EXPERIMENTAL WAVE EFFECTS ON VERTICAL RELATIVE MOTION

A Thesis

by

RAJITH PADMANABHAN

Submitted to the Office of Graduate Studies of
Texas A&M University
in partial fulfillment of the requirements for the degree of

MASTER OF SCIENCE

May 2006

Major Subject: Ocean Engineering

EXPERIMENTAL WAVE EFFECTS ON VERTICAL RELATIVE MOTION

A Thesis

by

RAJITH PADMANABHAN

Submitted to the Office of Graduate Studies of
Texas A&M University
in partial fulfillment of the requirements for the degree of

MASTER OF SCIENCE

Approved by:

Chair of Committee,	Cheung Hun Kim
Committee Members,	Moo-Hyun "Joseph" Kim
	Achim Stossel
Head of Department,	David V Rosowsky

May 2006

Major Subject: Ocean Engineering

ABSTRACT

Experimental Wave Effects on Vertical Relative Motion. (May 2006)
Rajith Padmanabhan, B.Tech., Cochin University of Science and Technology
Chair of Advisory Committee: Dr. Cheung Hun Kim

Ship motions are influenced by the sea state. Conventionally the responses are calculated in the frequency domain. This method, however, is valid only for narrow band spectra. As the seaway becomes more nonlinear, the ship motions cannot be readily predicted using the spectral method. Experiments conducted by Dalzell, have shown that the Response Amplitude Operator (RAO) decreased with increasing sea state or non linearity. Conventionally in the shipbuilding industry, the ship motions are studied by the linear RAOs and the energy density spectrum of the seaway. This method does not take into consideration any non linearities in the system. These are ignored and the ship seaway system is modeled linearly. The following work analyzes ship motions in the conventional linear approach and compares it to time domain simulations using the technique outlined in the work, viz. UNIOM (Universal Nonlinear Input Output Method). Time domain simulation of the SL-7 container ship hull is carried out. A comparison of the most probable peak value of the different modes of motion indicates that the linear theory tends to overpredict.

To Amma and Sampada

ACKNOWLEDGMENTS

This research was conducted at Texas A&M University with the support of the Department of Civil Engineering, through the Texas Engineering Experiment Station (TEEX). I wish to thank my chair, Dr. C.H.Kim, for his valuable contribution toward this thesis and for having shared with me his valuable insights in the field of Naval Architecture, Hydrodynamics and Statistics. I wish to thank Dr. M.H.Kim and Dr. Achim Stossel for their guidance throughout this research project. I wish to thank Adam Adil (Exmar Offshore) for having helped me out with the programs and Mr. Jeffery Arthur Richer (US Navy) for his support throughout this research work. For all things related to the use of the computer, from installing the hardware to debugging code and finally typesetting the whole work in LaTeX, my good friend Thomas has most patiently listened to and helped me solve every issue in the nick of time. I thank him for his patience and wholehearted support. I am indebted to my classmates, Mr. Basil Theckumpurath and Ms.Amal Chellappan, for their constant support and motivation. Special thanks to my family for their faith in me and constantly motivating me, without them I would not have been able to come this far.

TABLE OF CONTENTS

CHAPTER Page

CHAPTER Page

LIST OF TABLES

LIST OF FIGURES

FIGURE Page

FIGURE Page

FIGURE Page

FIGURE Page

FIGURE Page

FIGURE Page

FIGURE Page

FIGURE Page

FIGURE Page

CHAPTER I

INTRODUCTION

1. Motivation

Conventionally ship motion has been studied using linear method in the frequency domain. This method is a good choice for a preliminary study, being quick to compute and simplistic in nature. This method has hence been highly preferred by the industry as a good tool in calculation the ship responses. However this method is seen to be unreliable for highly nonlinear responses. For the linear theory to be valid, the ship should be wall sided and traveling on a straight course at constant speed in very low waves, experiencing very small motions in all modes, (Cummins 1973).The linear method is given by equation 1.1

$$U_{yy}(\omega) = U_{xx}(\omega) \mid G(\omega) \mid^2 \tag{1.1}$$

U_{xx} is the input wave spectrum

U_{yy} is the response wave spectrum and

$G(\omega)$ is the linear transfer function, also known as the **RAO**, which stands for **R**esponse **A**mplitude **O**perator.

This is not applicable in high sea states and ship motions in high sea states will divert away from the linear assumptions.

The journal model is *Journal of Ship Research.*

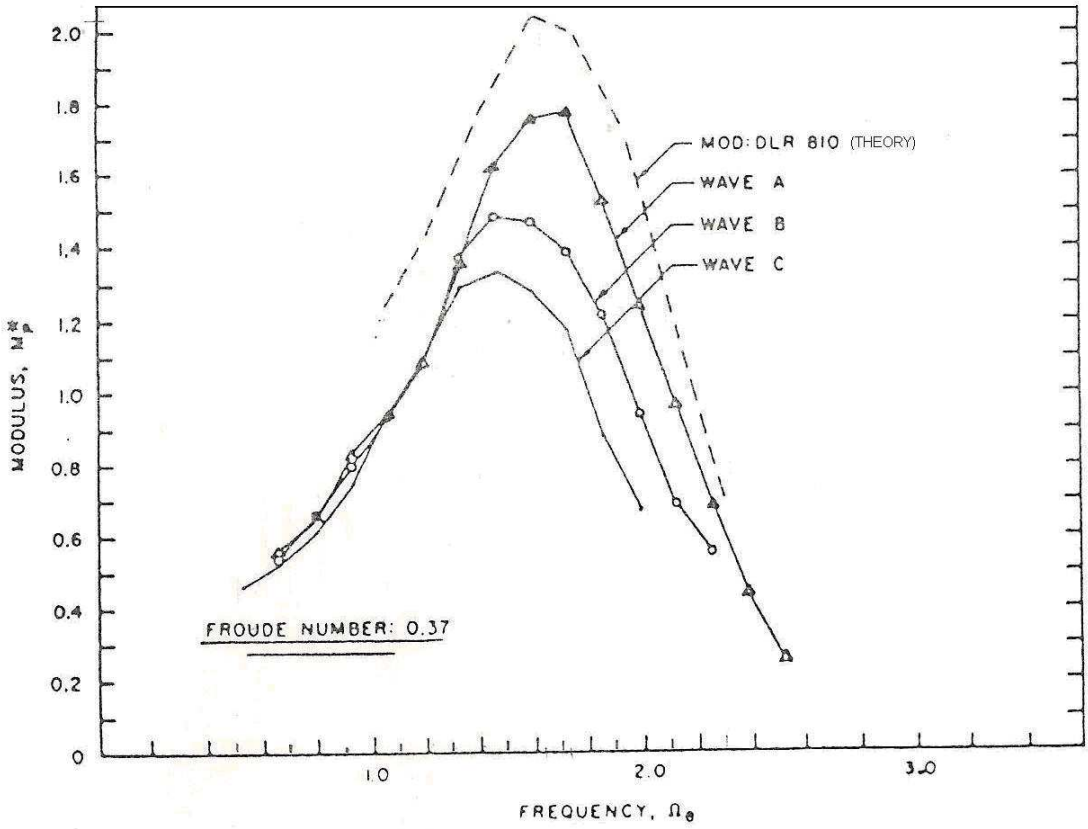

Fig. 1. Pitch transfer RAO from Dalzell's experiment [source: (Cummins 1973)]

1.1. Motivation

Ship motions calculated conventionally assumed the RAO to be constant regardless of the nonlinearities of the wave. The effect of nonlinearities have been studied by Dalzell, and his findings illustrate that the RAO of the ship at high sea states decreased. This is illustrated in figure 1.

In Dalzell's experiment (Dalzell 1982), a model long hull destroyer DD 692 was subject to three sea states. A- corresponding to a significant wave height of 2.3 percent of the model length; B - significant wave height of 6.1 percent of the model length and C - significant wave height of 9.3 percent of the ship length.

For these sea conditions, the hull was towed to find the pitch responses, from which RAOs were generated as shown in equation 1.2.

$$RAO = \frac{U_{xy}}{U_{xx}} \tag{1.2}$$

where the subscript x and y denote the input wave and the response respectively.

The objective of the study is to compare the motions predicted by the linear method in the frequency domain and simulation in the time domain. Analysis will be performed for different Froude numbers and headings. Such a study would confirm the application of UNIOM on more effective calculations of ship motion.

The additional margin that we may get using this method would help set lower margin to prevent the shipping of green water, which is dealt by classification societies by defining a minimum freeboard requirement. The International Load Line Convention (ILLC) 1996 has specified minimum freeboard requirements for the ship. The UNIOM model presented in this work will help us better understand the role of wave nonlinearities on the ship motions and thereby the margin of safety required.

1.2. Application

We apply a **U**niversal **N**onlinear **I**nput **O**utput **M**odel , henceforth called **UNIOM**. The method uses the linear RAO of the ship, and uses the nonlinear input wave to simulate a non-linear response model. This method uses the real wave, instead of a Gaussian wave package simulated using the sea spectrum. This approach has previously been used by Adil (Adil 2004) and Richer (Richer 2005). A detailed description of this method is given by Kim, C. H. (Kim 2006).

We do not have sufficient experimental data to confidently say that one method is superior to the other, however we can see how the responses from the linear and

the UNIOM approach differ as the sea state increases.

2. Approach

2.1. Linear and Nonlinear Model

For a Gaussian input wave pattern input into a linear system, the response is give by equation 1.1. A linear system thus can be analyzed using this approach. This approach is called the linear approach.

The non linear input into a linear system would produce a non linear response. This non linear response can be studied in the time domain using the relation

$$Out(t) = \Sigma \mid A_j \mid\mid RAO_j \mid e^{i(\omega_j t - \phi_j - \epsilon_j)} \tag{1.3}$$

The subscript j denotes the j^{th} frequency.

$Out(t)$ is the output time series, which depends on the RAO, RAO_j, if the RAO is the roll motion RAO then $Out(t)$ gives the time series of roll motion. Similarly on using the relative motion RAO in the formula, $Out(t)$ becomes the relative motion time series. Thus we can simulate any motion provided we know the RAO.

The RAO is generated from strip theory, and ϵ_j is the phase of the RAO. Since the input A_j is nonlinear, $Out(t)$, the resultant response of the vessel, even though the RAO is linear, is also nonlinear.

The above approach is called the UNIOM model.

CHAPTER II

THE UNIOM MODEL

UNIOM is based on the assumption that a non-linear input to a linear system would generate a nonlinear response. This is graphically shown in figure 2. In this work, the non linear input and output are the input waves and the ship response respectively. The linear system being the ship and seaway.

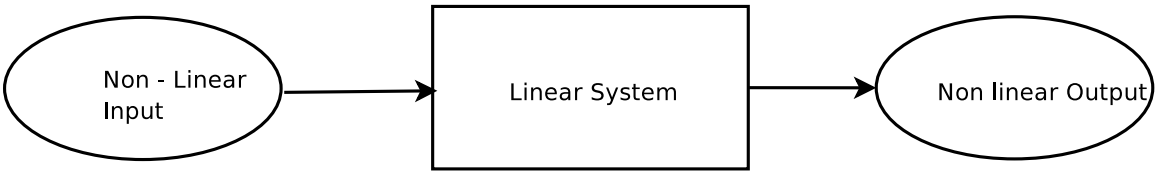

Fig. 2. The UNIOM model

1. Strip Theory

First introduced by Korvin-Kroukovsky (Kim et al 1980) in 1955 and Korvin-Kroukovsky and Jacobs (Kim et al 1980).This method of ship motion prediction consists of dividing the ship into a number of longitudinal strips. On each of these strips two-dimensional pulsating sources are applied on the boundary and the motion induced hydrodynamic forces and moments are evaluated. For our study we will use the program SHMB5 developed by Kim et al (Kim et al 1980). This program distributes pulsating sources on the strip (Frank-close-fit method) to evaluate the sectional motion induced and the wave-exciting forces and moments.

2. Equations of Motion

A ship has six degrees of freedom, we will denote them as 1,2,3,4,5,6. They are surge, sway, heave, roll, pitch, and yaw. Figure 4 shows these motions. For each of these degree of freedom, we may generalize the motion as

$$\sum_{i=1}^{6} \left(M_{kj} + A_{kj}\right) \ddot{X} + N_{kj}\dot{X} + B_{kj}X = F_k \tag{2.1}$$

k= 1,2,3,4,5,6

where: M_{kj}=Mass of the body in the j^{th} mode due to unit displacement in the k^th direction

A_{kj}=Added Mass of the body in the j^{th} mode due to unit displacement in the k^th direction, the term $(M + A)$ is called virtual mass and will be henceforth referred to as M,

N_{kj} is the damping force in the j^{th} mode per unit velocity along the k^{th} direction

B_kj is the restoring force in the j^{th} mode per unit displacement along the k^{th} direction

F_k is the force along the $k^{th} direction$

k= 1,3 and 5 : Surge, heave and pitch

k= 2,4 and 6 : Sway, roll and yaw motions

$\ddot{X}$, $\dot{X}$ and X denote the acceleration, velocity and the displacement

The motions are not really independent, heave and pitch are coupled and sway-roll-yaw are coupled, these are given in equations 2.4 - 2.5

An oblique regular wave is given by

$$h = ae^i \left(\nu_o x \cos\mu + \nu_o y \sin\mu - \omega t\right) \tag{2.2}$$

with

$$\omega = \omega_0 - \nu_0 U cos\mu \tag{2.3}$$

a is the wave amplitude,ν is the wave number and μ is the heading of the ship. x and y are the x and y distances of the point in consideration from the origin.

U is the forward velocity of the ship, ω is the encounter frequency of the wave and ω_0 is the intrinsic frequency of the wave.

The intrinsic frequency of the wave is the frequency of the wave as observed by a land based frame of reference, while the encounter frequency of the wave is the frequency observed by a frame of reference fixed on the ship.

Figure 3 shows a sketch of an oblique wave incident on a ship

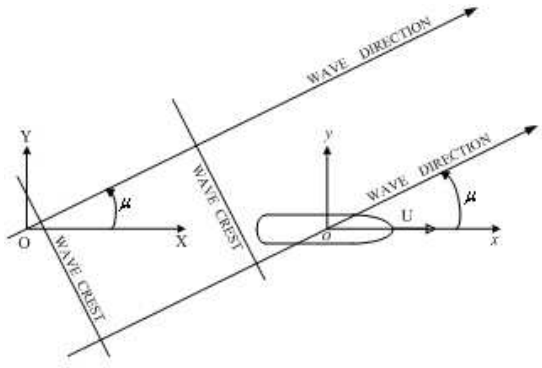

Fig. 3. Sketch of oblique wave trains incident on a ship [source: (Kim C H, 2006)]

The senses of the six degrees of freedom of the ship are illustrated in figure 4, where ξ, η, and ζ are surge ,sway, and yaw, respectively; And ϕ, ψ, and χ are roll, pitch, and yaw, respectively.

O represents the origin of the space fixed co-ordinate system. G is the origin of the frame of reference moving with the ship.

The ship motion in response to this wave is calculated by solving the linear

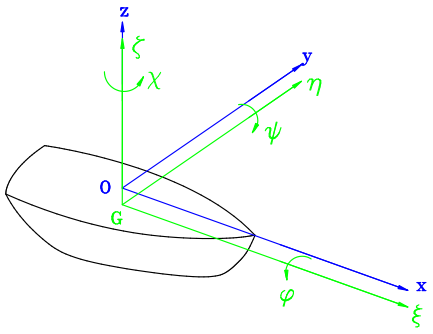

Fig. 4. Ship co-ordinate system showing the different degrees of freedom.

coupled heave-pitch equation2.4 and sway-yaw-roll equations 2.5

$$\begin{bmatrix} \{(B_{\zeta\zeta} - \omega^2 M_{\zeta\zeta}) - i\omega N_{\zeta\zeta}\}\{(B_{\psi\zeta} - \omega^2 M_{\psi\zeta}) - i\omega N_{\psi\zeta}\} \\ \{(B_{\zeta\psi} - \omega^2 M_{\zeta\psi}) - i\omega N_{\zeta\psi}\}\{(B_{\psi\psi} - \omega^2 M_{\psi\psi}) - i\omega N_{\psi\psi}\} \end{bmatrix} \begin{bmatrix} \frac{\zeta}{a} \\ \frac{\psi}{a} \end{bmatrix} = \begin{bmatrix} \frac{F_\zeta}{a} \\ \frac{F_\psi}{a} \end{bmatrix} \tag{2.4}$$

$$\begin{bmatrix} (-\omega^2 M_{\eta\eta}) - i\omega N_{\eta\eta})(-\omega^2 M_{\chi\eta} - i\omega N_{\chi\eta})(-\omega^2 M_{\phi\eta} - i\omega N_{\phi\eta}) \\ (-\omega^2 M_{\eta\chi}) - i\omega N_{\eta\chi})(-\omega^2 M_{\chi\chi} - i\omega N_{\chi\chi})(-\omega^2 M_{\phi\chi} - i\omega N_{\phi\chi}) \\ (-\omega^2 M_{\eta\phi}) - i\omega N_{\eta\phi})(-\omega^2 M_{\chi\phi} - i\omega N_{\chi\phi})(B_{\phi\phi} - \omega^2 M_{\phi\phi} - i\omega N_{\phi\phi}) \end{bmatrix} \begin{bmatrix} \frac{\eta}{a} \\ \frac{\chi}{a} \\ \frac{\phi}{a} \end{bmatrix} = \begin{bmatrix} \frac{F_\eta}{a} \\ \frac{F_\chi}{a} \\ \frac{F_\phi}{a} \end{bmatrix} \tag{2.5}$$

where the time factor $e^{-i\omega t}$ is omitted in both cases. The first subscript denotes the mode of motion and the second denotes the mode of induced force. SHMB calculates the motion by solving equations 2.4 and 2.5. Hydrodynamic pressure along the waterline on a hull surface induces the so called dynamic swell, which is used for estimation of relative motions between the at-rest waterline and the adjacent wave surface. The dynamic swell or the wave elevation due to the hydrodynamic pressure along the at-rest waterline is given by

$$\frac{p_{DS}}{\rho g a} = \frac{p_I + p_D + p_B}{\rho g a} \tag{2.6}$$

p_{DS} is the pressure due to dynamic swell, P_I, P_D, P_R are the pressure due of the

incident, diffraction and the radiation wave. the vertical motion $z_{\pm}$ of the at-rest waterline itself is given by

$$z_{\pm} = \zeta - x\psi + \frac{iU}{\omega}\psi \mp \frac{B(x)}{2}\phi \tag{2.7}$$

where $\pm$ indicates the right and left sides of the ship section along the waterline respectively. $\frac{B(x)}{2}$ indicates the half section beam in the waterplane. Therefore the relative motion between the at rest waterline and the wave surface, the dynamic swell is given by

$$\frac{r\pm}{a} = \frac{p_{DS}\pm}{\rho g a} - \frac{z\pm}{a} \tag{2.8}$$

3. The Ship Motion Program

The ship motion is analyzed using SHMB5, developed by Kim, C.H. et al. This program uses strip theory for computations, the use of this software has been validated and the method is specified in Kim, C.H et al (Kim et al 1980). The output from the program is further processed by the program PRDMR5, to give the relative motion.

3.1. Ship Particulars

The ship in consideration is a typical containership, SL-7 which has been extensively used in various ship motion studies at the Davidson laboratory of Stevens Institute of Technology, New Jersey. The ship is divided into 10 stations with two half stations at either ends. The ship particulars are given in table 1, the station we use for studying the vertical relative motion, the midship section. Figure 5 shows a wiremesh figure of the ship.

Table 1.: Main particulars of the SL 7 containership

LBP	175	m
B	25.4	m
T midship	9.5	m
Disp	24742	m^3
LCG	-2.48	m forward of midship
KB	5.4	m from baseline
KG	9.52	m from baseline
GM	1	m
Roll gyradius	8.33	m
Pitch gyradius	42	m
Yaw gyradius	42	m

4. Input Waves

For the present study, non linear waves generated at the Korea Research Institute of Ships and Ocean Engineering (KRISO) will be used. KRISO has provided wave time series data they generated in their basin using ITTC and the JONSWAP spectrum; these are specified in table 2.

In table 2 T_z denotes the zerocrossing period and T_p denotes the peak period, Hs stands for the significant wave height.

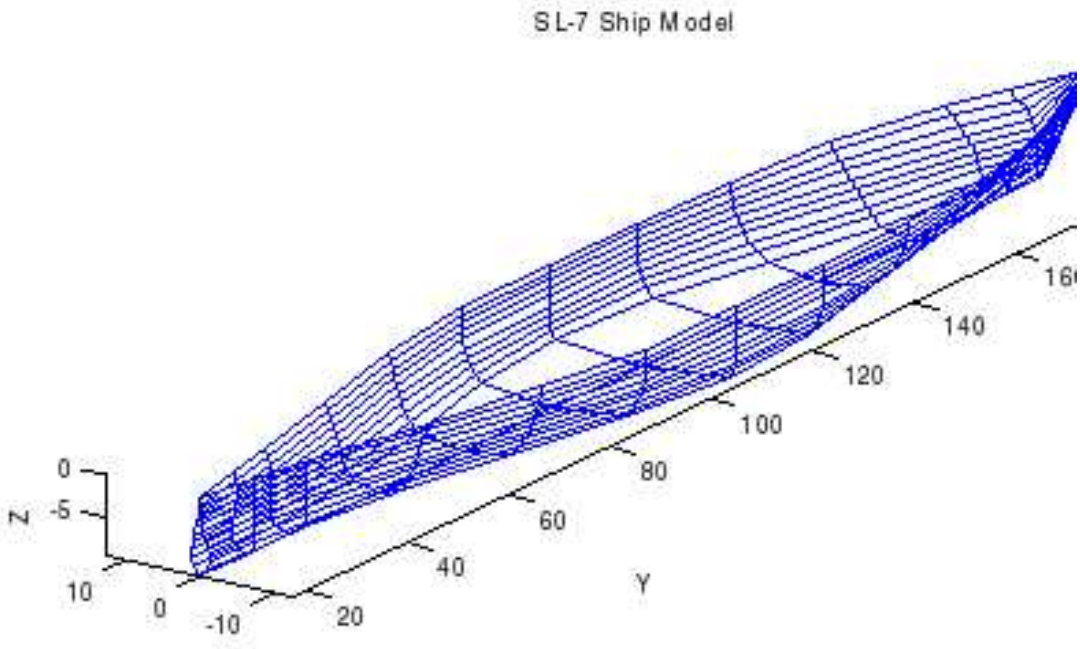

Fig. 5. Wiremesh model of containership hull SL 7

4.1. Froude Similitude Law

The experimental generation of waves in a wave basin is governed by Froude's Law shown in equation 2.9. Model testing and interpretation of the data are discussed indepth by Chakrabarti (Chakrabarti 1994).

$$F_n = \frac{V}{\sqrt{gL}} \tag{2.9}$$

The wave heights and peak period of the model and prototype are related as shown in equation 2.10 and equation 2.11.

$$\frac{Hs_{model}}{Hs_{prototype}} = \lambda \tag{2.10}$$

Table 2.: KRISO experimental wave specification

Data ID	**Proto**		**Model**		γ	**Spectrum**
	Hs(m)	**Tz/Tp**	**Hs(m)**	**Tz/Tp**		
#042	4.0	8.0/11.26	0.073	1.079/1.519	1.0	ITTC
#010	6.0	9.5/12.09	0.109	1.281/1.630	1.5	JONSWAP
#014	7.0	9.5/12.09	0.127	1.281/1.630	2.0	JONSWAP
#020	9.0	10.0/12.73	0.164	1.348/1.717	2.5	JONSWAP
#028	11.0	10.5/13.37	0.200	1.416/1.803	2.5	JONSWAP
#043	3.0	8.0/11.26	0.055	1.079/1.519	1.0	ITTC

$$\frac{Tp_{model}}{Tp_{prototype}} = \lambda^{\frac{1}{2}} \tag{2.11}$$

where λ is the scale length scale factor.

4.2. The Modified JONSWAP Spectrum

The Joint North Atlantic Sea Wave Project (JONSWAP) spectrum has been modified over the years to the following form to represent other sea ways too. This spectrum is representative of wind generated seas (Journee & Massie 2001).

$$S(\omega) = \frac{5}{16} H_s^2 \omega_m^4 \omega^{-5} exp\left\{-1.25\left(\frac{\omega_m}{\omega}\right)^4\right\} (1 - 0.287 \ln\gamma)\, \gamma^{exp\left[-\frac{(\omega-\omega_m)^2}{2\sigma^2\omega_m^2}\right]} \tag{2.12}$$

where $\gamma = 3.5$ and

$$\sigma = \begin{cases} 0.07 & \text{if } \omega <= \omega_m \\ 0.09 & \text{if } \omega > \omega_m \end{cases}$$

4.3. ITTC Spectrum

The 15^th International Towing Tank Conference (ITTC 1978) has proposed a theoretical spectrum for average sea conditions and not for fully developed seas, given the significant wave height and modal period.

$$S(\omega) = \frac{A}{\omega^2} exp\left(\frac{B}{\omega^4}\right), A = 173 H_s^2 T_1^{-4}, B = 691\left(T_1\right)^2 \tag{2.13}$$

The above spectra are discussed by Dean, Robert G. and Dalrymple, Robert A. (Dean & Dalrymple 1984)

4.4. Encounter Frequency Domain

As a ship moves, the number of waves the ship encounters, or in other words the encounter frequency, will be different from that when stationary. This is because the frame of reference (ship) is now moving relative to the wave. This has the effect of altering the apparent frequency. The ship will encounter waves at higher frequency in head seas and at a lower frequency in following seas. For beam seas there will be no difference in the intrinsic and encounter frequency.

The frequency observed with respect to the ship will be called the encounter frequency. The ship motion has the effect of spreading out the abscissa of the amplitude spectra without altering the phase or the amplitude.

For the energy density spectrum, not only does the abscissa change, but also the ordinates change (Bhattacharyya 1978). This assures that the total energy between frequencies are conserved. The encounter frequency is given by equation 2.14.

$$\omega_e = \omega - \frac{\omega^2}{g} U \cos\mu \tag{2.14}$$

The energy density spectrum will change with the encountering frequency as

below

$$U_{xx}(\omega_e) = U_{xx}(\omega)\left(1 - \frac{2\omega U}{g}\cos\mu\right)^{-1} \tag{2.15}$$

5. KRISO Data Analysis

Prototype waves from KRISO are processed through a Fast Fourier Transform (FFT) program to obtain the energy density spectrum. The energy density spectrum is smoothed to obtain a smooth curve. Accuracy of the KRISO generated waves are assured by comparing the measured spectrum to the target spectrum, a 10% error in variance is considered allowable. Table 3 shows the comparison of variance of the measured and target spectrum.

To facilitate visual inspection, graphs are plotted comparing the measured and target spectra for each sea state. Overall good agreement is seen between the measured and the target spectra. Figures 6(a) to 6(f) compares the measured and target spectra.

6. Response Analysis

We can now simulate the motion of the ship in time domain using equation 1.3

For response in the frequency domain the RAOs from SHMB5 and PRDMR5 are used in equation 1.1 and the input wave spectrum to obtain the response spectrum. This response will correspond to the linear response of the ship.

7. Spectral Response Analysis

From the spectral response calculated using equation 1.1 we can find the variance of the response, which is the area under the energy density spectrum. This is referred

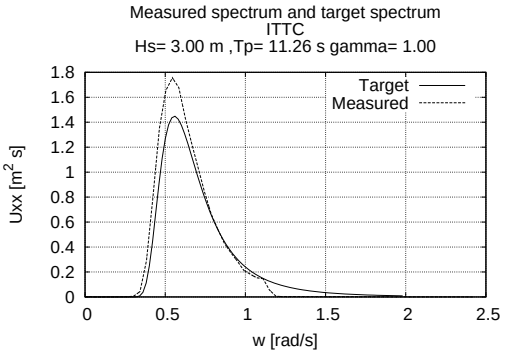

(a) wave #043, Hs=3.0 m, Tp=11.26 s

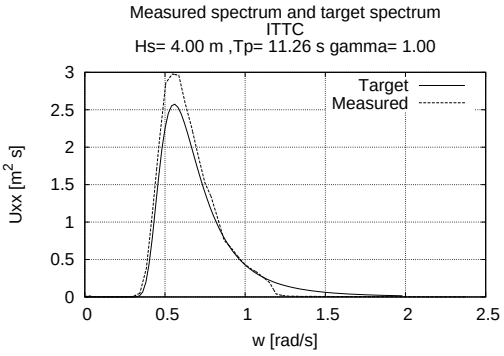

(b) wave #042, Hs=4.0 m, Tp=11.26 s

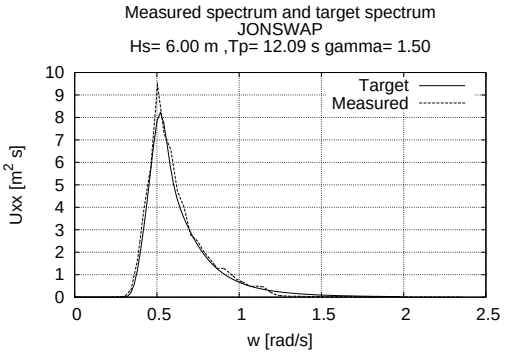

(c) wave #010, Hs=6.0 m, Tp=12.09 s

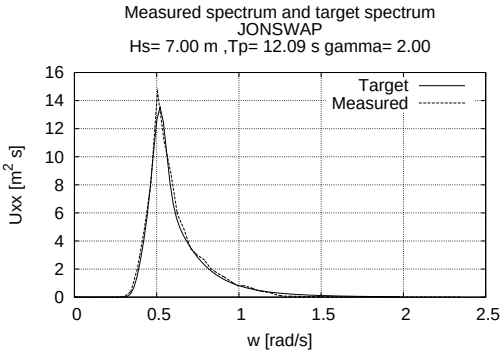

(d) wave #014, Hs=7.0 m, Tp=12.09 s

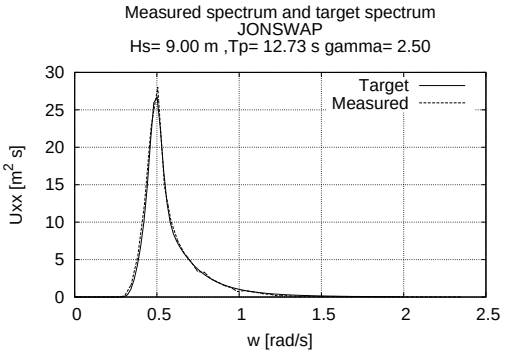

(e) wave #020, Hs=9.0 m, Tp=12.73 s

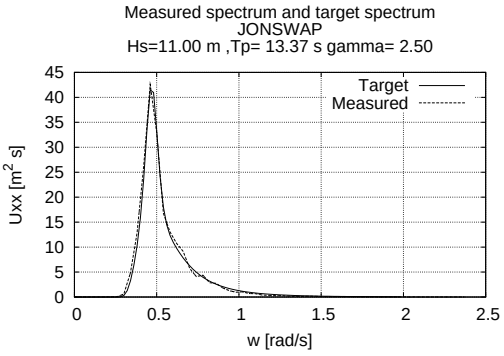

(f) wave #028, Hs=11.0 m, Tp=13.37 s

Fig. 6. Comparison of measured and target spectra

Table 3.: Comparison of variance of measured spectrum and the target spectrum, an error of up to 10% is considered acceptable

Data ID	**Variance** $[m^2]$		**Error** [%]
	Target	**Measured**	
#043	0.6138	0.5589	8.94
#042	1.0888	0.9936	8.74
#010	2.4248	2.2572	6.91
#014	3.2537	3.1044	4.59
#020	5.3625	5.1845	3.32
#028	7.9625	7.7495	2.67

to as the 1^{st} spectral moment denoted by m_0.

$$\sigma^2 = E\left[(x-\mu_x)^2\right] = \frac{1}{T}\int_0^T (x-\mu_x)^2\,dt = \frac{1}{N-1}\sum_{j=1}^{j=N}(x_j-\mu_x)^2 \tag{2.16}$$

μ_x is the mean value of the data.

The n^th spectral moment is given by the equation,

$$m_n = \int_0^\infty \omega^n U_{xx}(\omega)d\omega \tag{2.17}$$

The zerocrossing period of the wave is the average time period between successive up crossings or down crossings. For this study we will use only the zero upcrossings periods, represented by T_z. T_z can be calculated from the spectral moments by

equation 2.18. This holds good only for a narrow banded process and there will be marked deviations from this for a broad banded process.

$$T_z = 2\pi\sqrt{\frac{m_0}{m2}} \tag{2.18}$$

8. Zero Crossing Analysis

The zero crossing analysis program is included in the appendix. We use the matlab routine to do this. The routine records for each zero crossing - the wave height, the crest height, the trough height and the period.

9. Probability of Exceedence

For the current study, the irregular seaway is modeled as a narrow band spectrum of Rayleigh distribution of wave elevations. The probability that a wave crest will exceed a given peak value of a is given by

$$Pr\left\{peaks >= a\right\} = exp\left(\frac{-a^2}{2m_0}\right) \tag{2.19}$$

Nonlinearity will be indicated if the probability of exceedence of the time series doesn't agree with that of the Rayleigh distribution.

10. Most Probable Peak Analysis

For a wave record of infinite length, the probable peak value in N observations, where N is the number of zero crossings is given by

$$\hat{a}_N = \sqrt{2\ln N}\sqrt{m_0} \tag{2.20}$$

The number of observations N is the number of zero crossings in the time record

of length T.

$$N = \frac{T}{T_z} \tag{2.21}$$

CHAPTER III

SHIP MOTION CALCULATION

1. Input Wave Spectra

The input waves given in table 2 are analyzed using a Fast Fourier Transform (FFT) program and the one sided spectra of the same are calculated. Figure6(c) through 6(f) show the input wave spectra for the KRISO data.

2. Linear Transfer Function or RAO

A linear system like the one given in equation 2.1 is characterized by a frequency response function or a linear transfer function (LTF). We can obtain the frequency response function as above by performing an FFT to 2.1

$$G(\omega) = \frac{A_{out}}{A_{in}} \tag{3.1}$$

Thus the ratio of the Fourier transform of the output to that of the input is identical to the linear frequency response function. The frequency response function here is called RAO.

The ship SL 7 will be analyzed at different speeds, or Froude numbers in different headings. We will study, heave, pitch, roll, sway, and yaw motions. The program SHMB has a limitation of the range of frequencies it can analyze. For any other heading than head seas, the RAOs can be calculated from a minimum frequency of 0.3 radians only. However for our study since the wave spectra under consideration have very low energy in the bandwidth from 0.0 radians to 0.3 radians, we may ignore this limitation, and for the present study SHMB5 and PRDMR5 are deemed adequate in spite of this limitation.

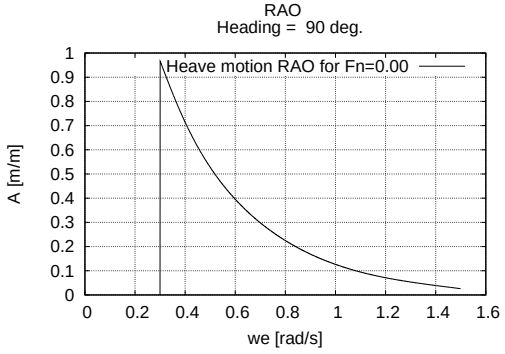

(a) heave RAO

Fig. 7. RAO for Fn=0.00 and Heading =90^o

Since following seas will cause the energy density spectrum to shift to the low frequency side, we are limited to analyzing only headings between 180^o and 135^o.

Furthermore, irregular frequencies appear in the RAOs between 1.5 and 1.6 radians. This limits our analysis to lower Froude numbers so that the energy density doesn't spread out too far into the irregular frequencies in the encounter spectrum.

3. Response Amplitude Operator

This section will detail the RAOs used in this study.

3.1. Heading=90^o, Froude number=0.00

The RAOs for a heading of 90^o and Froude number, F_n=0.00 is shown in figures 7(a) to 8(f)

3.2. Heading=90^o, Froude number=0.15

The RAOs for a heading of 90^o and Froude number, F_n=0.15 is shown in figures 9(a) to 10(f)

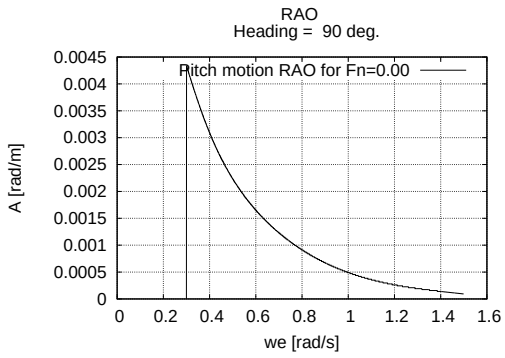

(a) pitch RAO

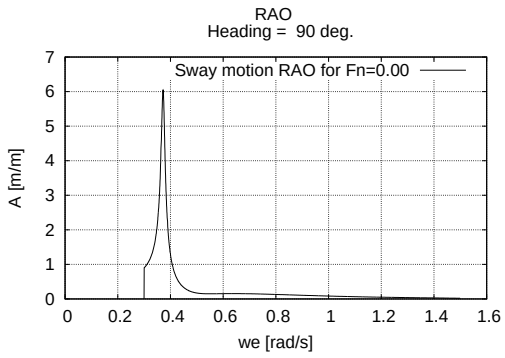

(b) sway RAO

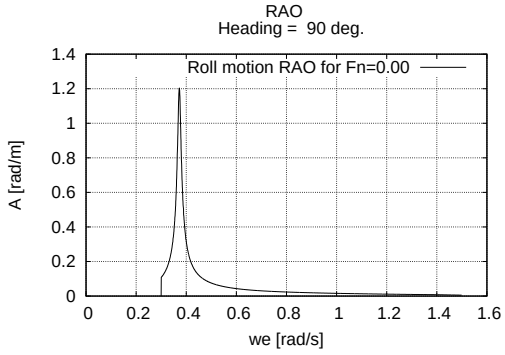

(c) roll RAO

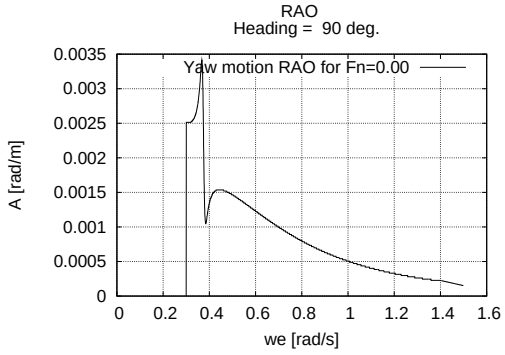

(d) yaw RAO

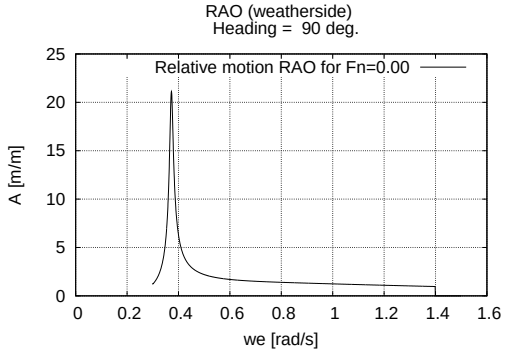

(e) vertical relative motion RAO (weather side)

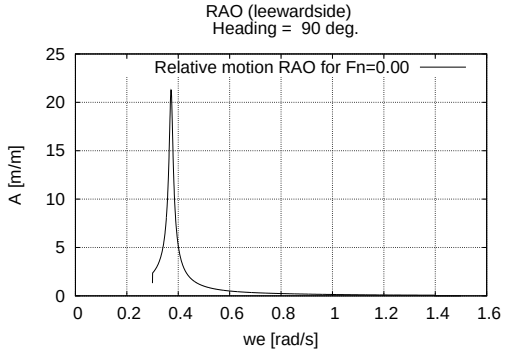

(f) vertical relative motion RAO (leeward side)

Fig. 8. Ship RAO for Fn=0.00 and Heading $=90^o$, calculated using SHMB

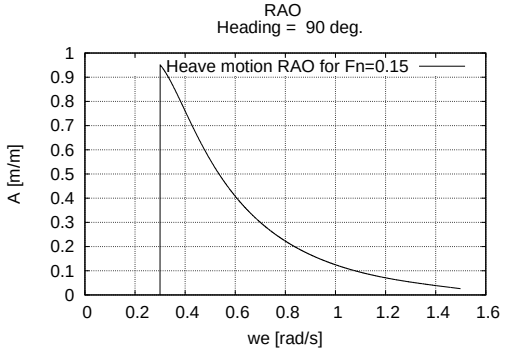

(a) heave RAO

Fig. 9. RAO for Fn=0.15 and Heading =90^o

3.3. Heading=135^o, Froude number=0.00

The RAOs for a heading of 135^o and Froude number, F_n=0.00 is shown in figures 11(a) to 12(f)

3.4. Heading=135^o, Froude number=0.15

The RAOs for a heading of 135^o and Froude number, F_n=0.15 is shown in figures 13(a) to 14(f)

4. Results from the Linear Method and UNIOM

Using the RAOs and the input wave spectrum we can compute the motions by the linear method using equation 1.1 or through UNIOM using the equation 1.3.

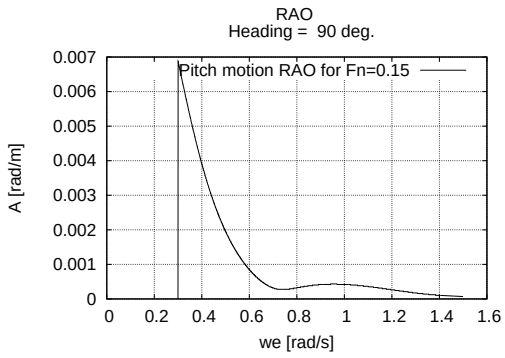

(a) pitch RAO

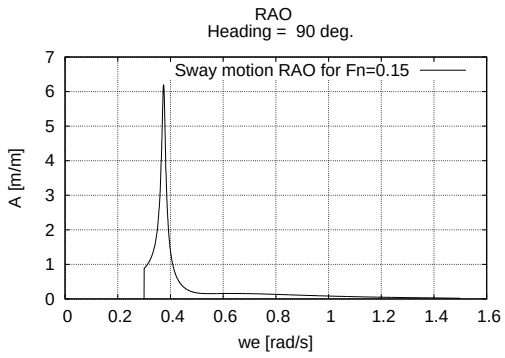

(b) sway RAO

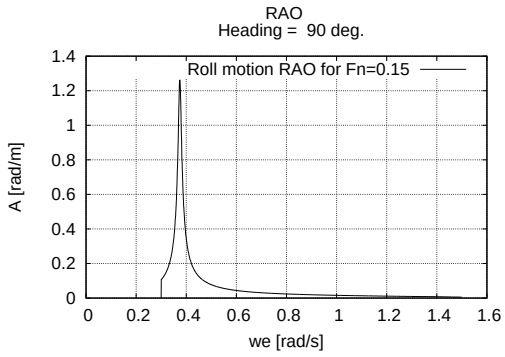

(c) roll RAO

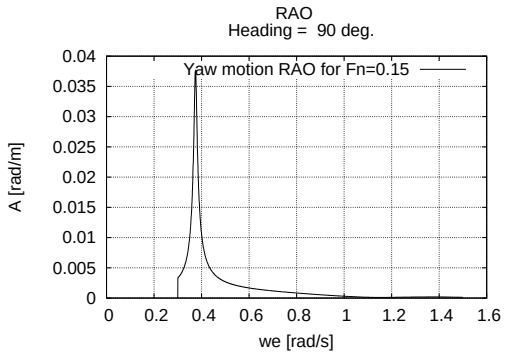

(d) yaw RAO

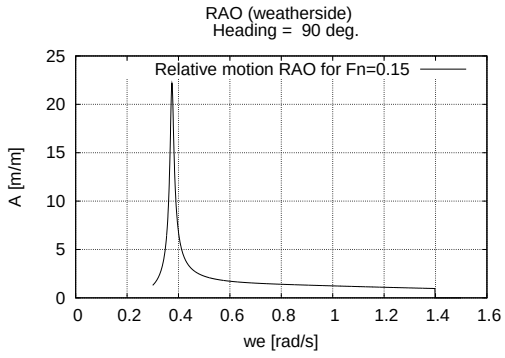

(e) vertical relative motion RAO (weather side)

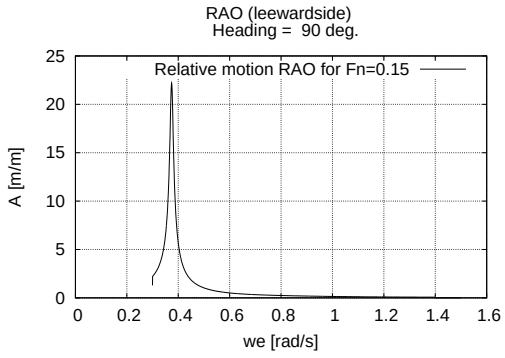

(f) vertical relative motion RAO (leeward side)

Fig. 10. Ship RAO for Fn=0.15 and Heading $=90^o$, calculated using SHMB

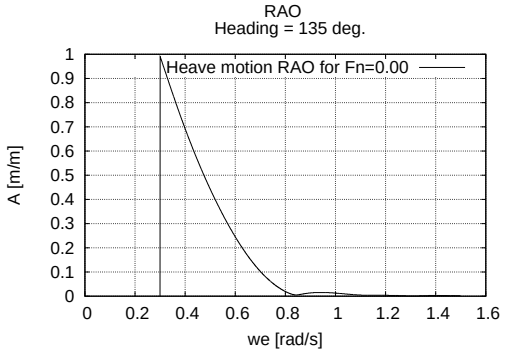

(a) heave RAO

Fig. 11. RAO for Fn=0 and Heading $=135^o$

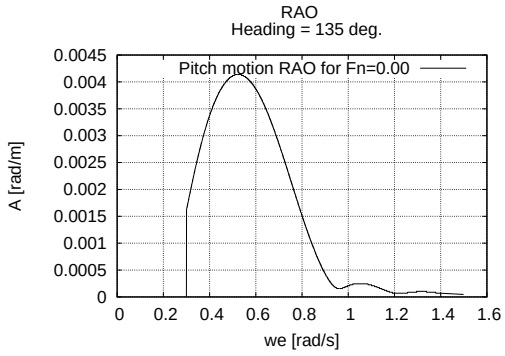

(a) pitch RAO

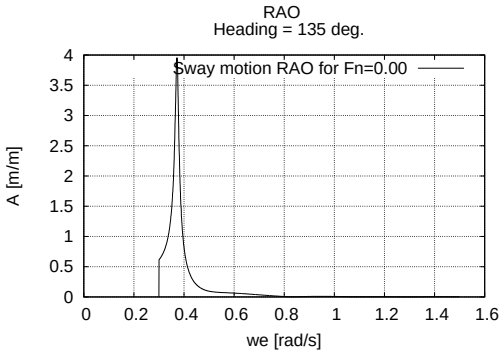

(b) sway RAO

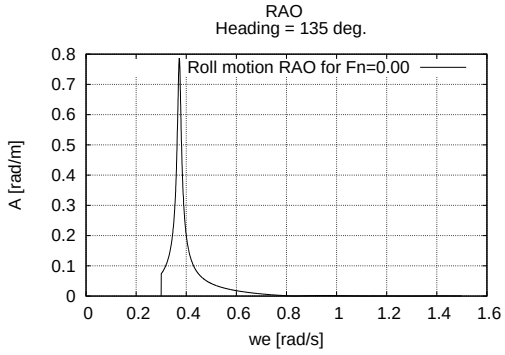

(c) roll RAO

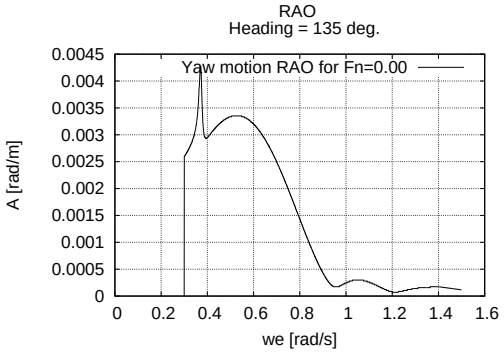

(d) yaw RAO

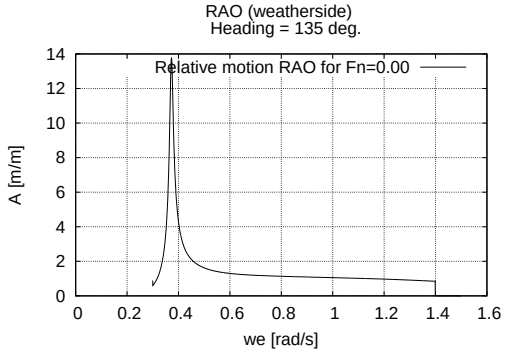

(e) vertical relative motion RAO (weather side)

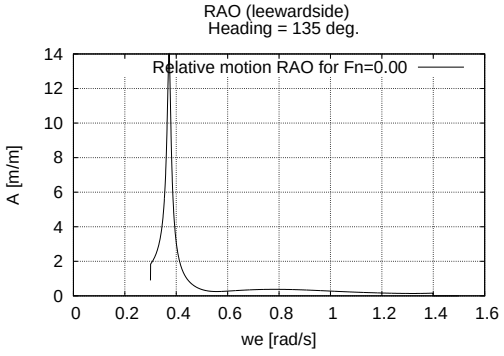

(f) vertical relative motion RAO (leeward side)

Fig. 12. Ship RAO for Fn=0 and Heading $=135^o$, calculated using SHMB

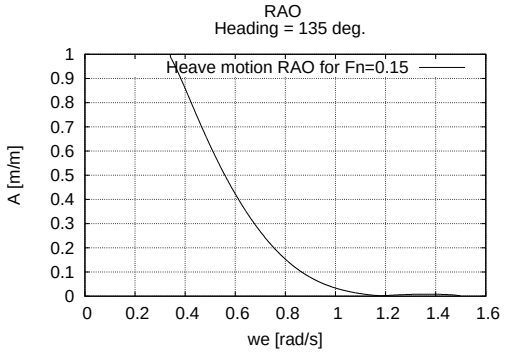

(a) heave RAO

Fig. 13. RAO for Fn=0.15 and Heading $=135^o$

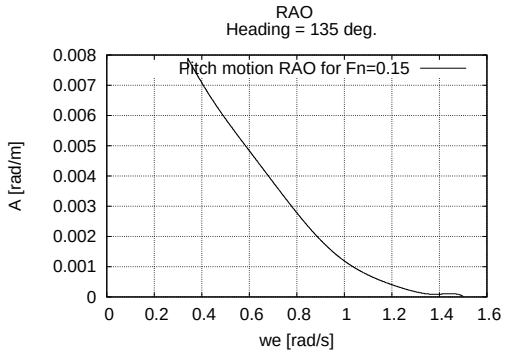

(a) pitch RAO

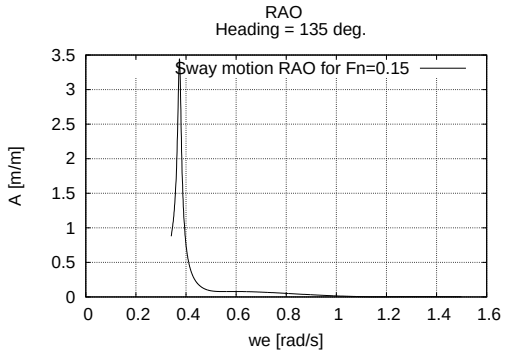

(b) sway RAO

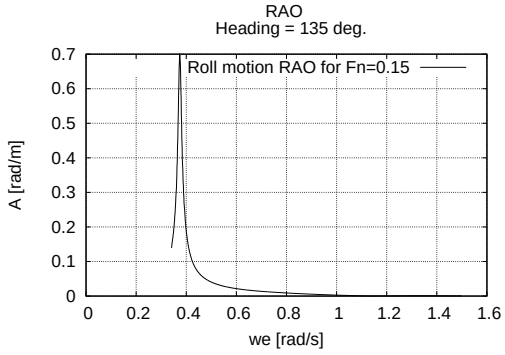

(c) roll RAO

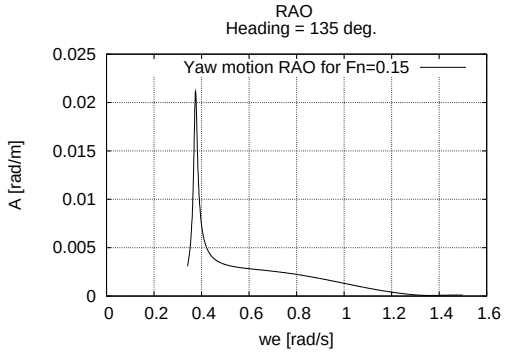

(d) yaw RAO

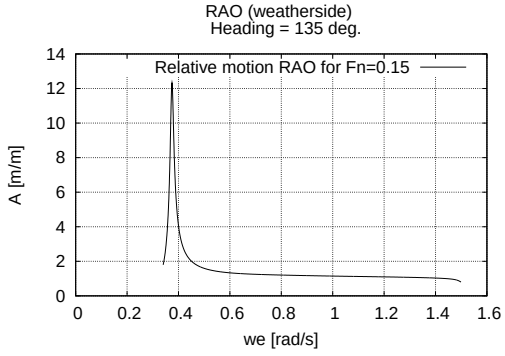

(e) vertical relative motion RAO (weather side)

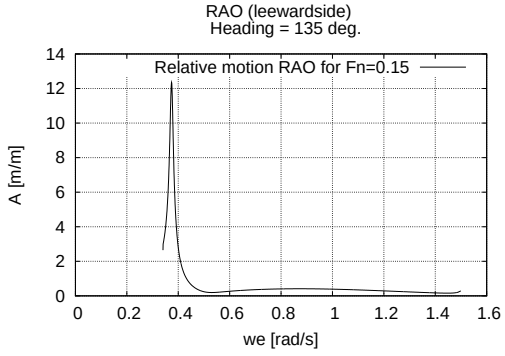

(f) vertical relative motion RAO (leeward side)

Fig. 14. Ship RAO for Fn=0.15 and Heading =135^o, calculated using SHMB

CHAPTER IV

ANALYSIS RESULTS FOR HEADING = 90^O AND $F_N = 0.00$

The motions of the container ship SL 7 for $Fn = 0$ and headings of 90^o are calculated using the linear approach and using UNIOM.

1. Simulation Results

In this section, the results from using the linear theory and UNIOM are compared. The simulation using UNIOM is carried out for 3600 seconds, but for the plots to be readable, only 1500 seconds of data is shown. The time steps used for the simulations is 1 second. The peak values are found corresponding to a time duration of 3600 seconds.

2. Probability of Exceedence

The probability of exceedence for the wave as well as the response motions are calculated. The following pages show the input wave and the responses.

2.1. Case 1 $H_s = 3.0m$

Figures 15 to 22 shows the input wave profile, heave, pitch, sway, roll, yaw, weather-side relative motion response and the leeward side relative motion response for KRISO wave data ID #043. The probability of exceedence of these wave are given in figures 23(a) to 24(d)

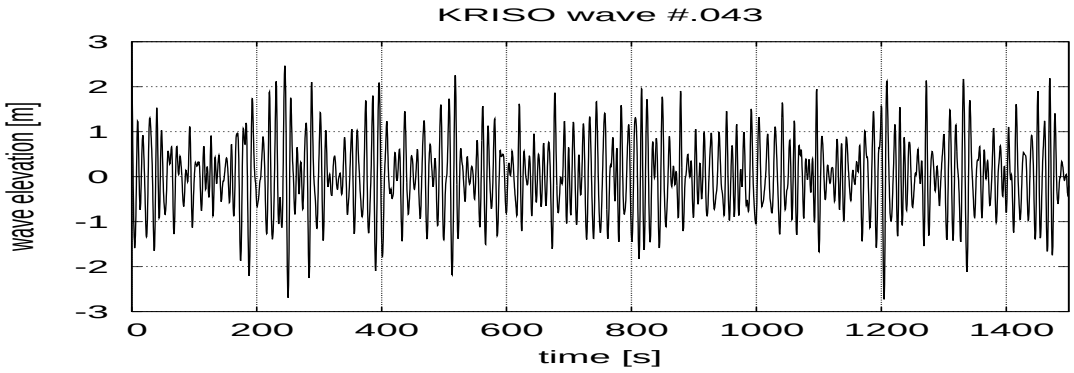

Fig. 15. Input wave $H_s = 3.0m$

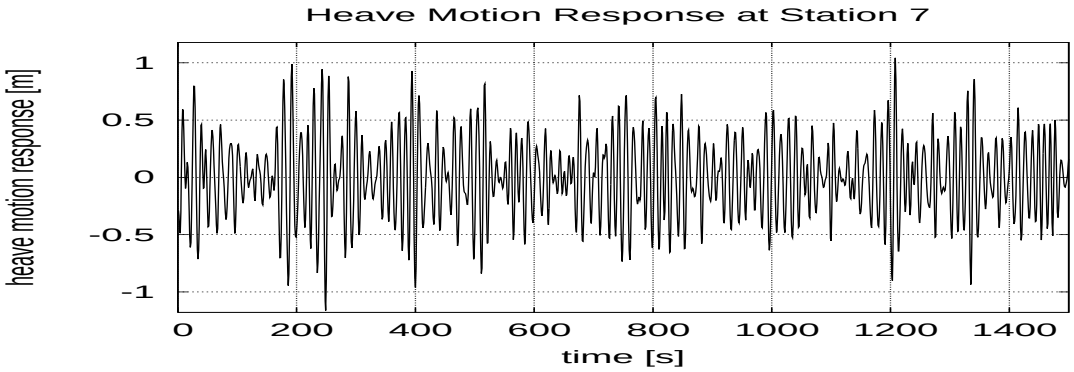

Fig. 16. Heave Motion for heading 90^o and $H_s = 3.0m$

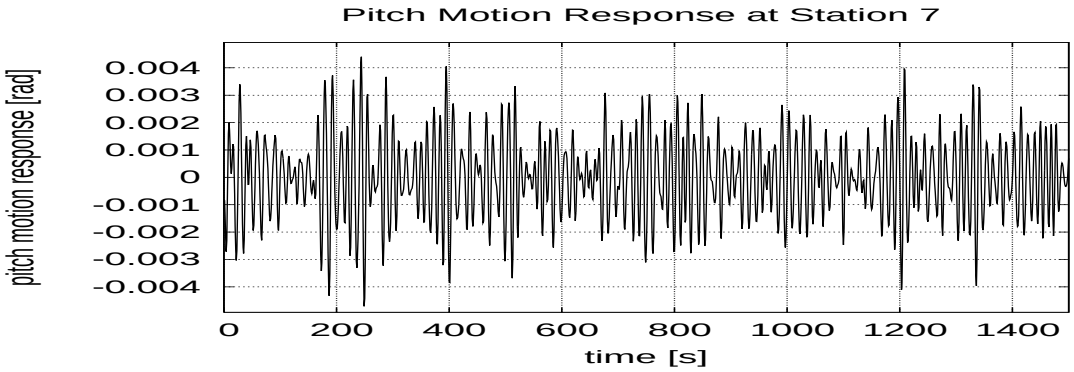

Fig. 17. Pitch Motion for heading 90^o and $H_s = 3.0m$

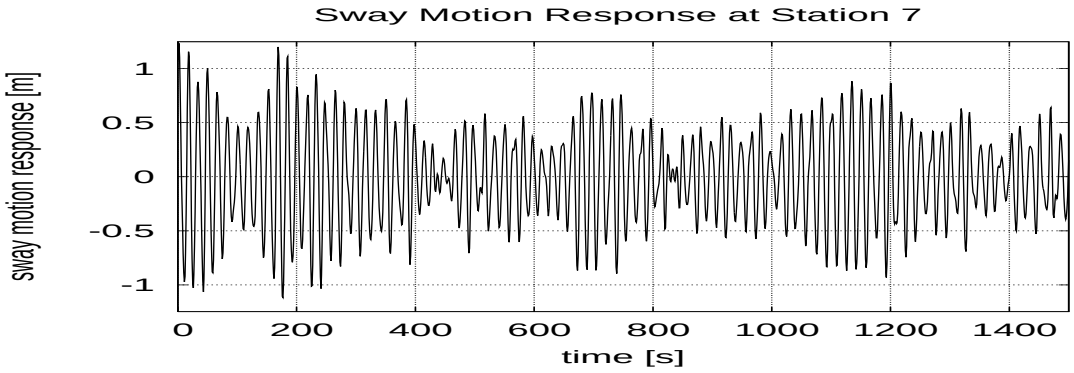

Fig. 18. Sway Motion for heading 90^o and $H_s = 3.0m$

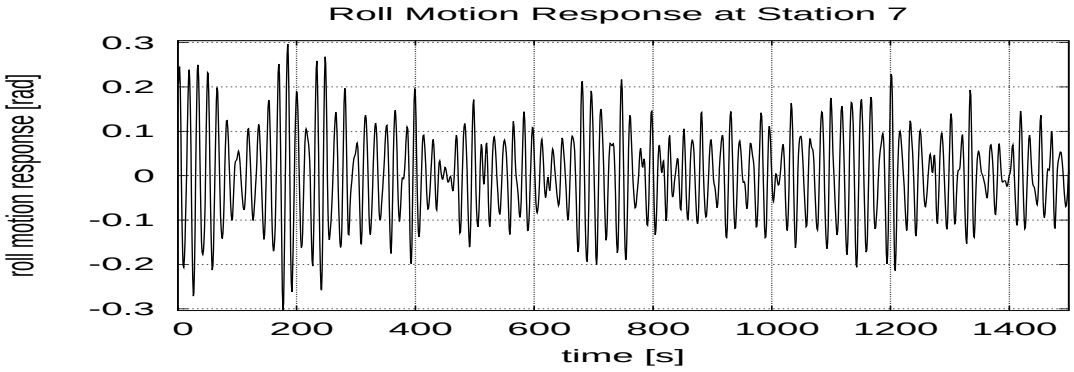

Fig. 19. Roll Motion for heading 90^o and $H_s = 3.0m$

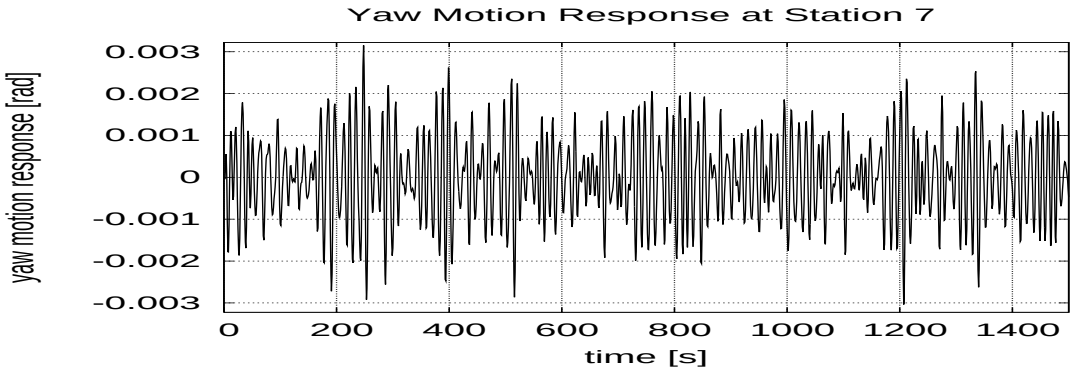

Fig. 20. Yaw Motion for heading 90^o and $H_s = 3.0m$

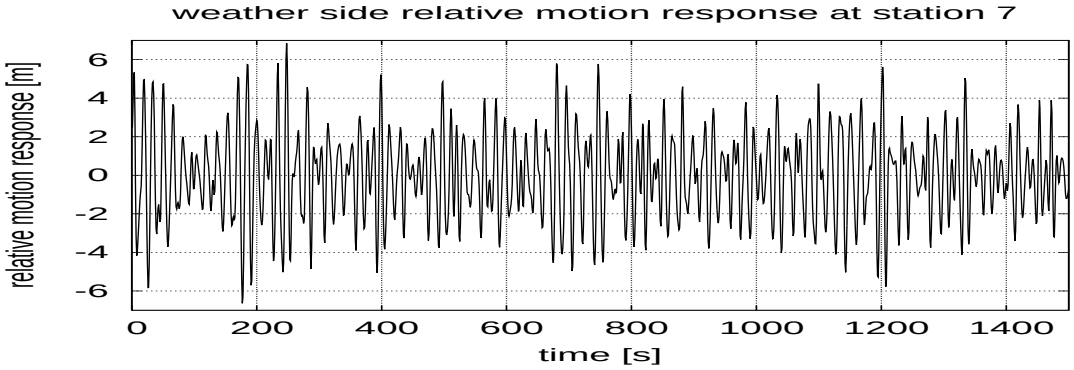

Fig. 21. Relative Motion at weather side for heading 90^o and $H_s = 3.0m$

2.2. Case 2 $H_s = 4.0m$

Figures 25 to 32 shows the input wave profile, heave, pitch, sway, roll, yaw,weatherside relative motion response and the leeward side relative motion response for KRISO wave data ID #042.The probability of exceedence of these wave are given in figures 33(a) to 34(d)

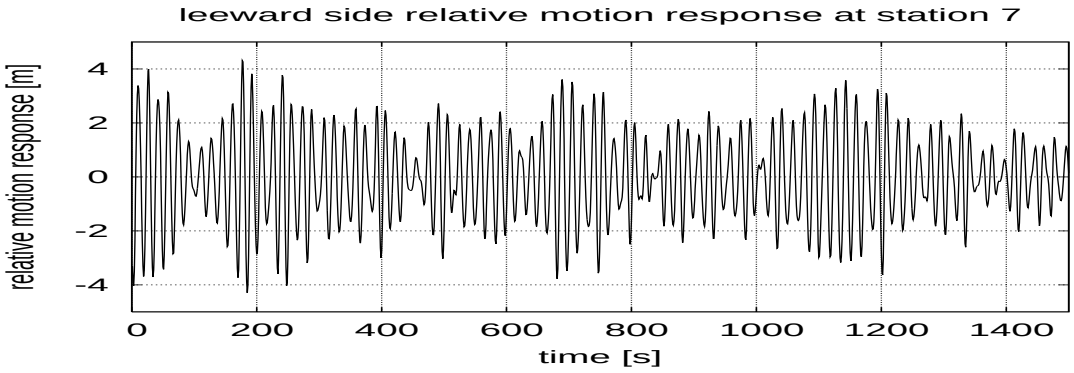

Fig. 22. Relative Motion at leeward side for heading 90^o and $H_s = 3.0m$

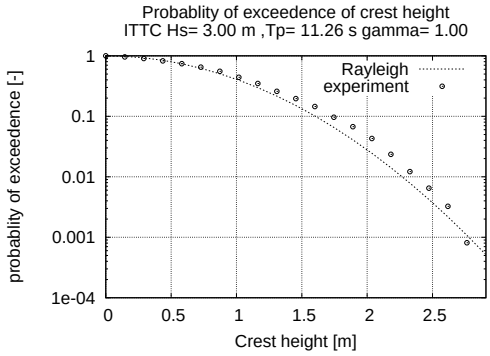

(a) Input wave

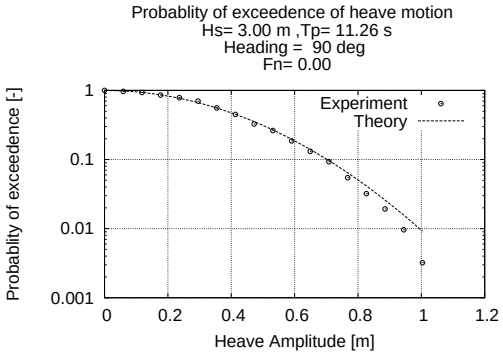

(b) Heave motion

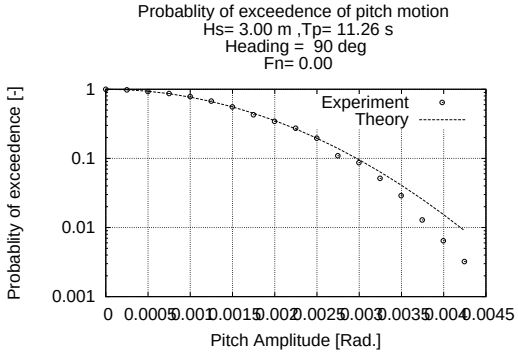

(c) Pitch motion

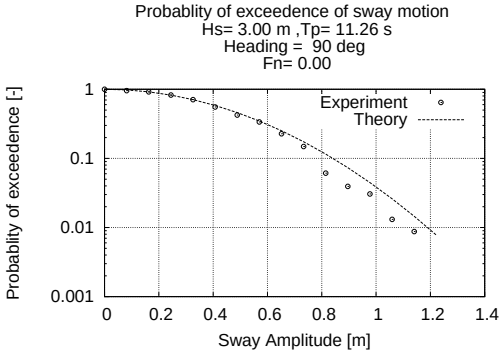

(d) Sway motion

Fig. 23. Probability of exceedence for the input wave and resultant motion Hs=3.00m, Fn=0.00 and Heading = 90^o

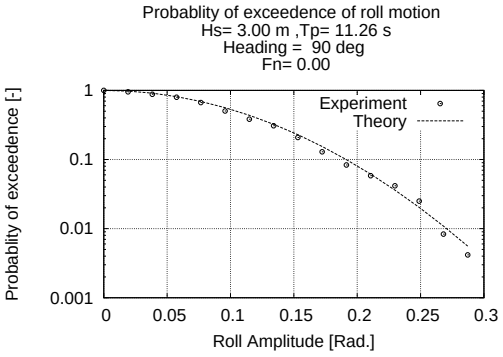

(a) Roll motion

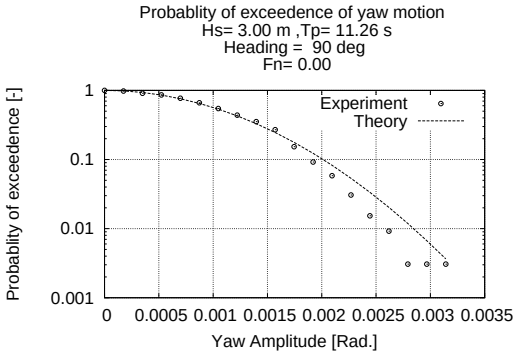

(b) Yaw motion

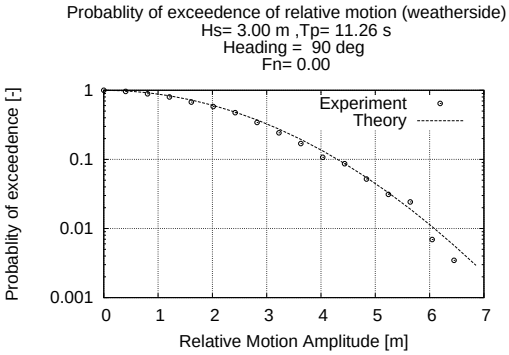

(c) vertical relative motion (weather side)

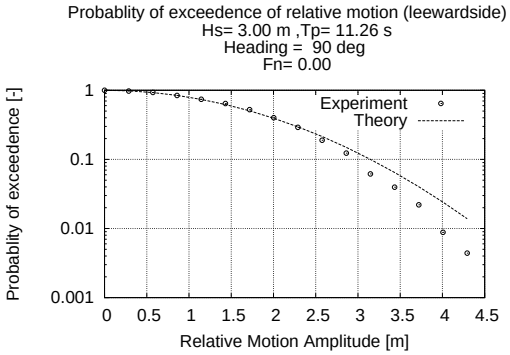

(d) vertical relative motion (leeward side)

Fig. 24. Probability of exceedence for the input wave and resultant motion Hs=3.00m, Fn=0.00 and Heading = 90^o

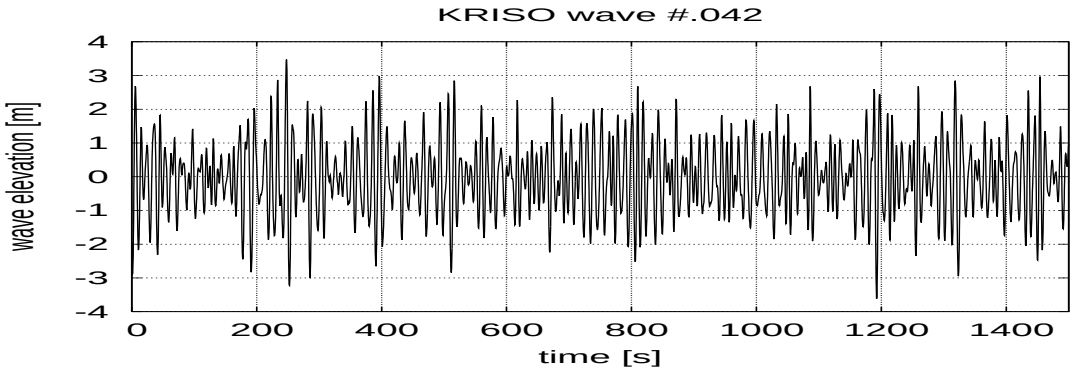

Fig. 25. Input wave $H_s = 4.0m$

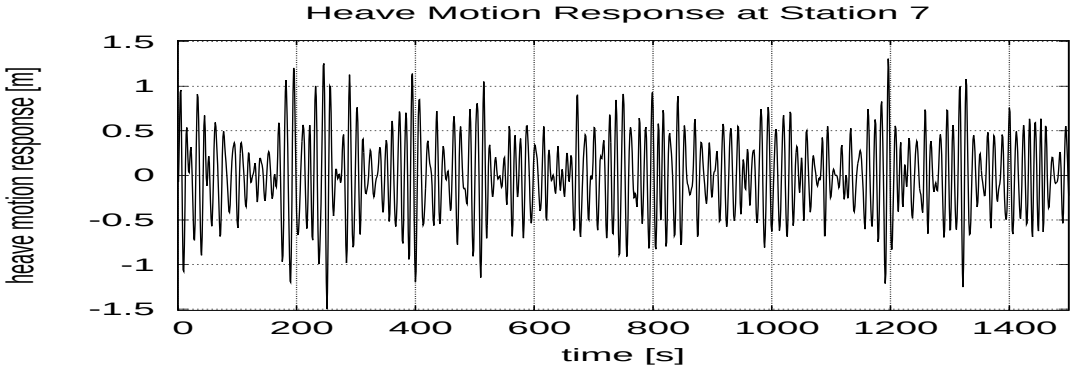

Fig. 26. Heave Motion for heading 90^o and $H_s = 4.0m$

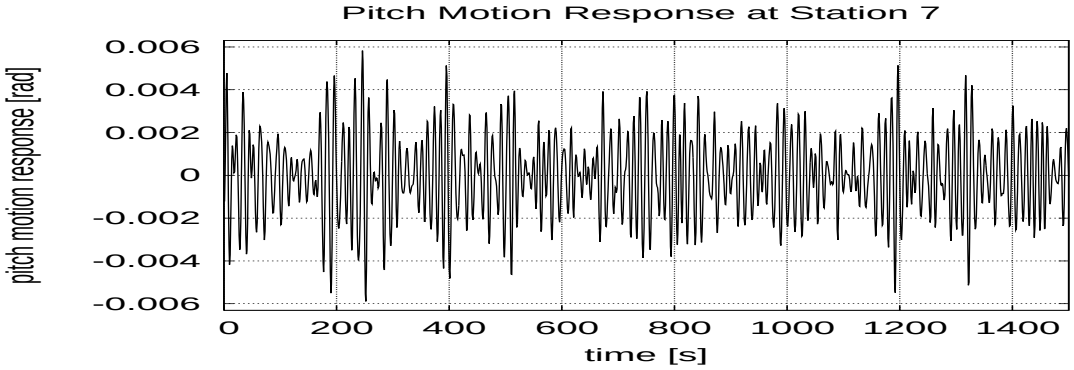

Fig. 27. Pitch Motion for heading 90^o and $H_s = 4.0m$

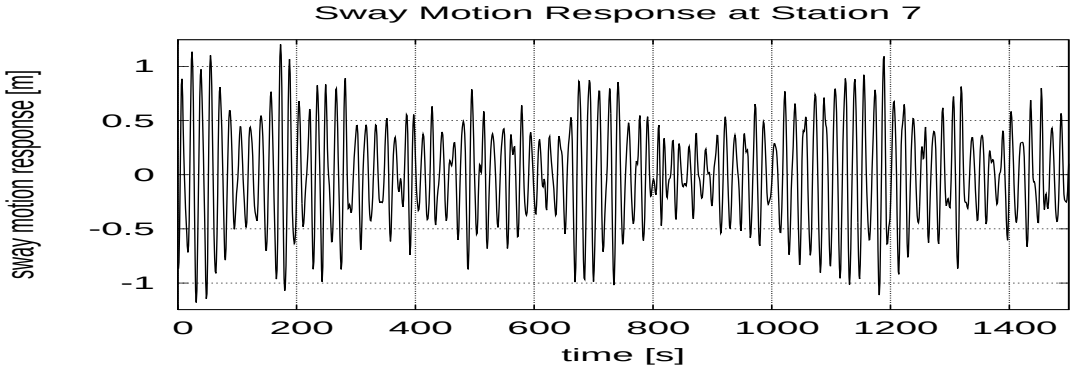

Fig. 28. Sway Motion for heading 90^o and $H_s = 4.0m$

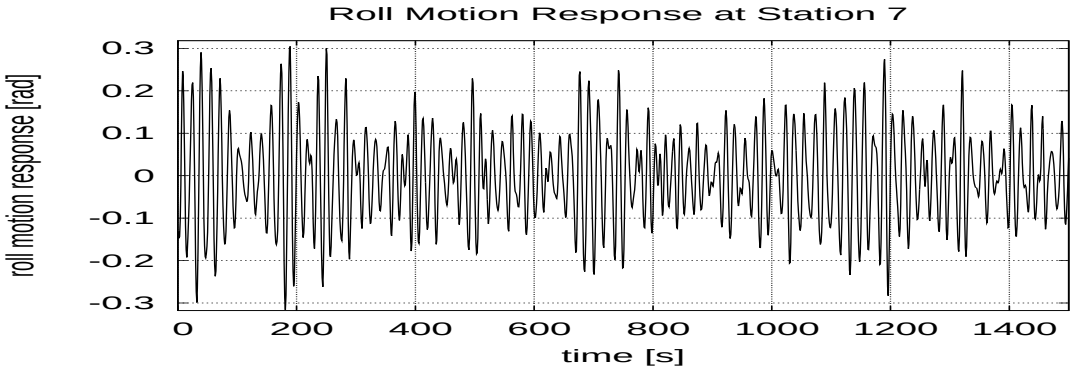

Fig. 29. Roll Motion for heading 90^o and $H_s = 4.0m$

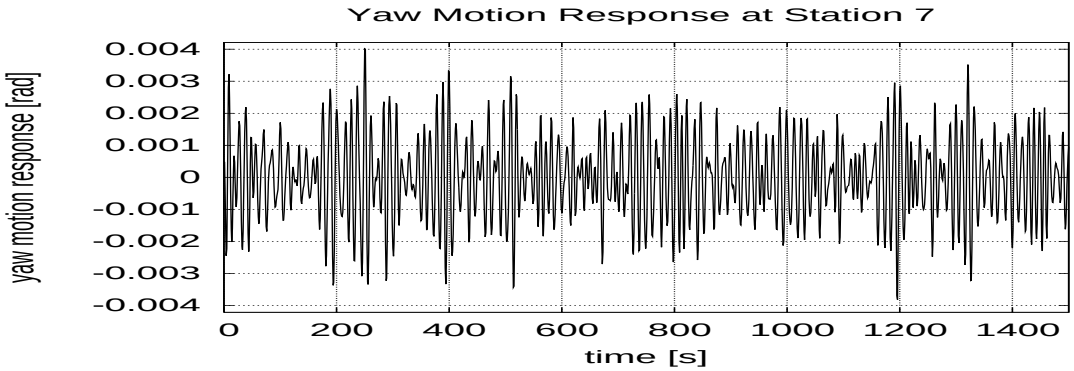

Fig. 30. Yaw Motion for heading 90^o and $H_s = 4.0m$

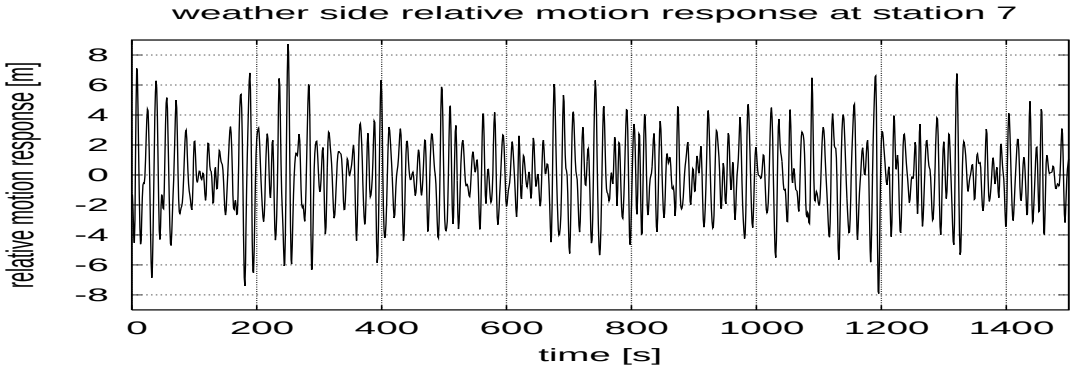

Fig. 31. Relative Motion at weather side for heading 90^o and $H_s = 4.0m$

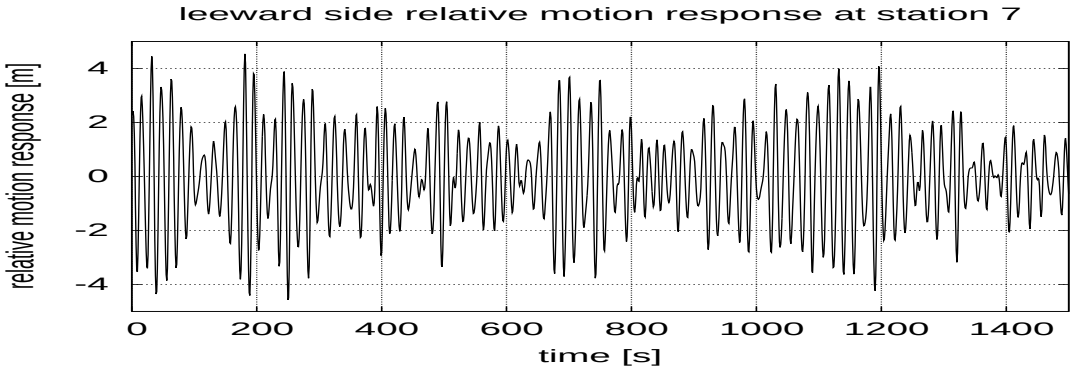

Fig. 32. Relative Motion at leeward side for heading 90^o and $H_s = 4.0m$

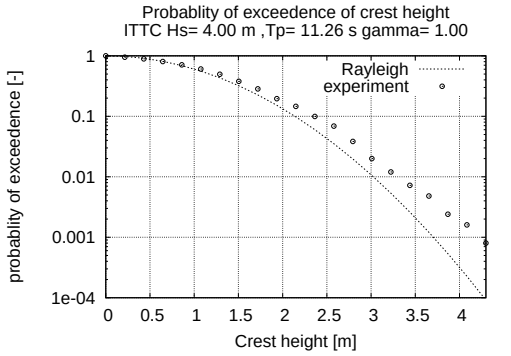

(a) input wave

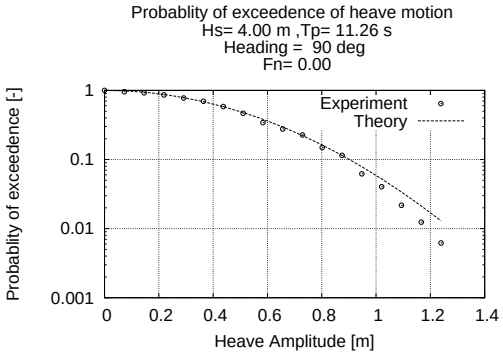

(b) heave motion

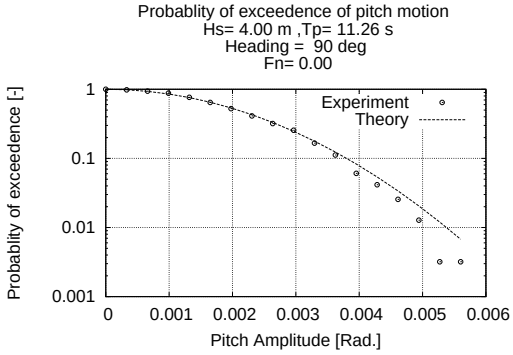

(c) pitch motion

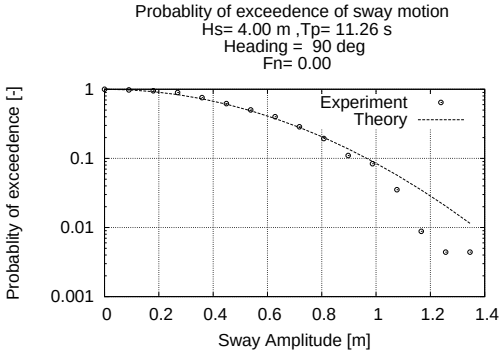

(d) sway motion

Fig. 33. Probability of exceedence for the input wave and resultant motion Hs=4.00m, Fn=0.00 and Heading = 90^o

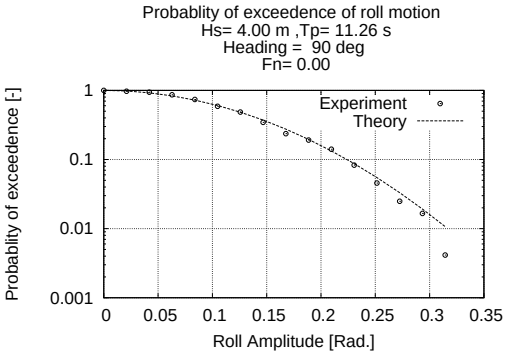

(a) roll motion

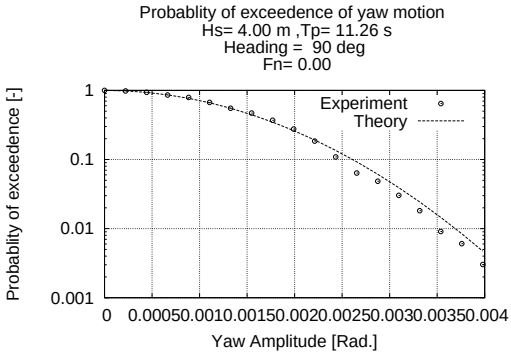

(b) yaw motion

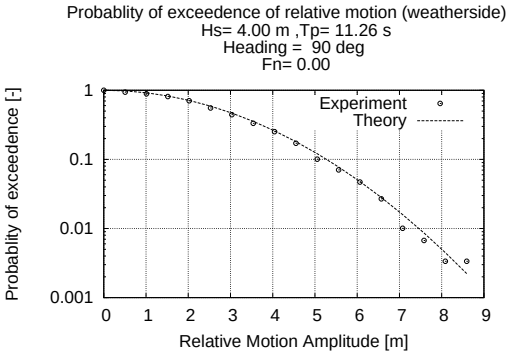

(c) vertical relative motion (weather side)

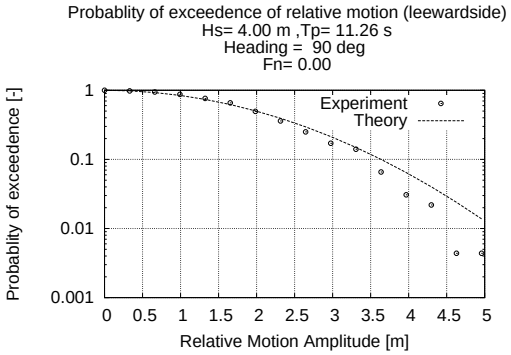

(d) vertical relative motion (leeward side)

Fig. 34. Probability of exceedence for the input wave and resultant motion Hs=4.00m, Fn=0.00 and Heading = 90^o

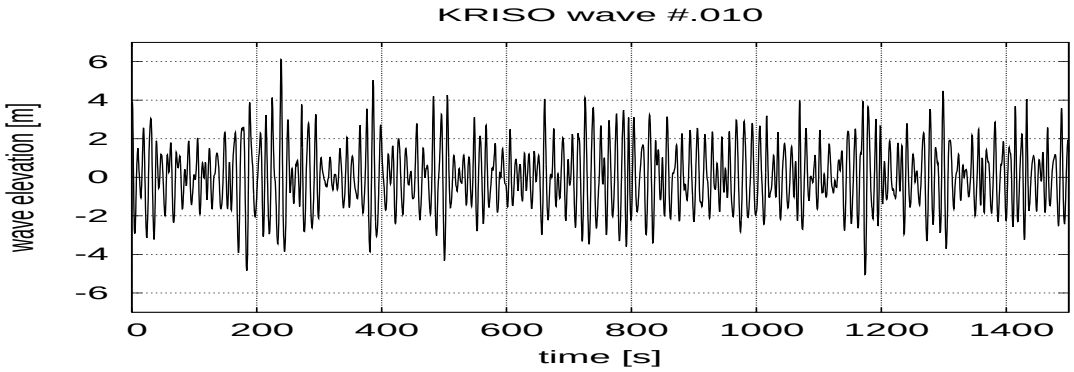

Fig. 35. Input wave $H_s = 6.0m$

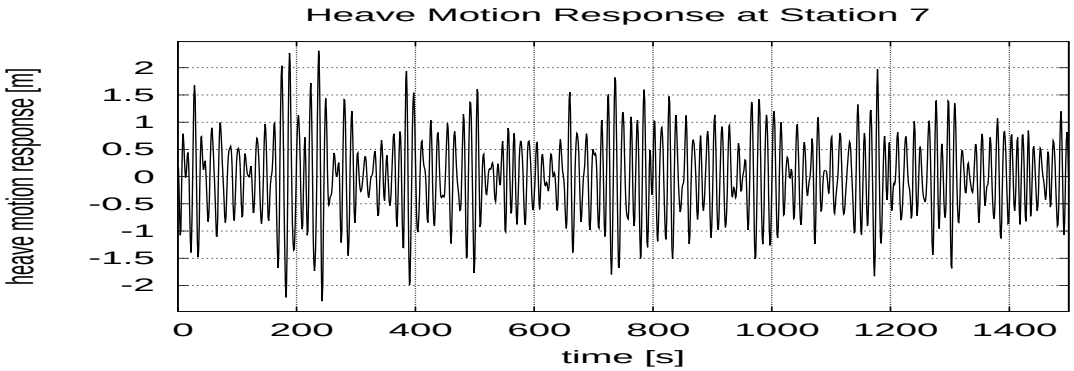

Fig. 36. Heave Motion for heading 90^o and $H_s = 6.0m$

2.3. Case 3 $H_s = 6.0m$

Figures 35 to 42 shows the input wave profile, heave, pitch, sway, roll, yaw, weather-side relative motion response and the leeward side relative motion response for KRISO wave data ID #010.The probability of exceedence of these wave are given in figures 43(a) to 44(d)

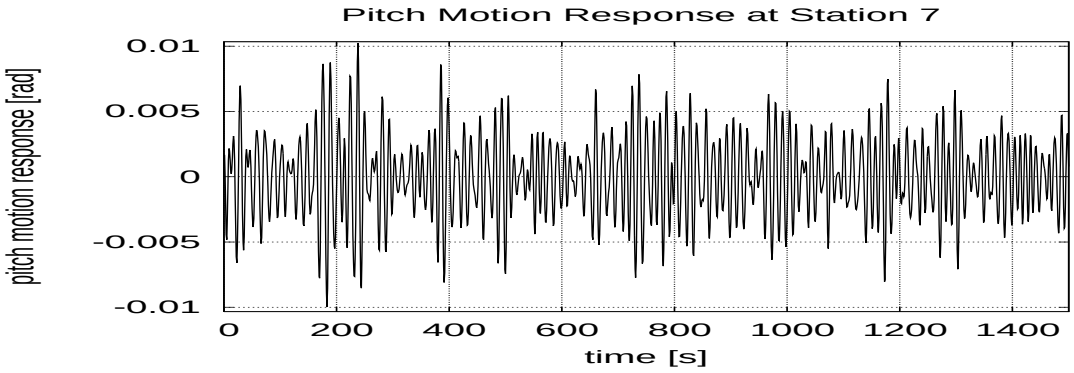

Fig. 37. Pitch Motion for heading 90^o and $H_s = 6.0m$

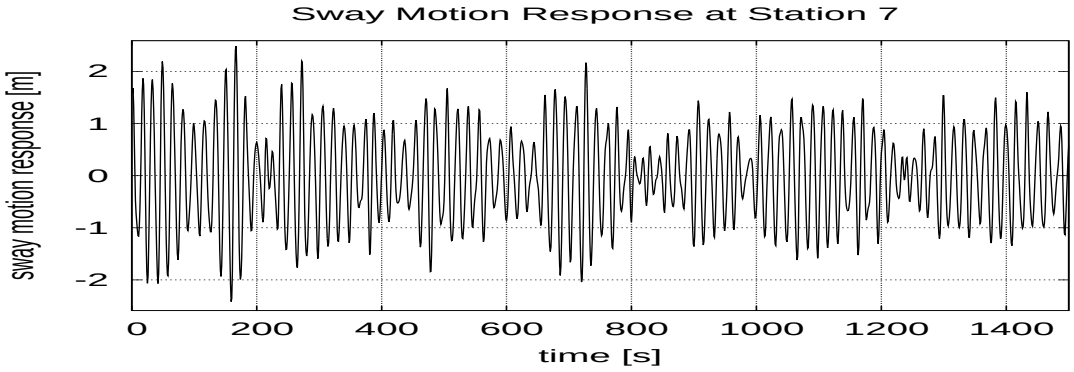

Fig. 38. Sway Motion for heading 90^o and $H_s = 6.0m$

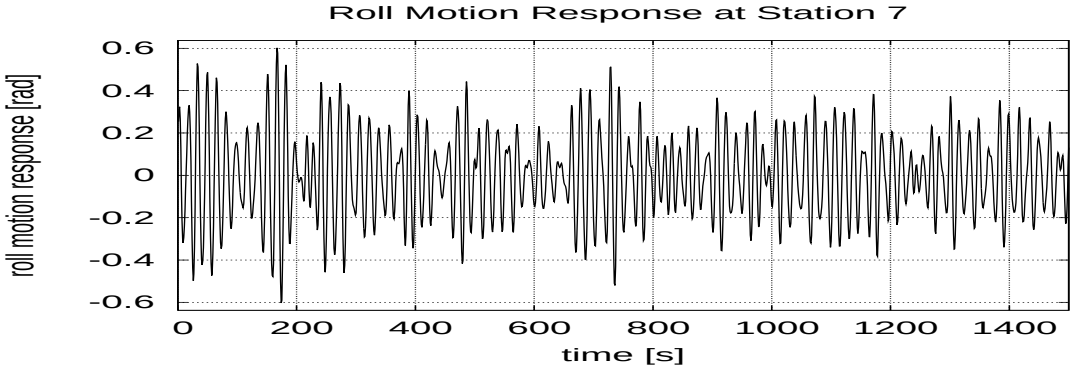

Fig. 39. Roll Motion for heading 90^o and $H_s = 6.0m$

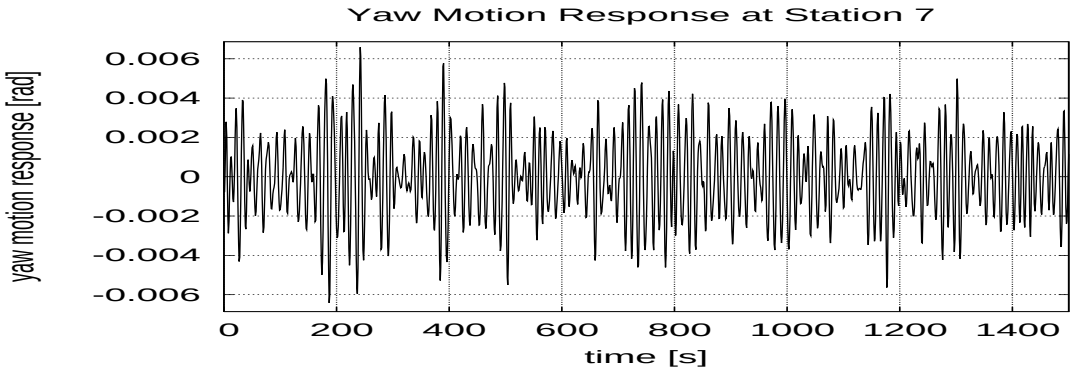

Fig. 40. Yaw Motion for heading 90^o and $H_s = 6.0m$

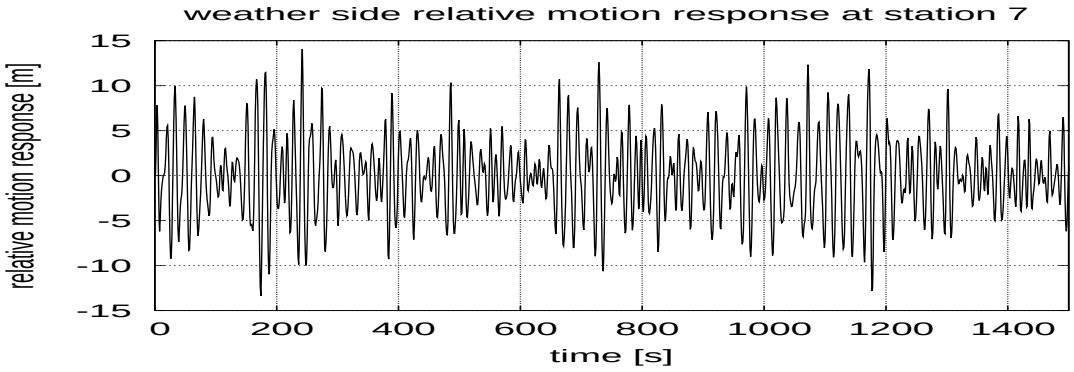

Fig. 41. Relative Motion at weather side for heading 90^o and $H_s = 6.0m$

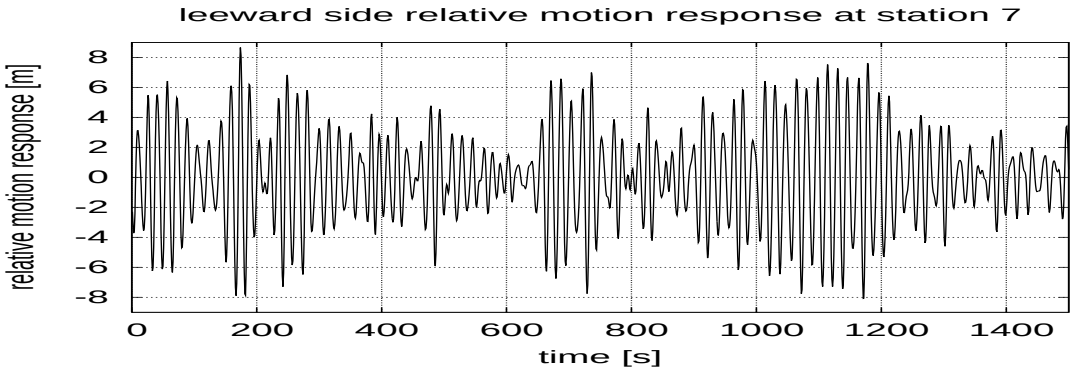

Fig. 42. Relative Motion at leeward side for heading 90^o and $H_s = 6.0m$

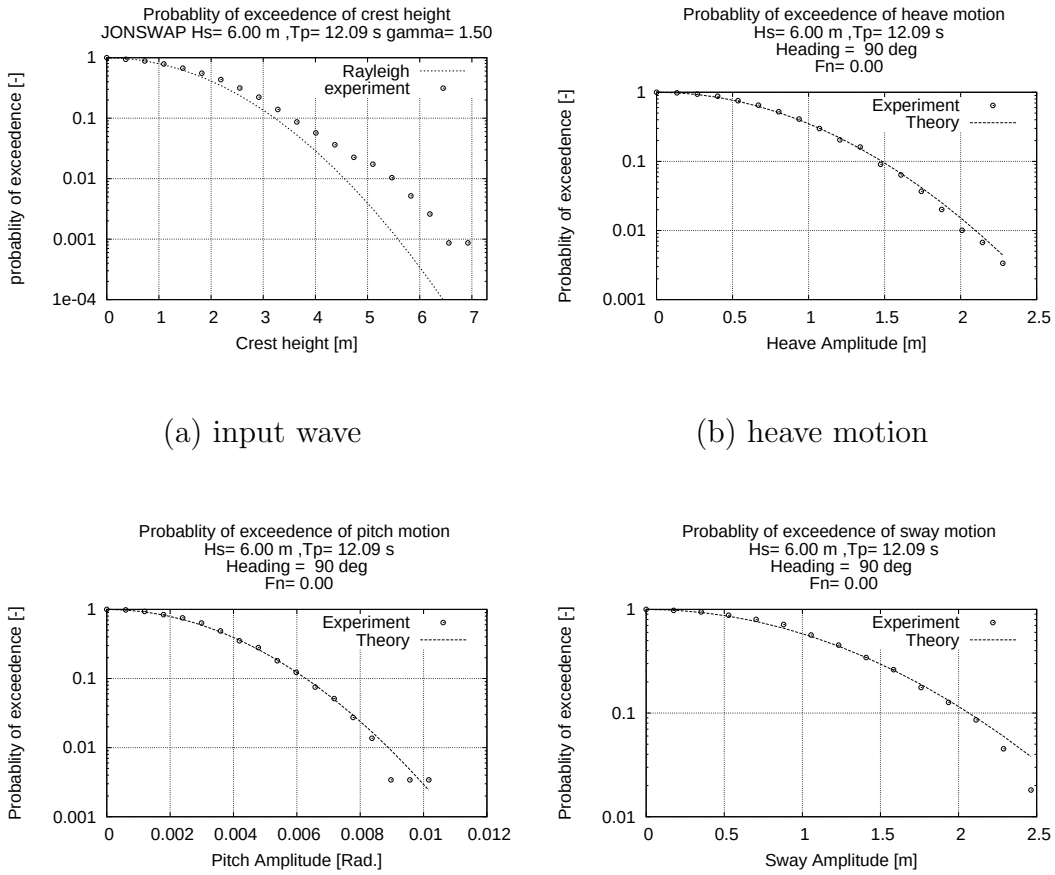

(a) input wave

(b) heave motion

(c) pitch motion

(d) sway motion

Fig. 43. Probability of exceedence for the input wave and resultant motion Hs=6.00m, Fn=0.00 and Heading = 90^o

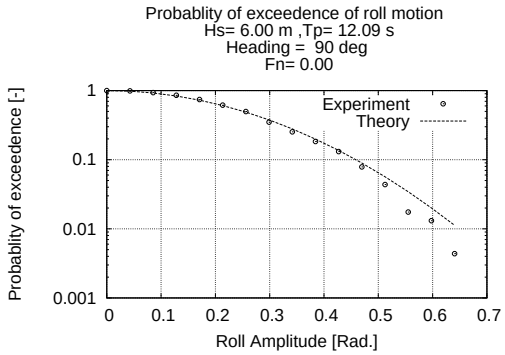

(a) roll motion

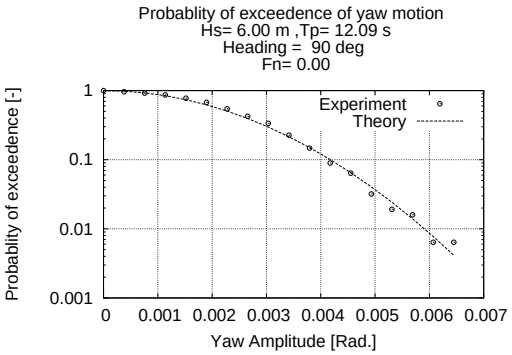

(b) yaw motion

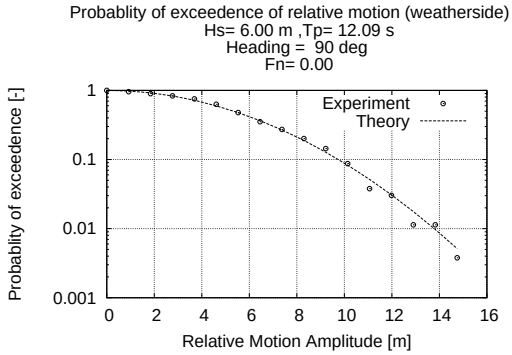

(c) vertical relative motion (weather side)

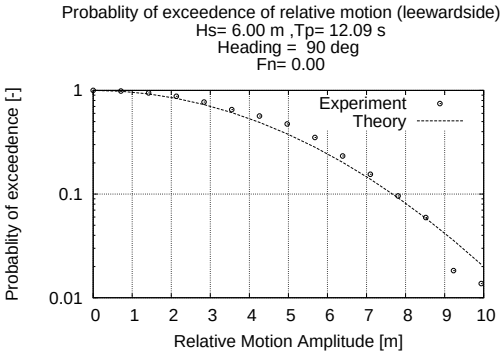

(d) vertical relative motion (leeward side)

Fig. 44. Probability of exceedence for the input wave and resultant motion Hs=6.00m, Fn=0.00 and Heading = 90^o

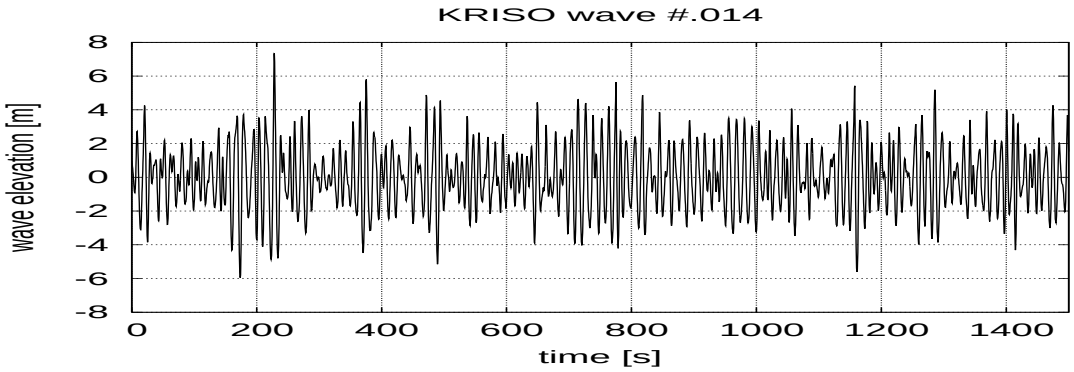

Fig. 45. Input wave $H_s = 7.0m$

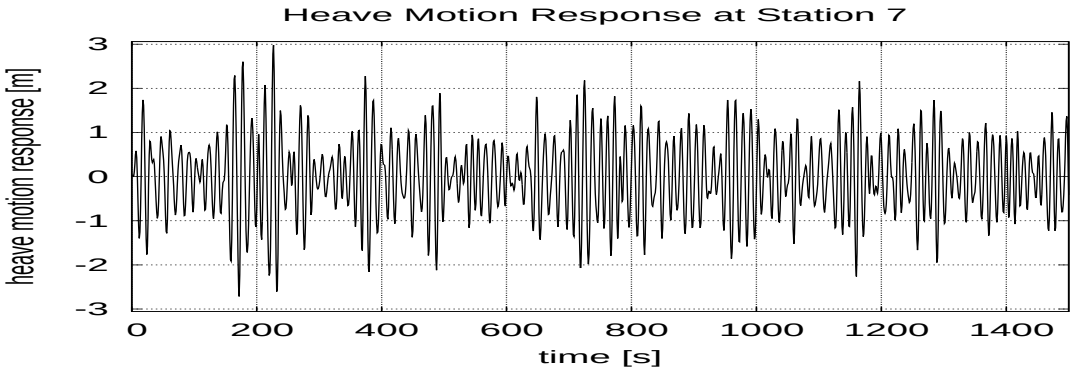

Fig. 46. Heave Motion for heading 90^o and $H_s = 7.0m$

2.4. Case 4 $H_s = 7.0m$

Figures 45 to 52 shows the input wave profile, heave, pitch, sway, roll, yaw, weather-side relative motion response and the leeward side relative motion response for KRISO wave data ID #014.The probability of exceedence of these wave are given in figures 53(a) to 54(d)

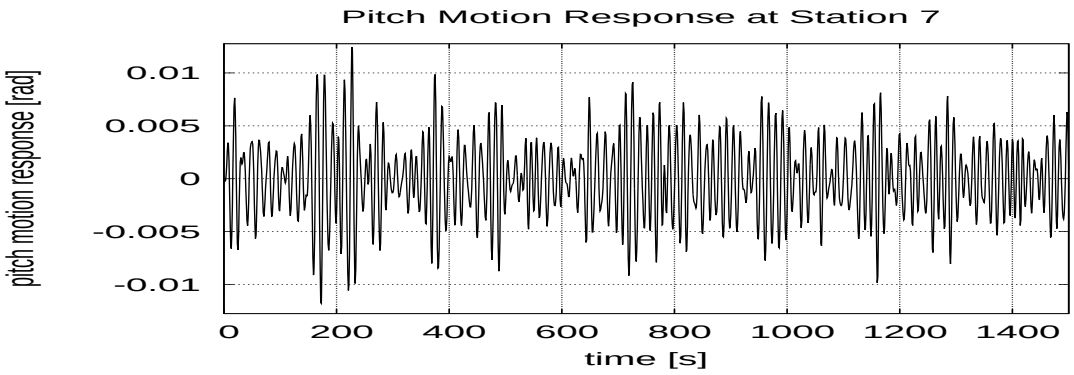

Fig. 47. Pitch Motion for heading 90^o and $H_s = 7.0m$

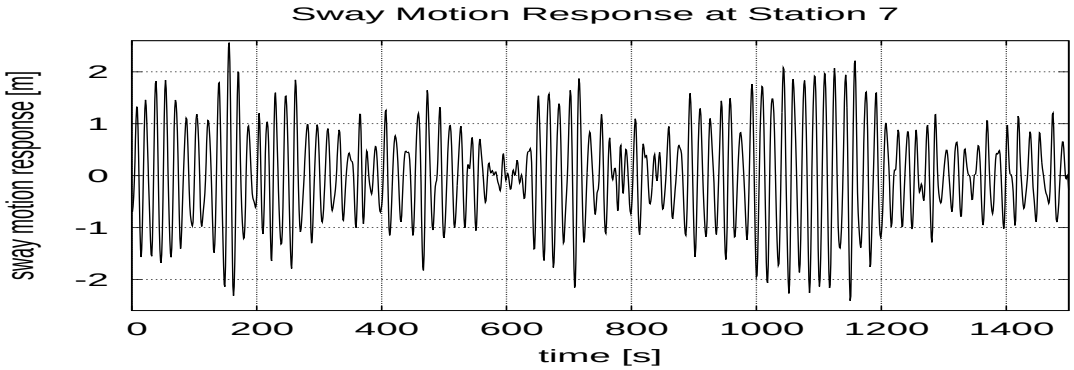

Fig. 48. Sway Motion for heading 90^o and $H_s = 7.0m$

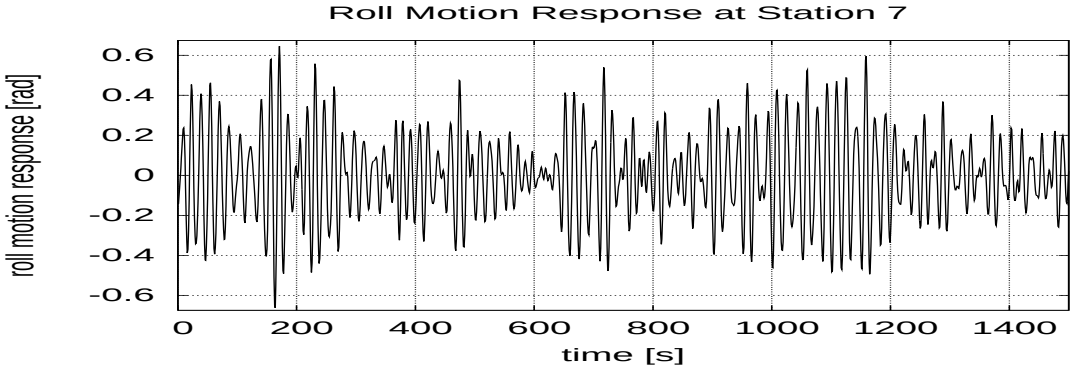

Fig. 49. Roll Motion for heading 90^o and $H_s = 7.0m$

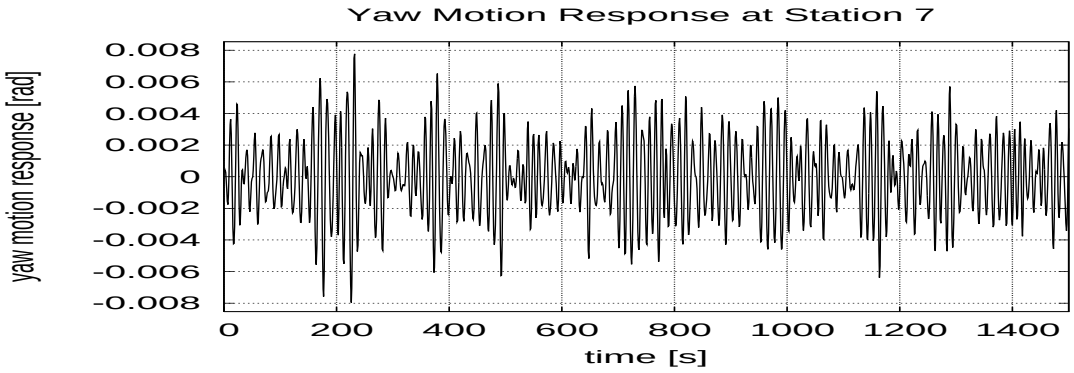

Fig. 50. Yaw Motion for heading 90^o and $H_s = 7.0m$

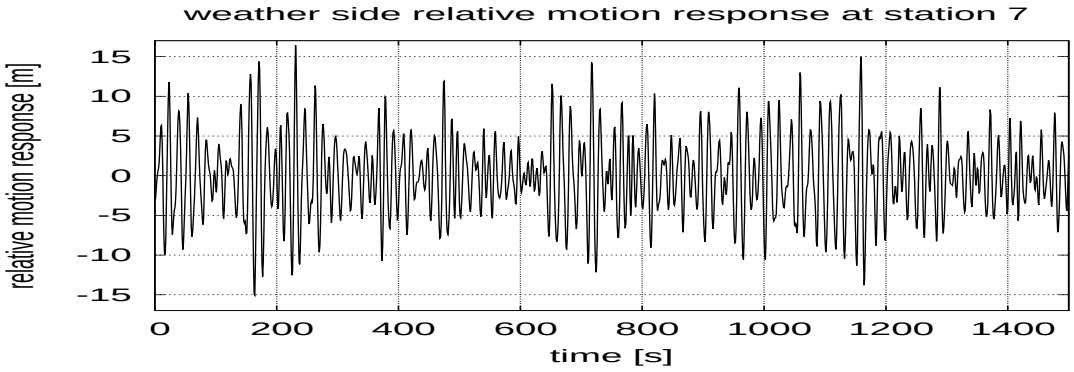

Fig. 51. Relative Motion at weather side for heading 90^o and $H_s = 7.0m$

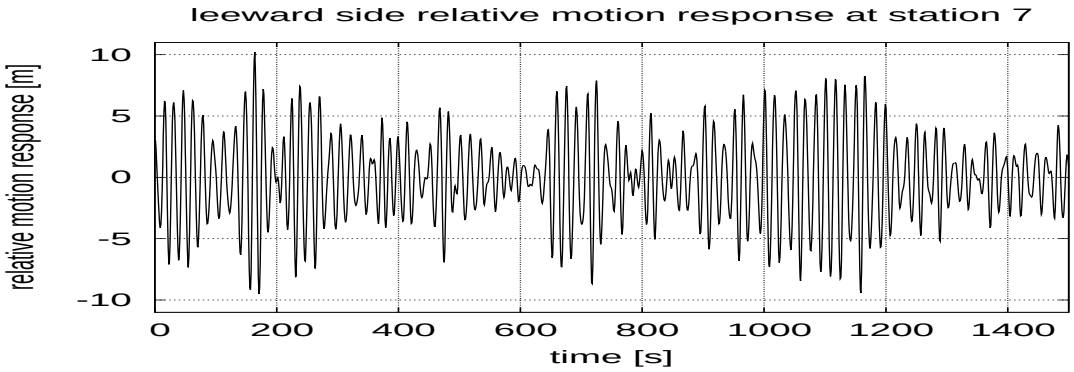

Fig. 52. Relative Motion at leeward side for heading 90^o and $H_s = 7.0m$

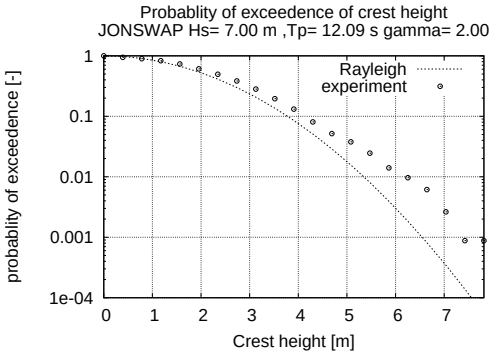

(a) input wave

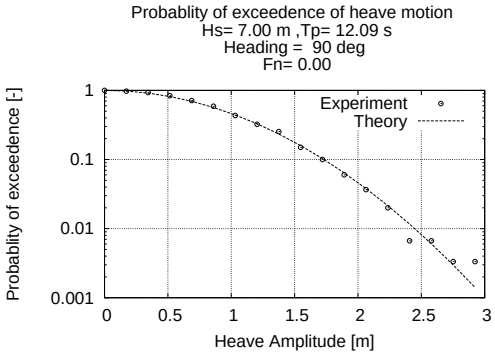

(b) heave motion

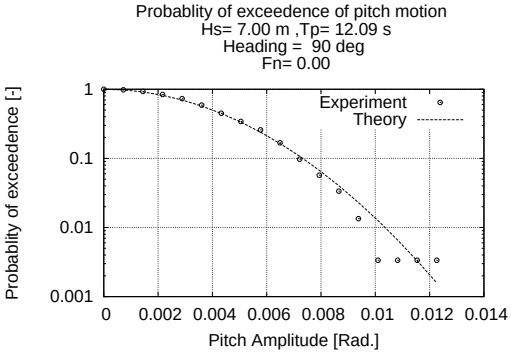

(c) pitch motion

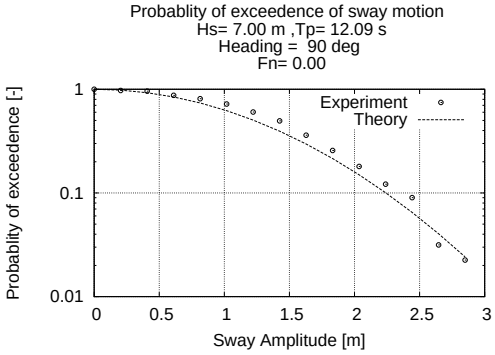

(d) sway motion

Fig. 53. Probability of exceedence for the input wave and resultant motion Hs=7.00m, Fn=0.00 and Heading = 90^o

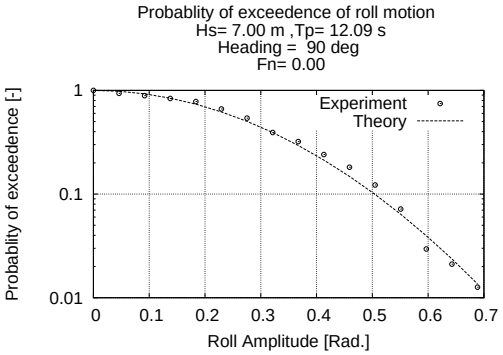

(a) roll motion

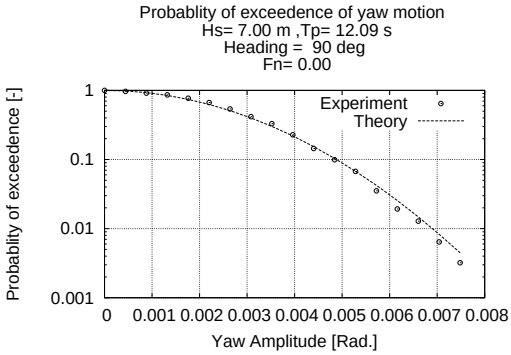

(b) yaw motion

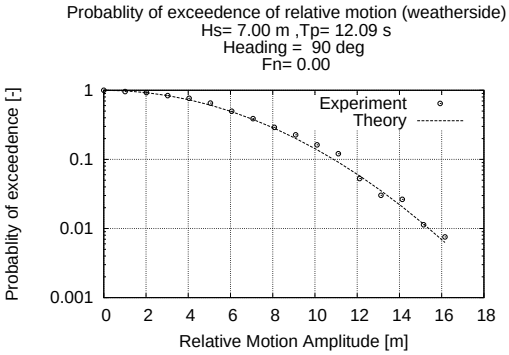

(c) vertical relative motion (weather side)

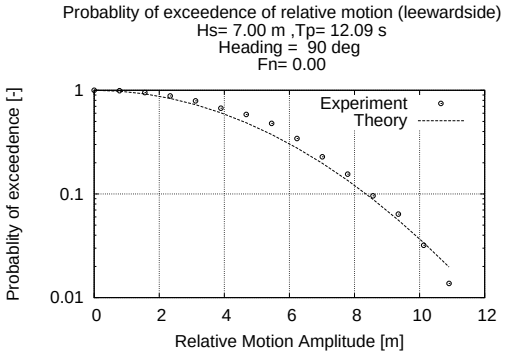

(d) vertical relative mnotion (leeward side)

Fig. 54. Probability of exceedence for the input wave and resultant motion Hs=7.00m, Fn=0.00 and Heading = 90^o

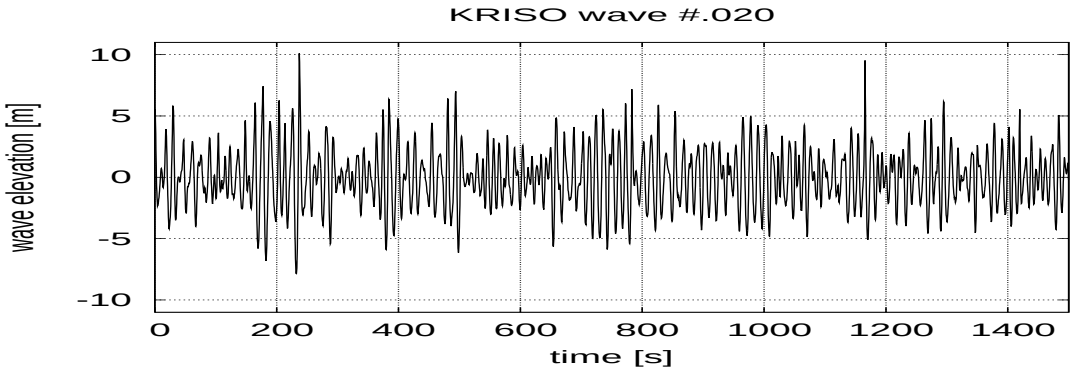

Fig. 55. Input wave $H_s = 9.0m$

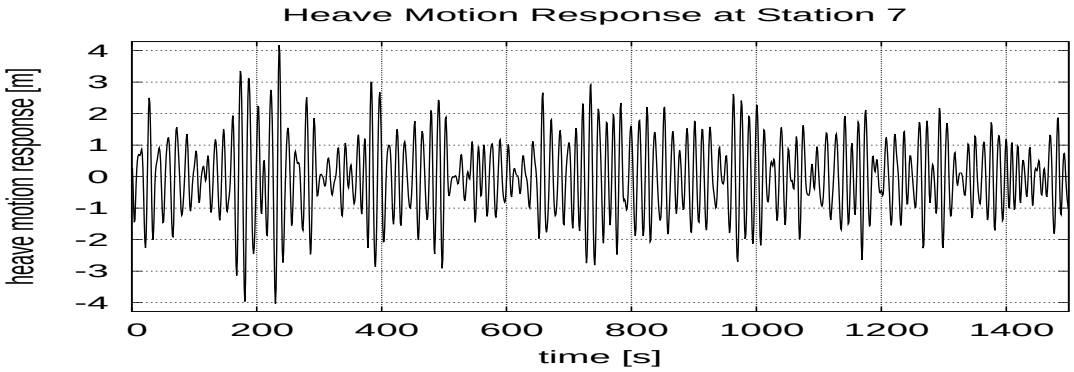

Fig. 56. Heave Motion for heading 90^o and $H_s = 9.0m$

2.5. Case 5 $H_s = 9.0m$

Figures 55 to 62 shows the input wave profile, heave, pitch, sway, roll, yaw, weather-side relative motion response and the leeward side relative motion response for KRISO wave data ID #020.The probability of exceedence of these wave are given in figures 63(a) to 64(d)

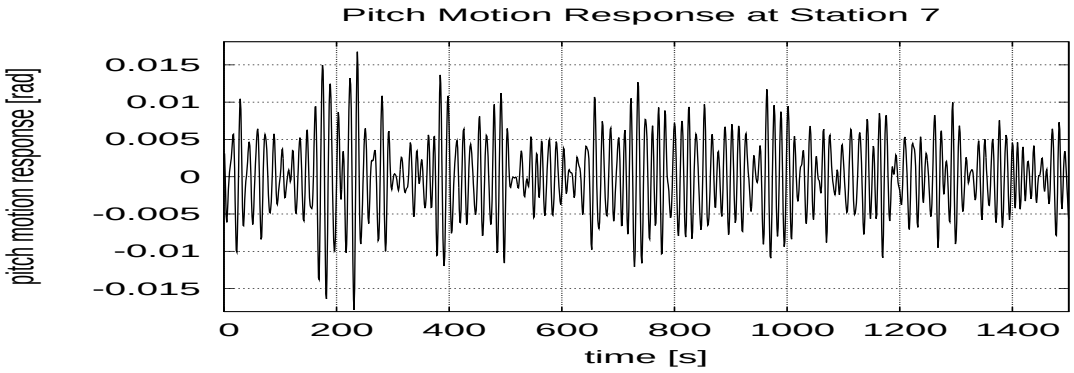

Fig. 57. Pitch Motion for heading 90^o and $H_s = 9.0m$

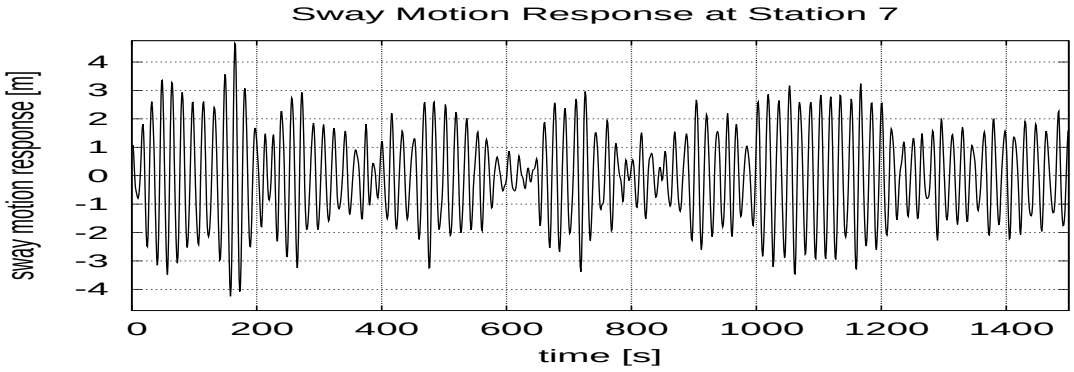

Fig. 58. Sway Motion for heading 90^o and $H_s = 9.0m$

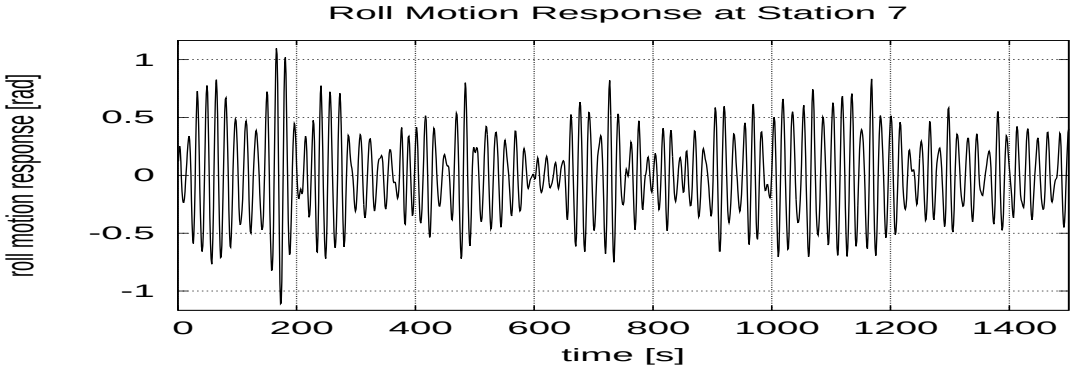

Fig. 59. Roll Motion for heading 90^o and $H_s = 9.0m$

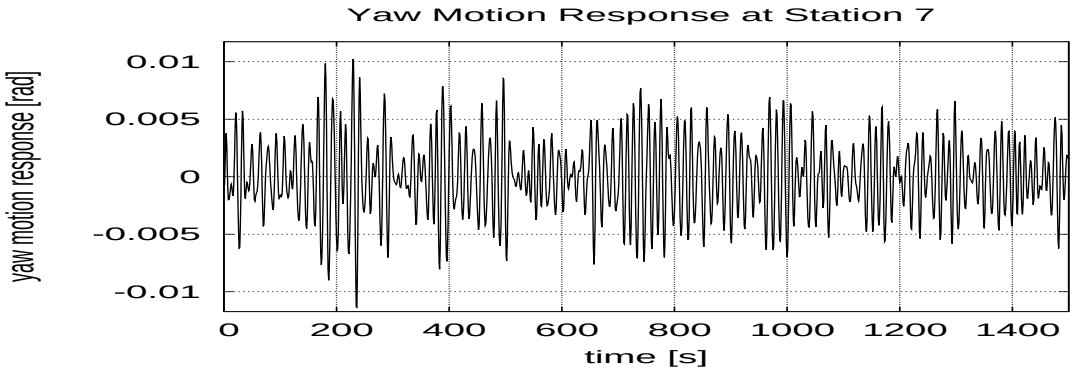

Fig. 60. Yaw Motion for heading 90^o and $H_s = 9.0m$

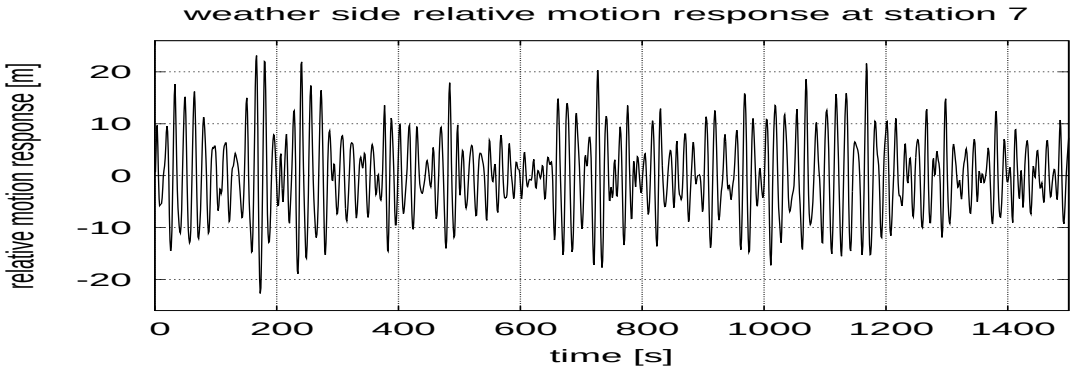

Fig. 61. Relative Motion at weather side for heading 90^o and $H_s = 9.0m$

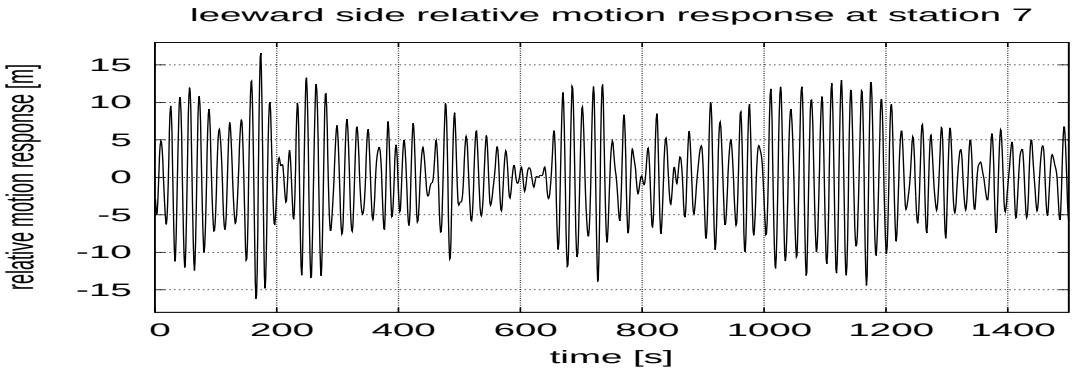

Fig. 62. Relative Motion at leeward side for heading 90^o and $H_s = 9.0m$

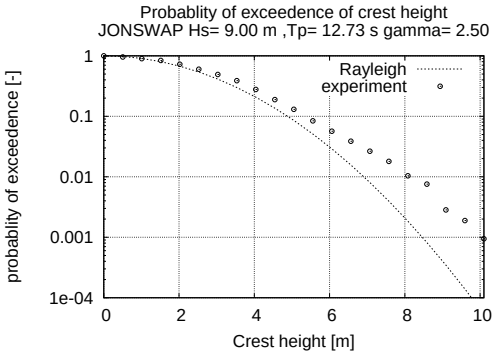

(a) input wave

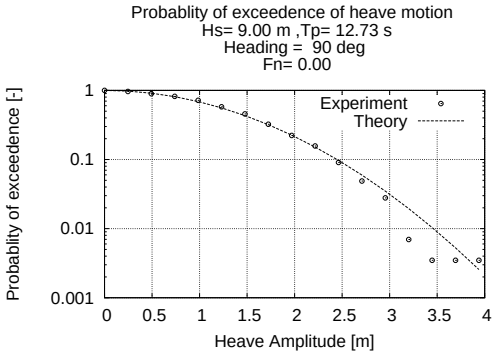

(b) heave motion

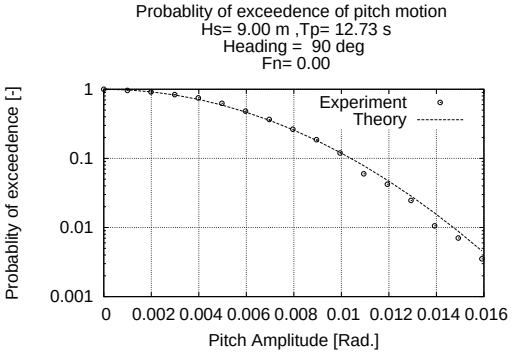

(c) pitch motion

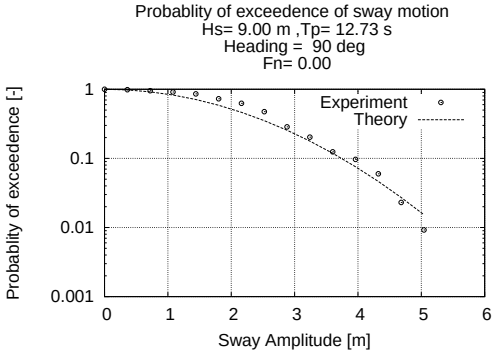

(d) sway motion

Fig. 63. Probability of exceedence for the input wave and resultant motion Hs=9.00m, Fn=0.00 and Heading = 90^o

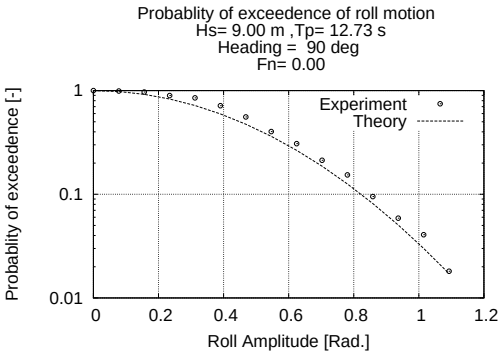

(a) roll motion

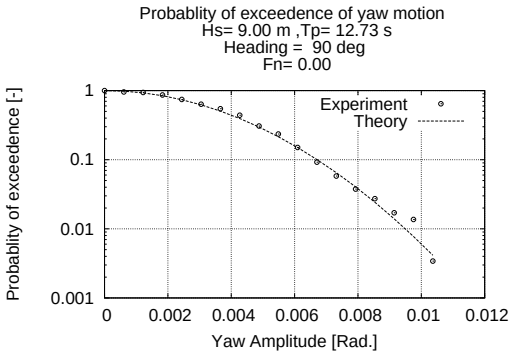

(b) yaw motion

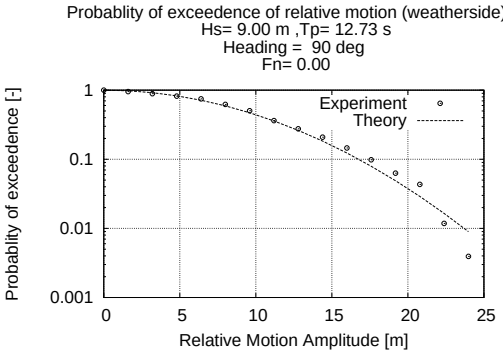

(c) vertical relative motion (weather side)

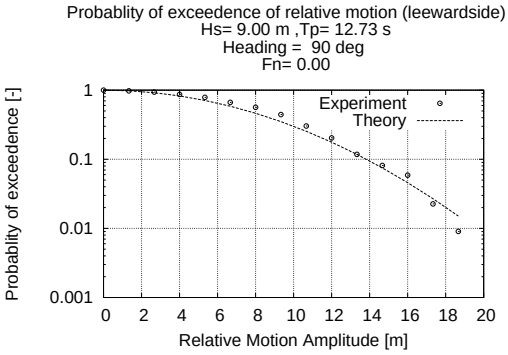

(d) vertical relative motion (leeward side)

Fig. 64. Probability of exceedence for the input wave and resultant motion Hs=9.00m, Fn=0.00 and Heading = 90^o

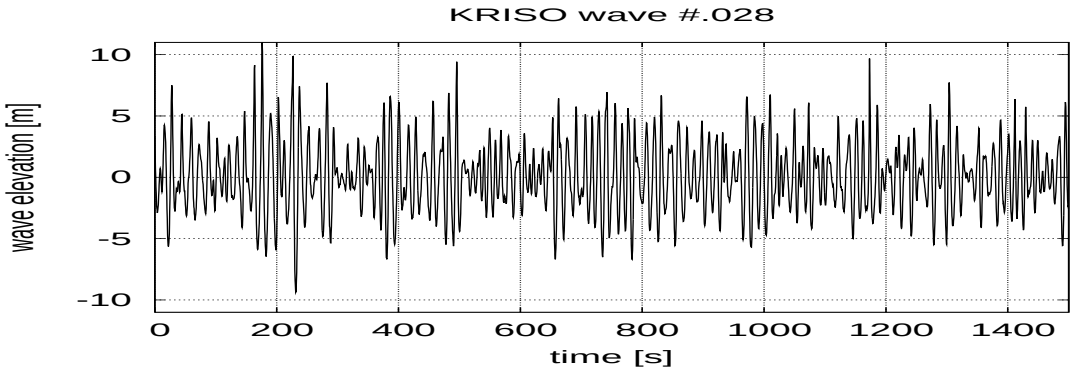

Fig. 65. Input wave $H_s = 11.0m$

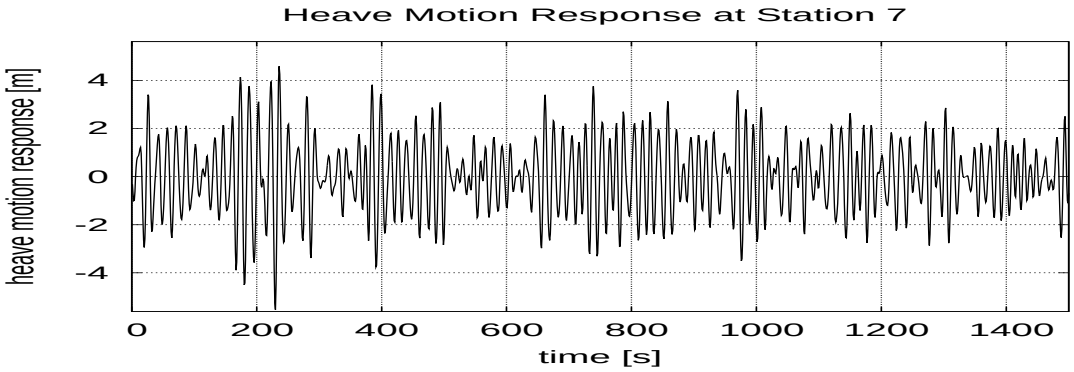

Fig. 66. Heave Motion for heading 90^o and $H_s = 11.0m$

2.6. Case 6 $H_s = 11.0m$

Figures 65 to 72 shows the input wave profile, heave, pitch, sway, roll, yaw, weather-side relative motion response and the leeward side relative motion response for KRISO wave data ID #028.The probability of exceedence of these wave are given in figures 73(a) to 74(d)

3. Most Probable Peak Value

The most probable peak values for the different sea states, for each sea condition is shown in figure 75(a) to 3.

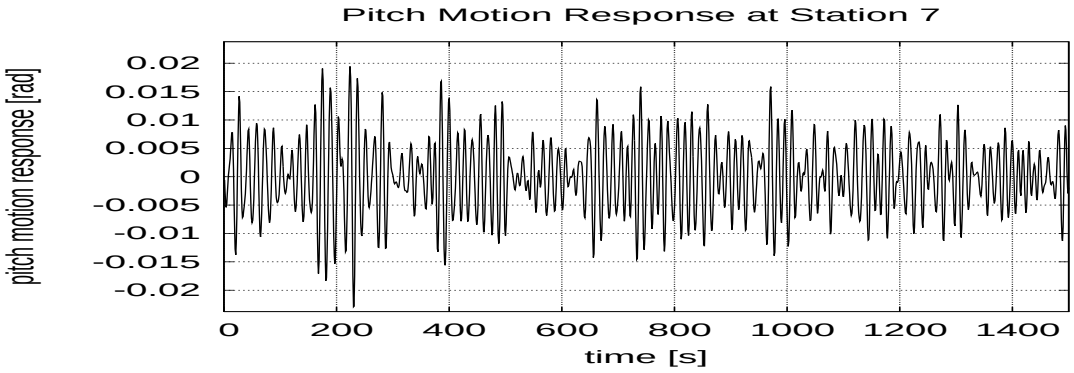

Fig. 67. Pitch Motion for heading 90^o and $H_s = 11.0m$

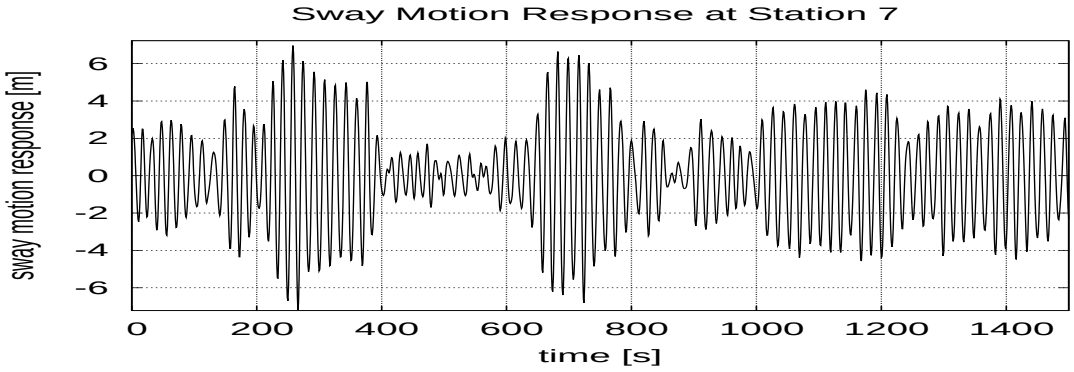

Fig. 68. Sway Motion for heading 90^o and $H_s = 11.0m$

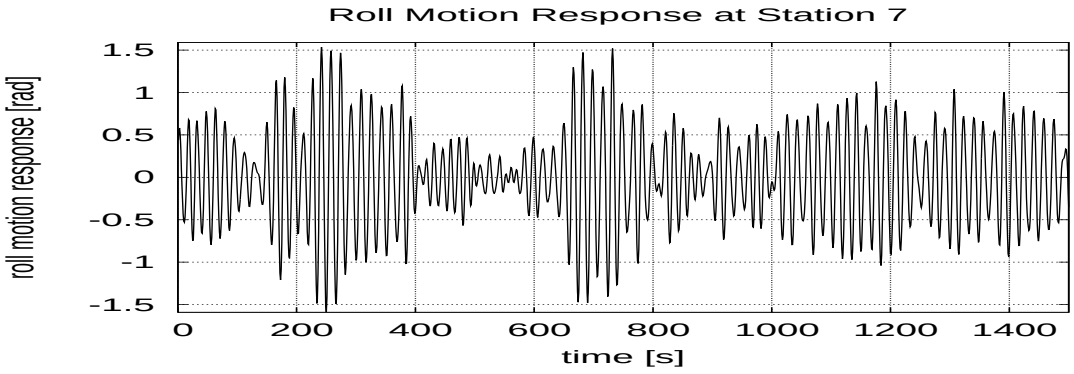

Fig. 69. Roll Motion for heading 90^o and $H_s = 11.0m$

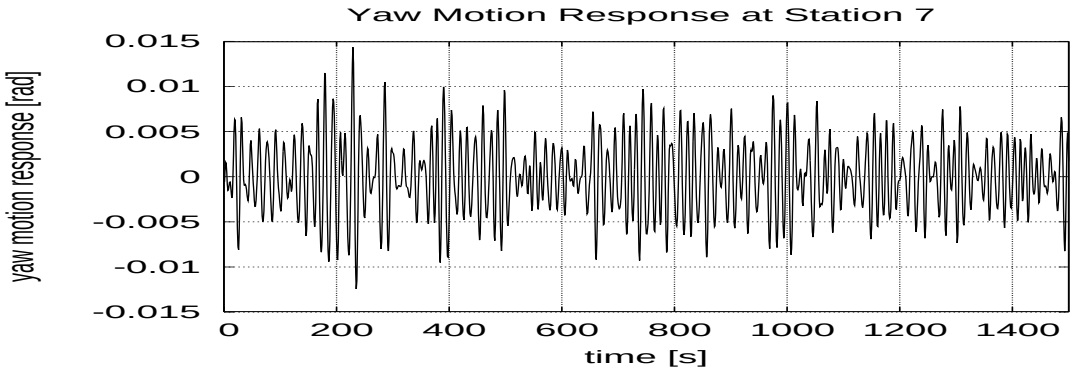

Fig. 70. Yaw Motion for heading 90^o and $H_s = 11.0m$

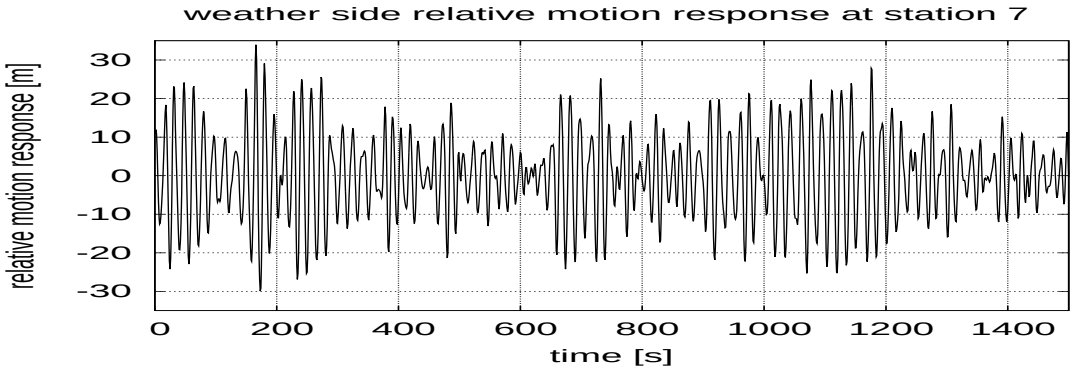

Fig. 71. Relative Motion at weather side for heading 90^o and $H_s = 9.0m$

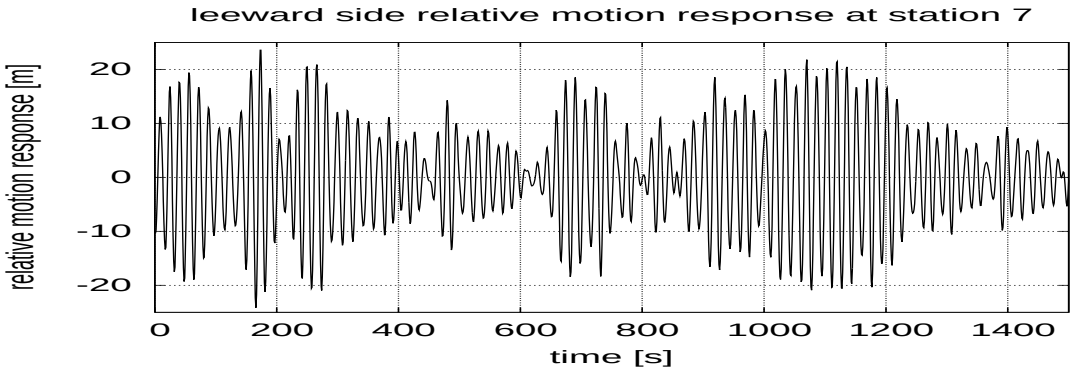

Fig. 72. Relative Motion at leeward side for heading 90^o and $H_s = 9.0m$

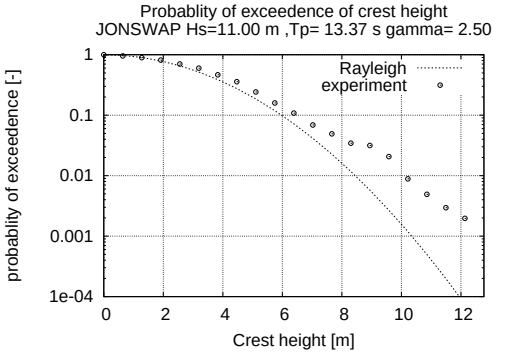

(a) input wave

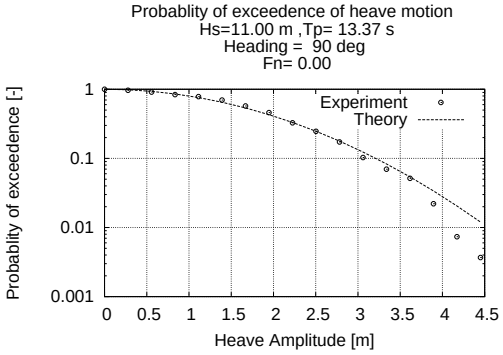

(b) heave

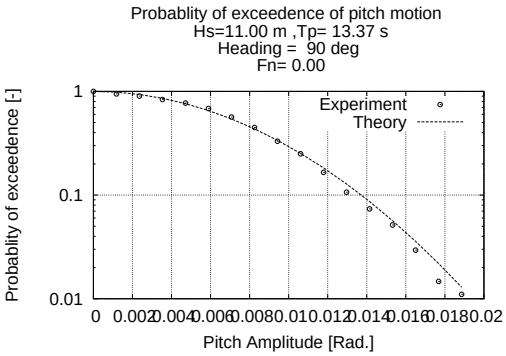

(c) pitch

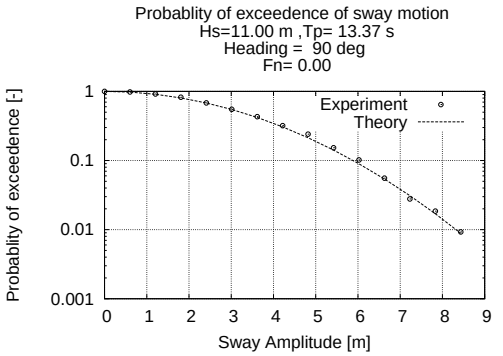

(d) sway

Fig. 73. Probability of exceedence for the input wave and resultant motion Hs=11.00m, Fn=0.00 and Heading = 90^o

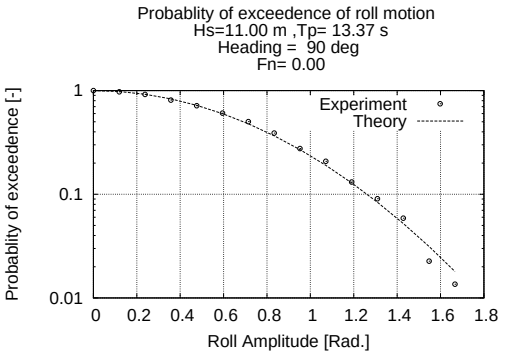

(a) roll

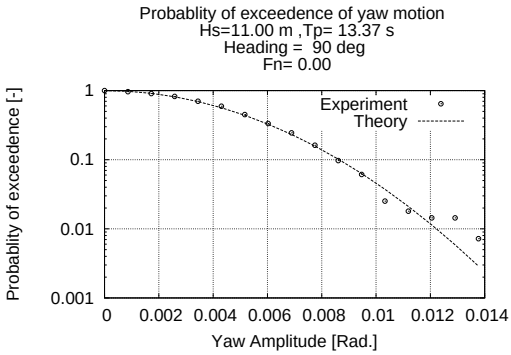

(b) yaw

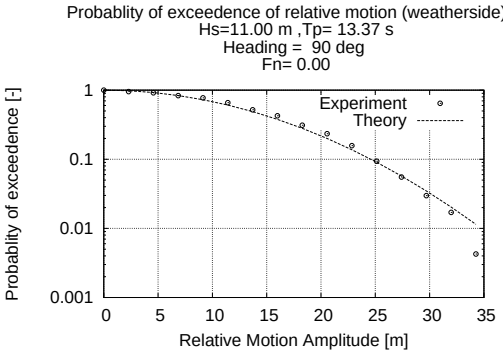

(c) vertical relative motion (weather side)

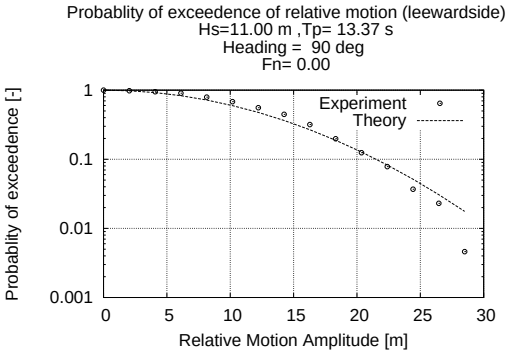

(d) vertical relative motion (leeward)

Fig. 74. Probability of exceedence for the input wave and resultant motion Hs=11.00m, Fn=0.00 and Heading = 90^o

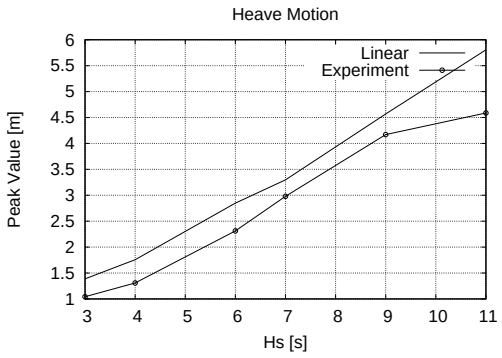

(a) heave

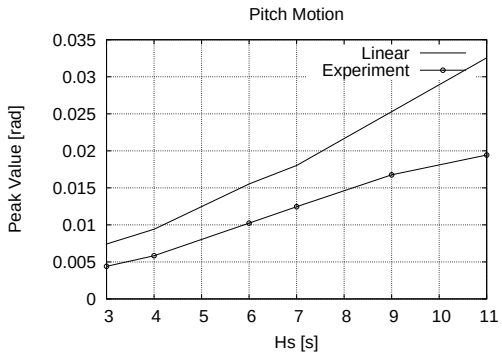

(b) pitch

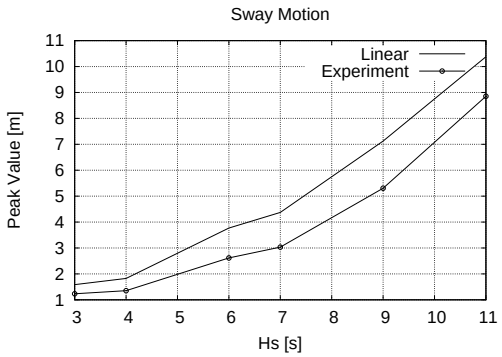

(c) sway

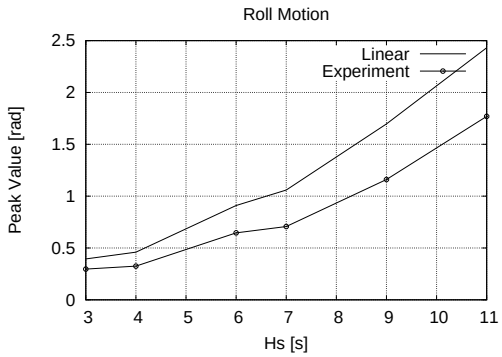

(d) roll

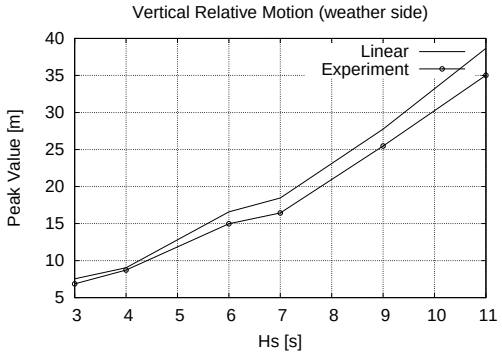

(e) weather side

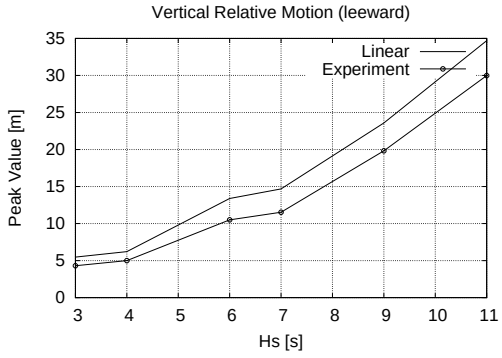

(f) leeward side

Fig. 75. Peak value comparison for heave, pitch,sway,roll and vertical relative motions (weather side and leeward side) for Fn=0.00 and Heading = 90^o

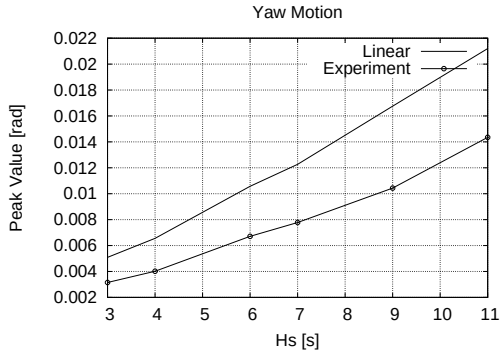

Fig. 76. Peak value comparison for yaw motion, Fn=0.00 and Heading = 90^o

4. Inference of Results

The figures 75(a) to 3, shows that the linear method overestimates the peak values, the margin of over prediction increases with the sea state.

CHAPTER V

ANALYSIS RESULTS FOR HEADING = 135^O AND $F_N = 0.15$

The motions of the container ship SL 7 for $Fn = 0.15$ and headings of 135^o are calculated using the linear approach and using UNIOM.

1. Simulation Results

In this section, the results from using the linear theory and UNIOM are compared. The simulation using UNIOM is carried out for 3600 seconds, but for the plots to be readable, only 1500 seconds of data is shown. The time steps used for the simulations is 1 second. The peak values are found corresponding to a time duration of 3600 seconds.

2. Probability of Exceedence

The probability of exceedence for the wave as well as the response motions are calculated. The following pages show the input wave and the responses.

2.1. Case 1 $H_s = 3.0m$

Figures 77 to 84 shows the input wave profile, heave, pitch, sway, roll, yaw, weather-side relative motion response and the leeward side relative motion response for KRISO wave data ID #043. The probability of exceedence of these wave are given in figures 85(a) to 86(d)

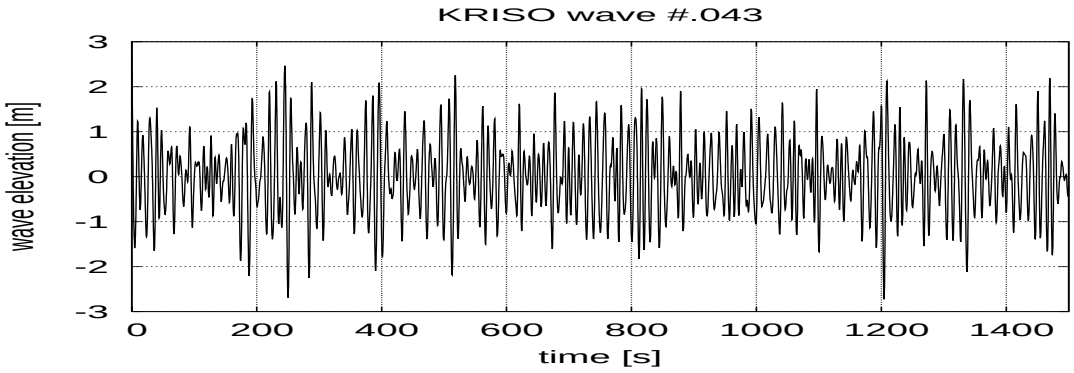

Fig. 77. Input wave $H_s = 3.0m$

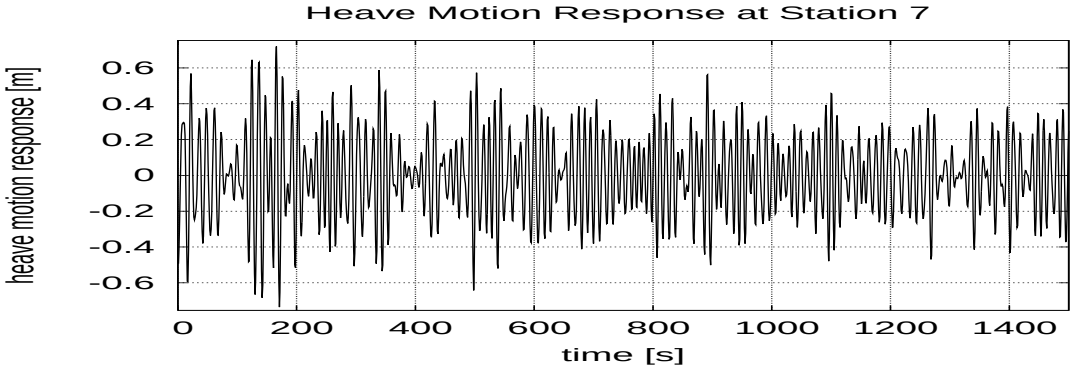

Fig. 78. Heave Motion for heading 135^o and $H_s = 3.0m$

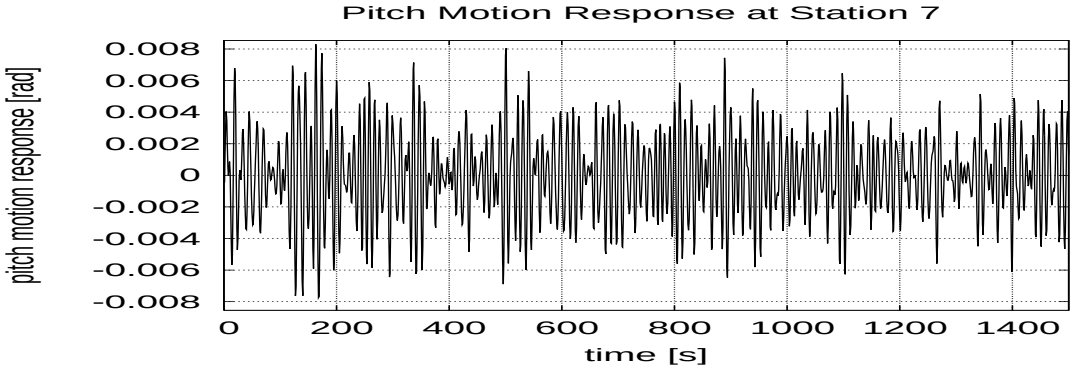

Fig. 79. Pitch Motion for heading 135^o and $H_s = 3.0m$

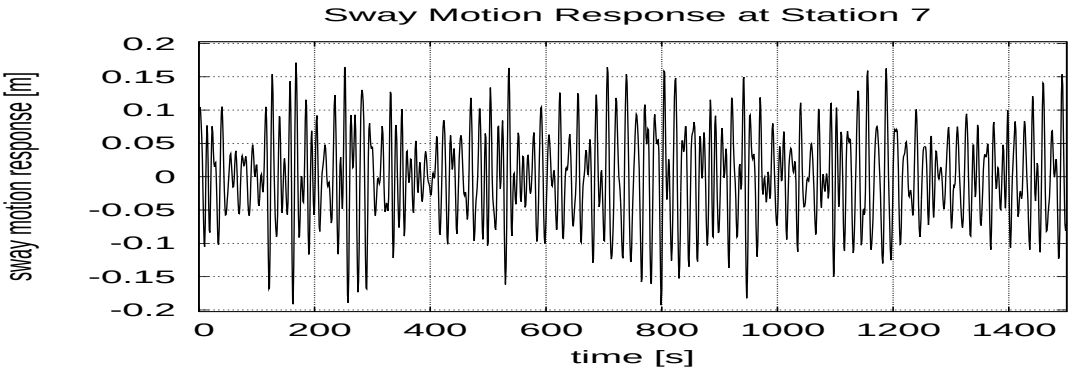

Fig. 80. Sway Motion for heading 135^o and $H_s = 3.0m$

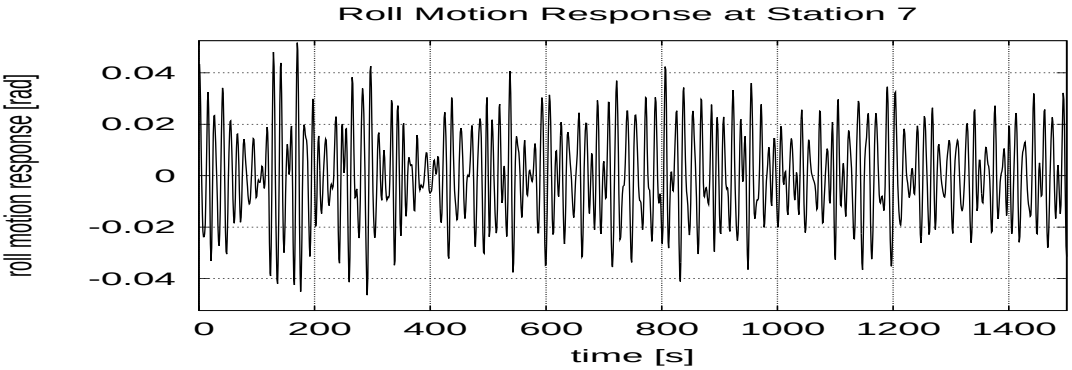

Fig. 81. Roll Motion for heading 135^o and $H_s = 3.0m$

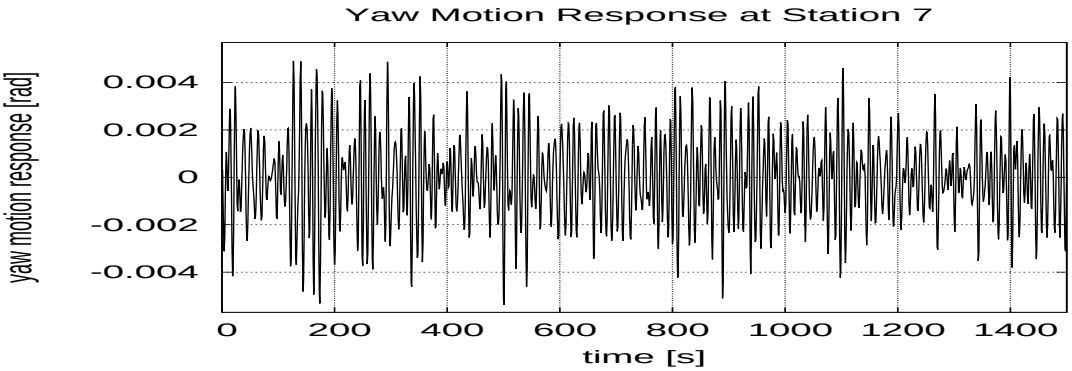

Fig. 82. Yaw Motion for heading 135^o and $H_s = 3.0m$

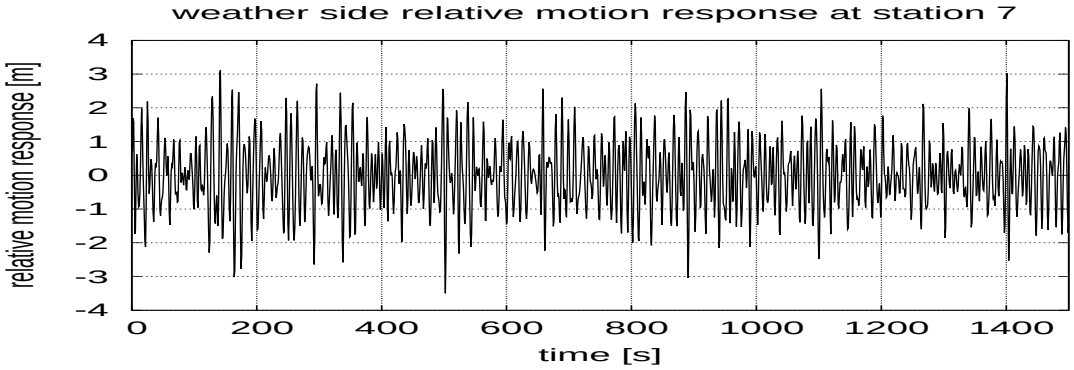

Fig. 83. Relative Motion at weather side for heading 135^o and $H_s = 3.0m$

2.2. Case 2 $H_s = 4.0m$

Figures 87 to 94 shows the input wave profile, heave, pitch, sway, roll, yaw,weatherside relative motion response and the leeward side relative motion response for KRISO wave data ID #042.The probability of exceedence of these wave are given in figures 95(a) to 96(d)

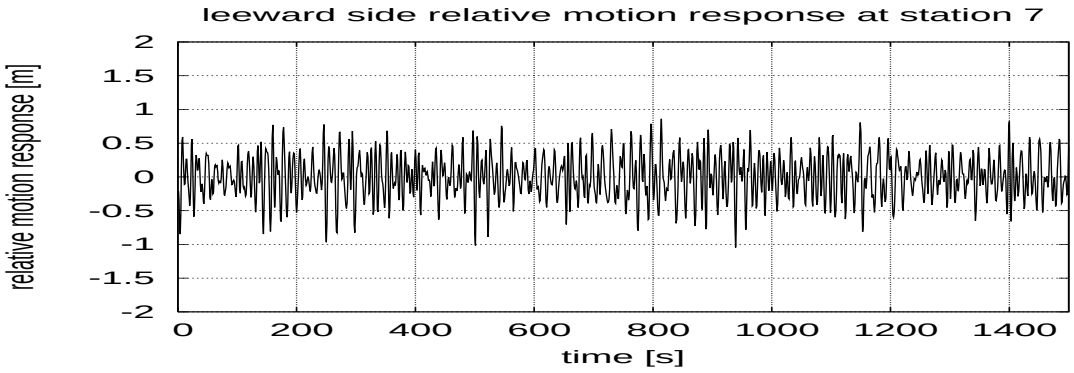

Fig. 84. Relative Motion at leeward side for heading 135^o and $H_s = 3.0m$

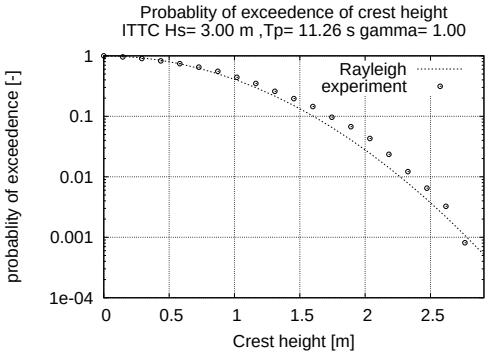

(a) Input wave

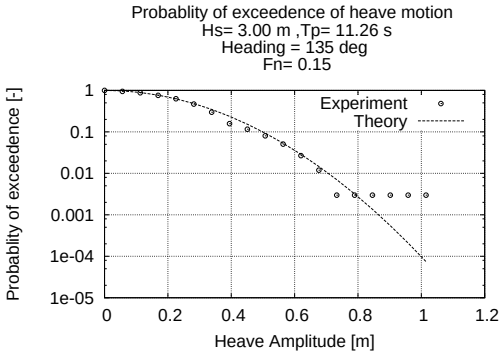

(b) Heave motion

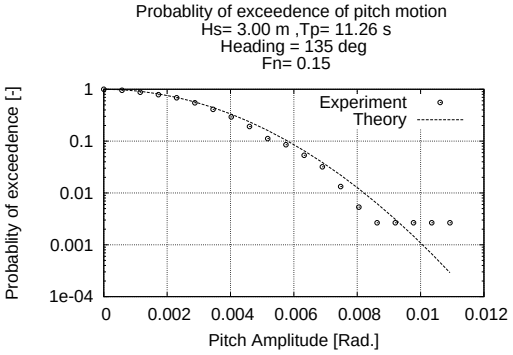

(c) Pitch motion

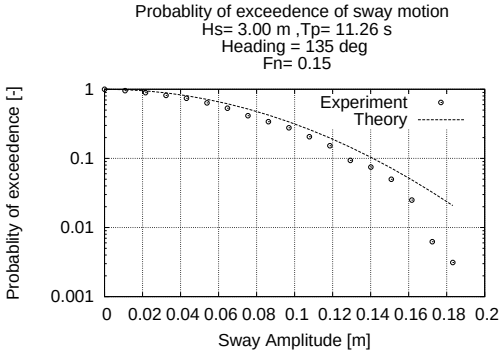

(d) Sway motion

Fig. 85. Probability of exceedence for the input wave and resultant motion Hs=3.00m, Fn=0.15 and Heading = 135^o

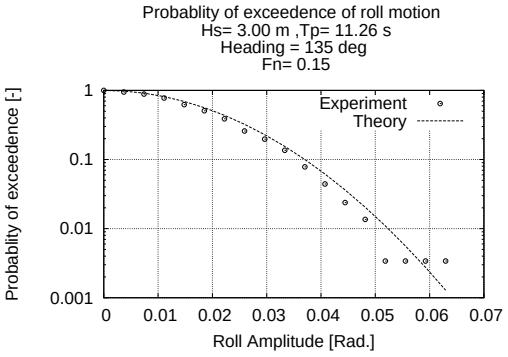

(a) Roll motion

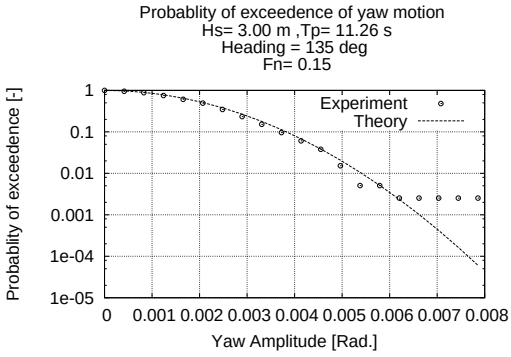

(b) Yaw motion

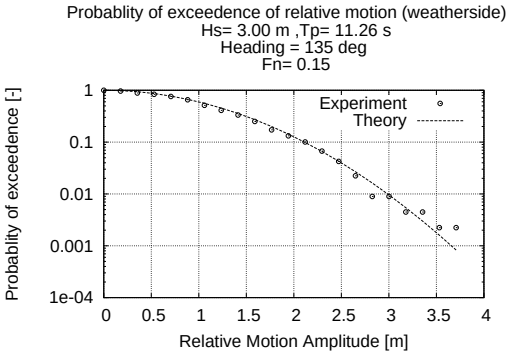

(c) vertical relative motion (weather side)

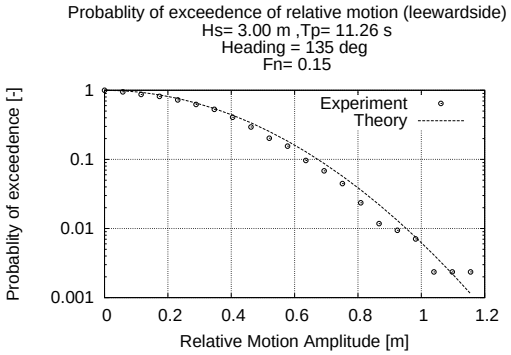

(d) vertical relative motion (leeward side)

Fig. 86. Probability of exceedence for the input wave and resultant motion Hs=3.00m, Fn=0.15 and Heading = 135^o

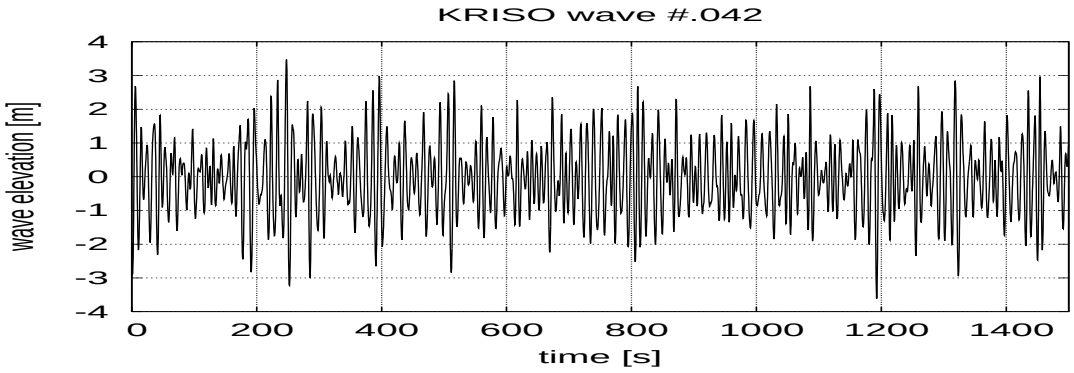

Fig. 87. Input wave $H_s = 4.0m$

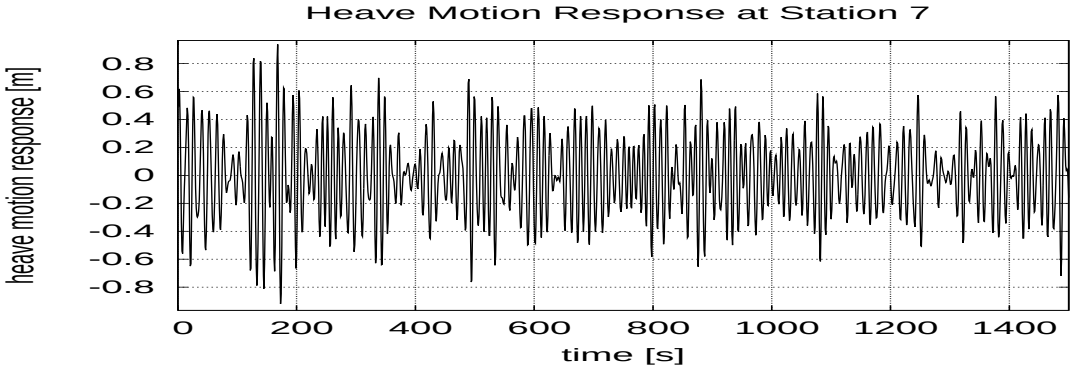

Fig. 88. Heave Motion for heading 135^o and $H_s = 4.0m$

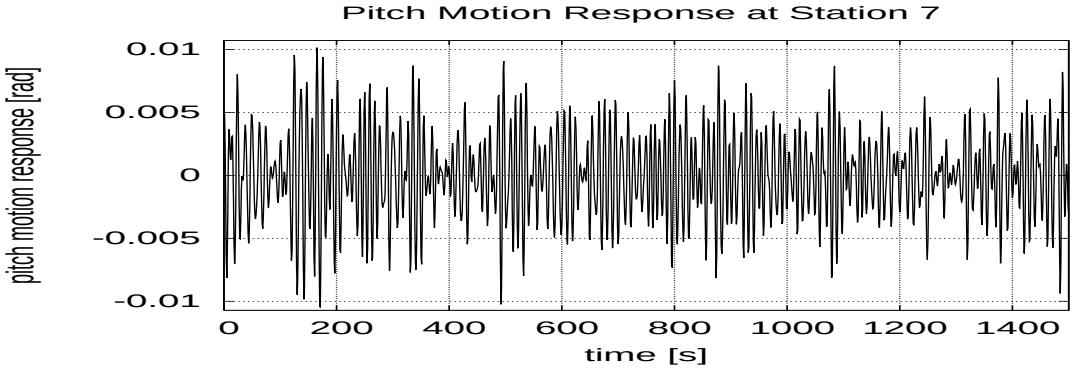

Fig. 89. Pitch Motion for heading 135^o and $H_s = 4.0m$

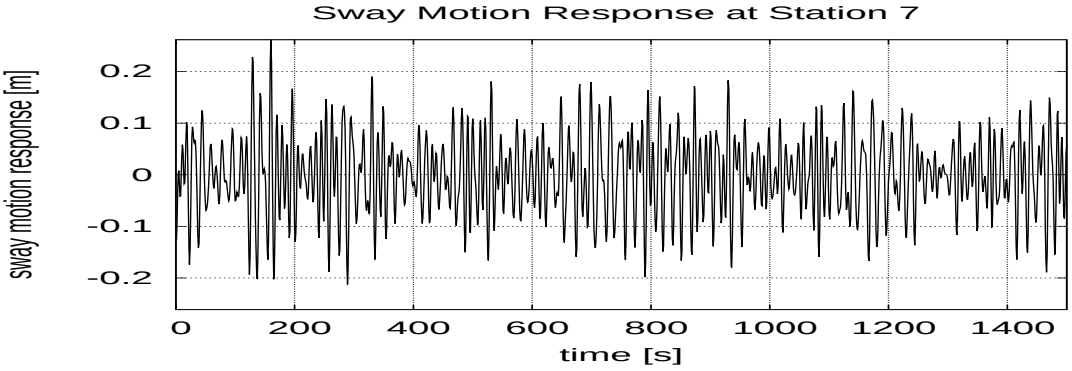

Fig. 90. Sway Motion for heading 135^o and $H_s = 4.0m$

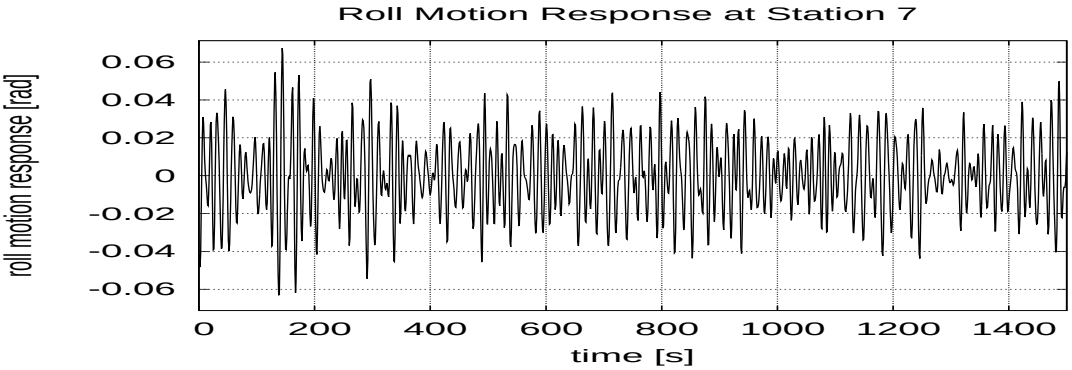

Fig. 91. Roll Motion for heading 135^o and $H_s = 4.0m$

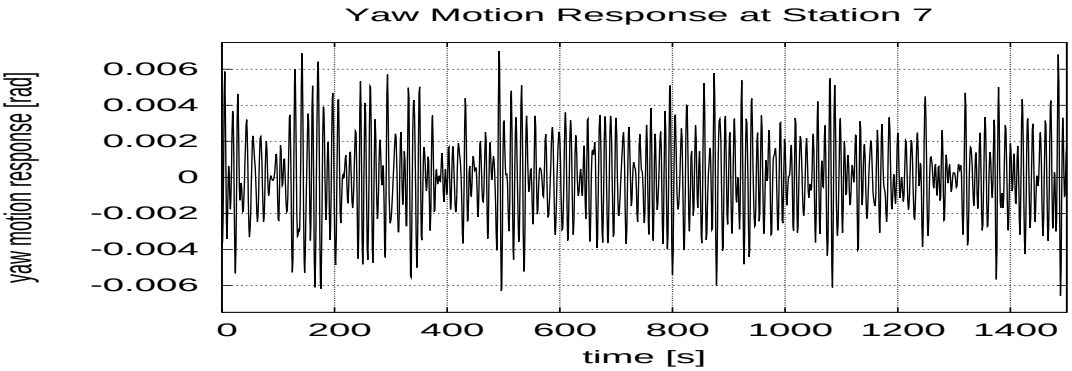

Fig. 92. Yaw Motion for heading 135^o and $H_s = 4.0m$

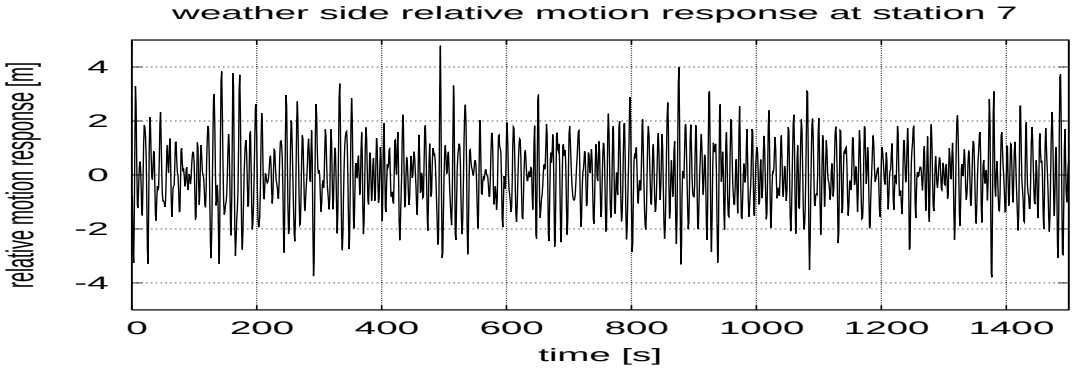

Fig. 93. Relative Motion at weather side for heading 135^o and $H_s = 4.0m$

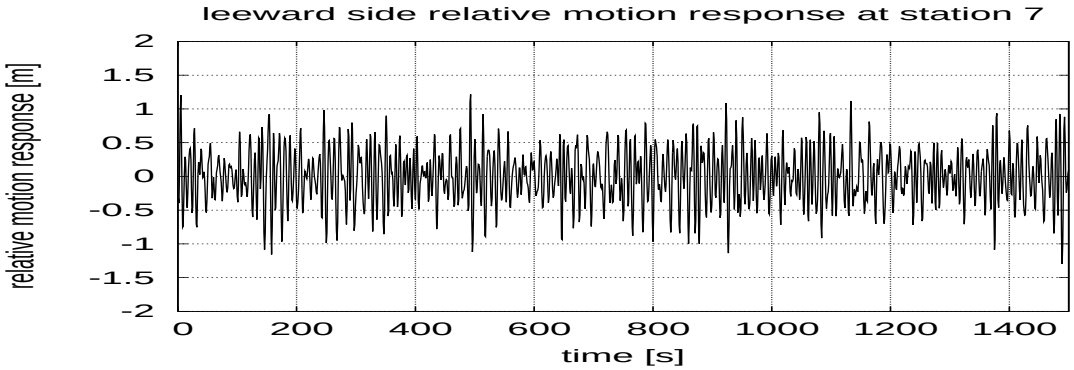

Fig. 94. Relative Motion at leeward side for heading 135^o and $H_s = 4.0m$

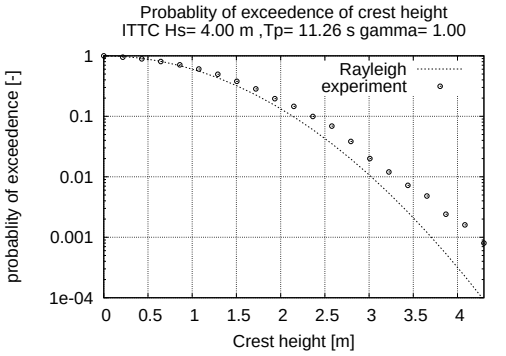

(a) input wave

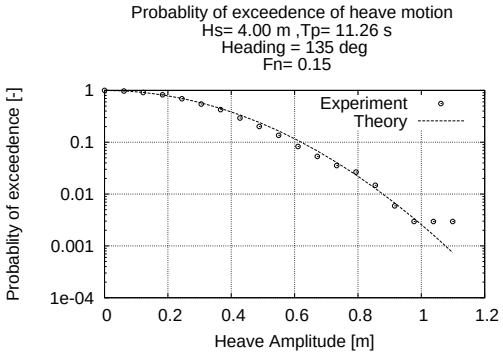

(b) heave motion

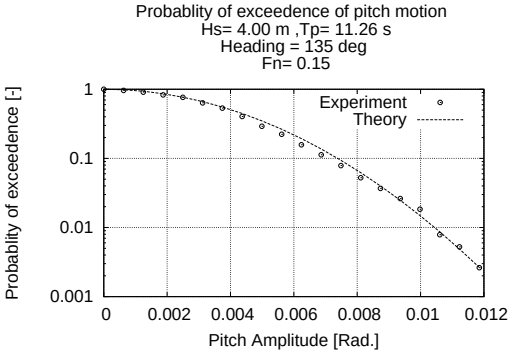

(c) pitch motion

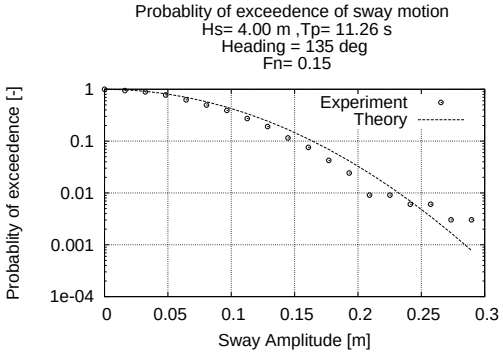

(d) sway motion

Fig. 95. Probability of exceedence for the input wave and resultant motion Hs=4.00m, Fn=0.15 and Heading = 135^o

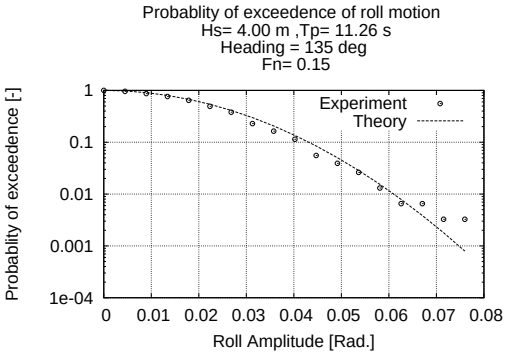

(a) roll motion

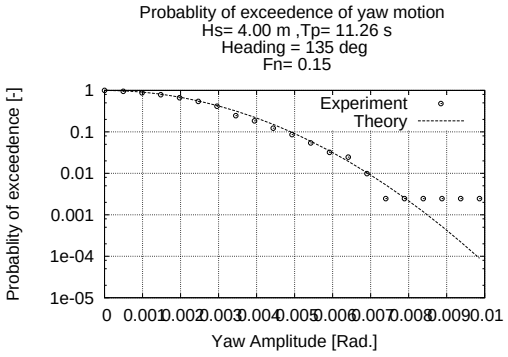

(b) yaw motion

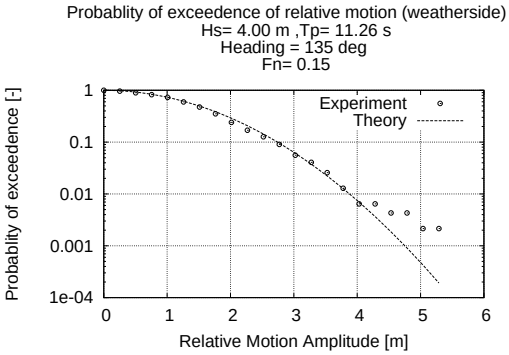

(c) vertical relative motion (weather side)

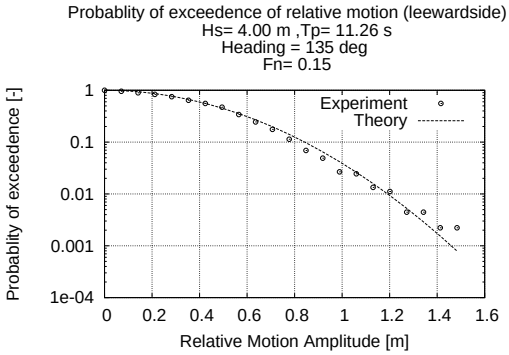

(d) vertical relative motion (leeward side)

Fig. 96. Probability of exceedence for the input wave and resultant motion Hs=4.00m, Fn=0.15 and Heading = 135^o

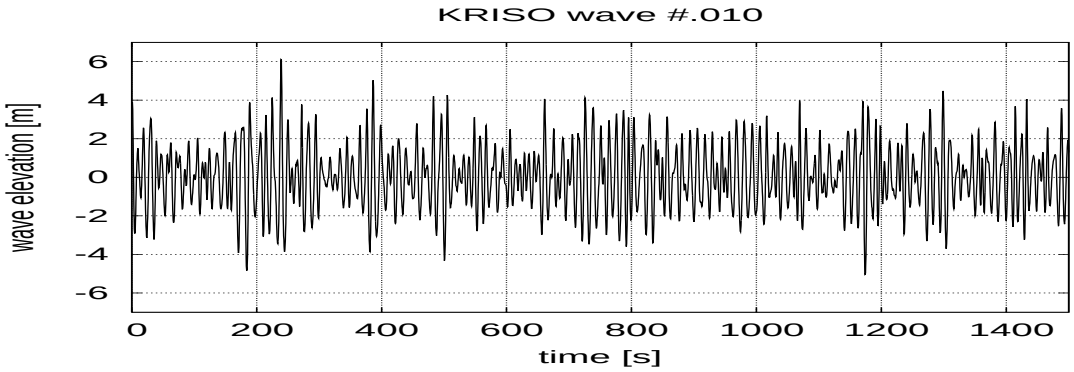

Fig. 97. Input wave $H_s = 6.0m$

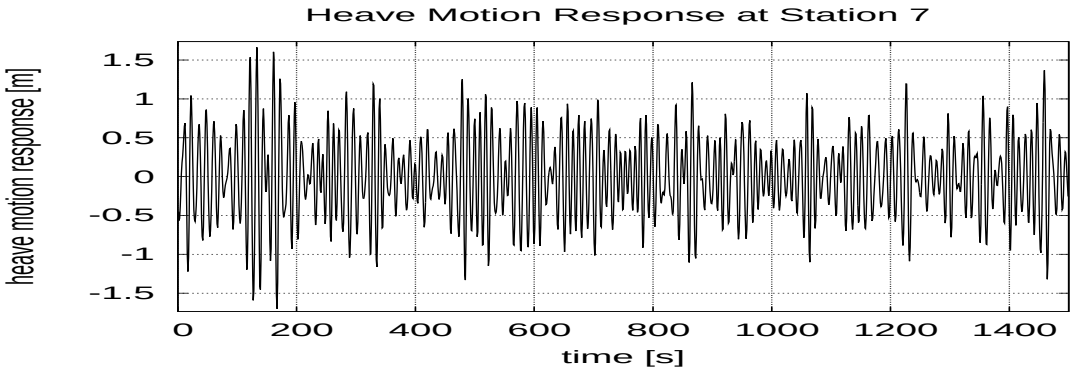

Fig. 98. Heave Motion for heading 135^o and $H_s = 6.0m$

2.3. Case 3 $H_s = 6.0m$

Figures 97 to 104 shows the input wave profile, heave, pitch, sway, roll, yaw,weatherside relative motion response and the leeward side relative motion response for KRISO wave data ID #010.The probability of exceedence of these wave are given in figures 105(a) to 106(c)

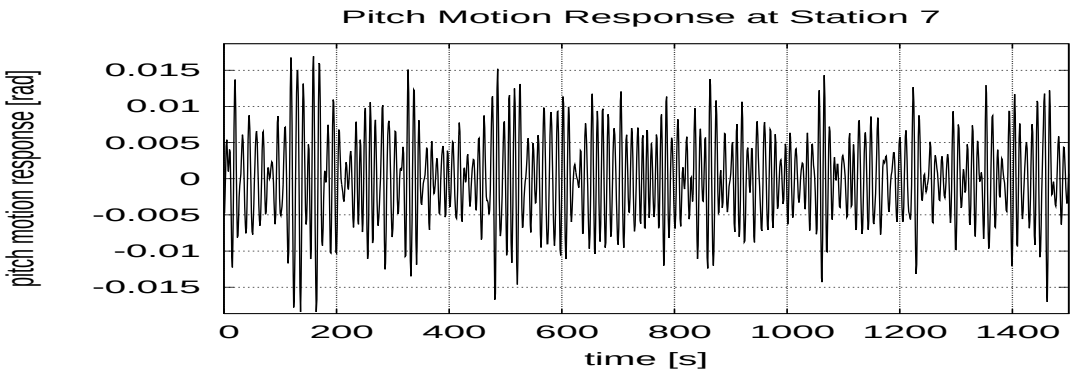

Fig. 99. Pitch Motion for heading 135^o and $H_s = 6.0m$

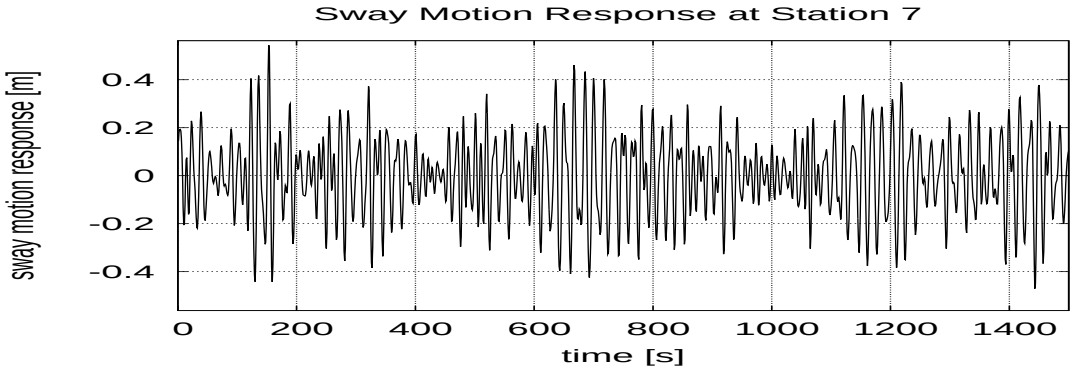

Fig. 100. Sway Motion for heading 135^o and $H_s = 6.0m$

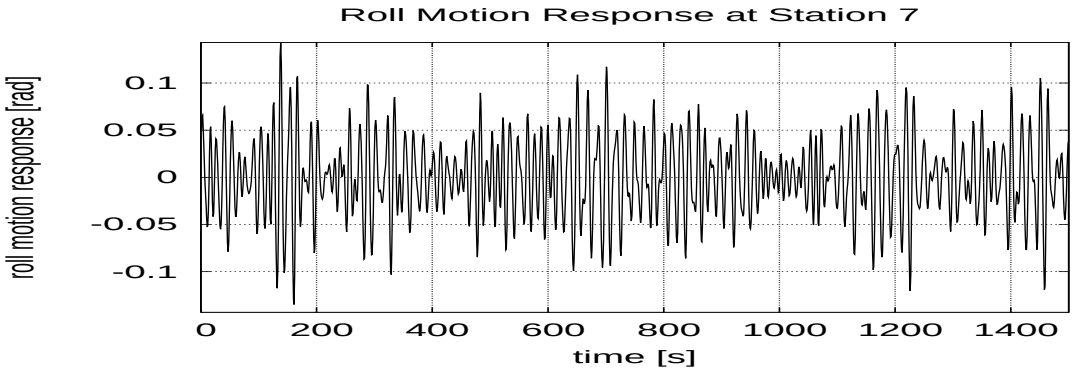

Fig. 101. Roll Motion for heading 135^o and $H_s = 6.0m$

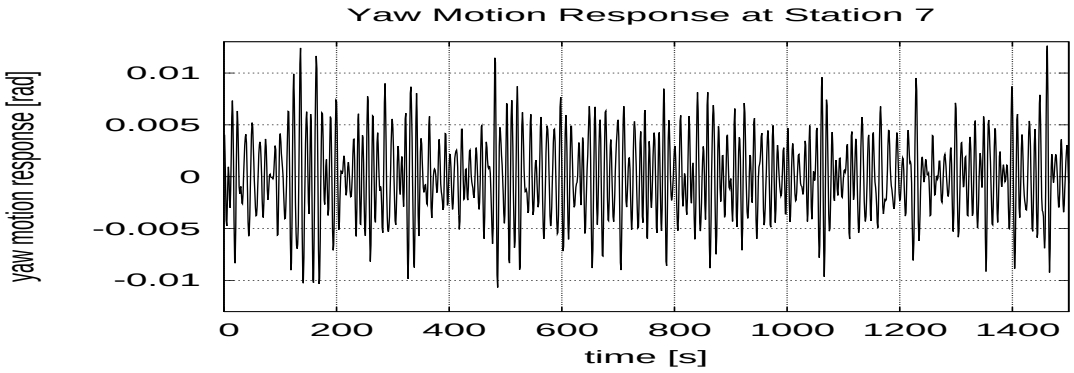

Fig. 102. Yaw Motion for heading 135^o and $H_s = 6.0m$

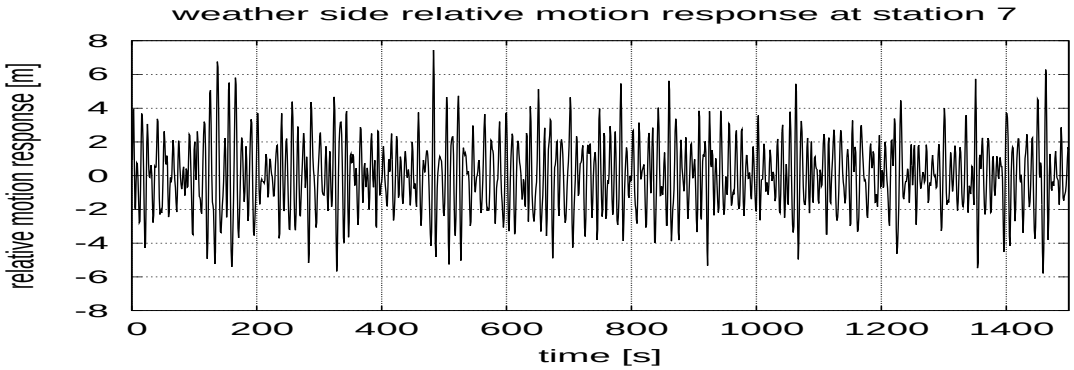

Fig. 103. Relative Motion at weather side for heading 135^o and $H_s = 6.0m$

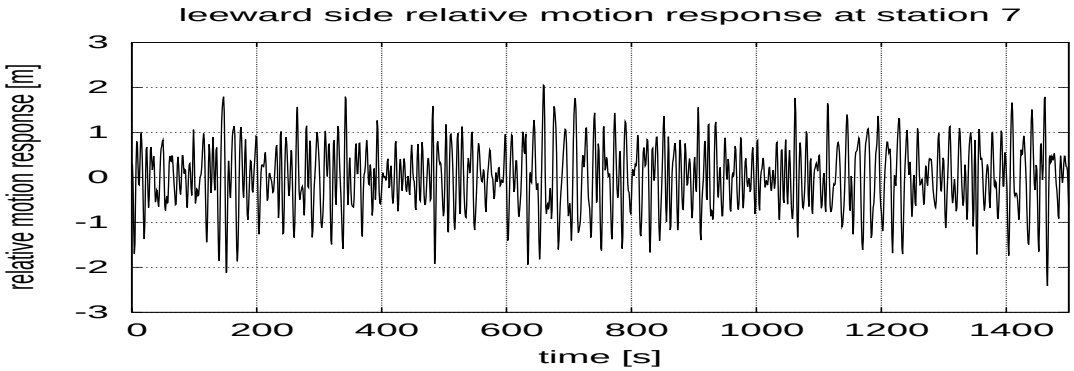

Fig. 104. Relative Motion at leeward side for heading 135^o and $H_s = 6.0m$

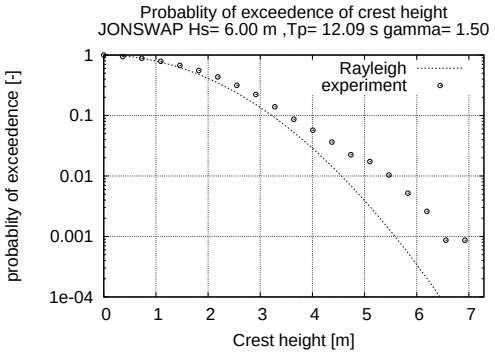

(a) input wave

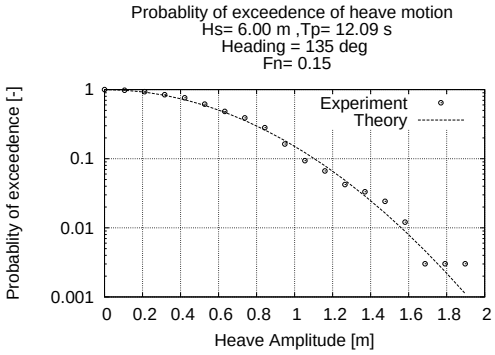

(b) heave motion

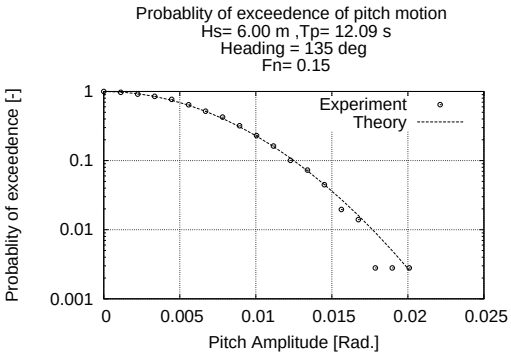

(c) pitch motion

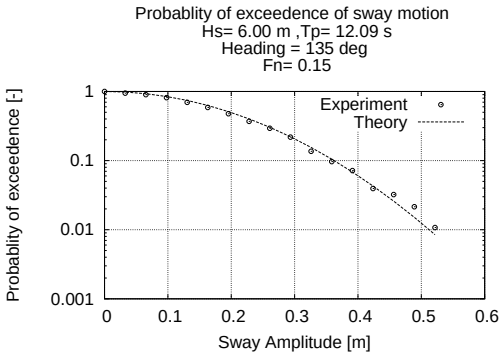

(d) sway motion

Fig. 105. Probability of exceedence for the input wave and resultant motion Hs=6.00m, Fn=0.15 and Heading = 135^o

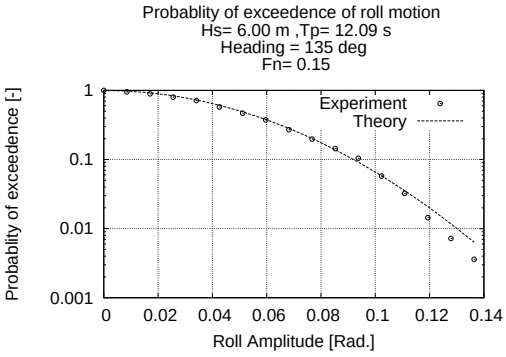

(a) roll motion

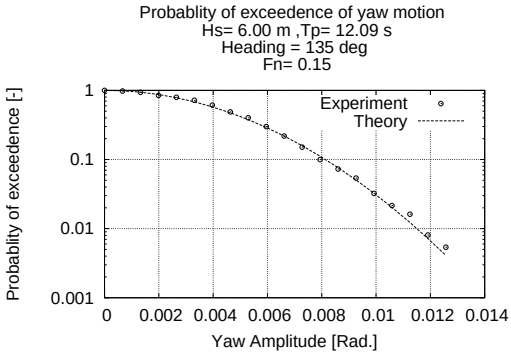

(b) yaw motion

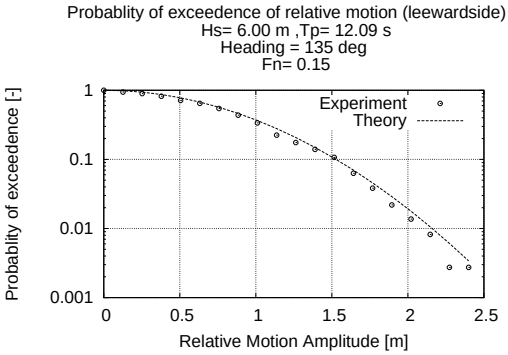

(c) vertical relative motion (leeward side)

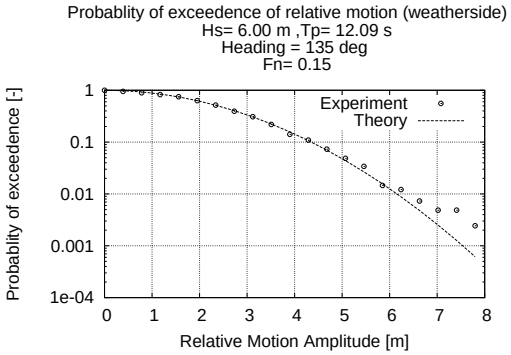

(d) vertical relative motion (weather side)

Fig. 106. Probability of exceedence for the input wave and resultant motion Hs=6.00m, Fn=0.15 and Heading = 135^o

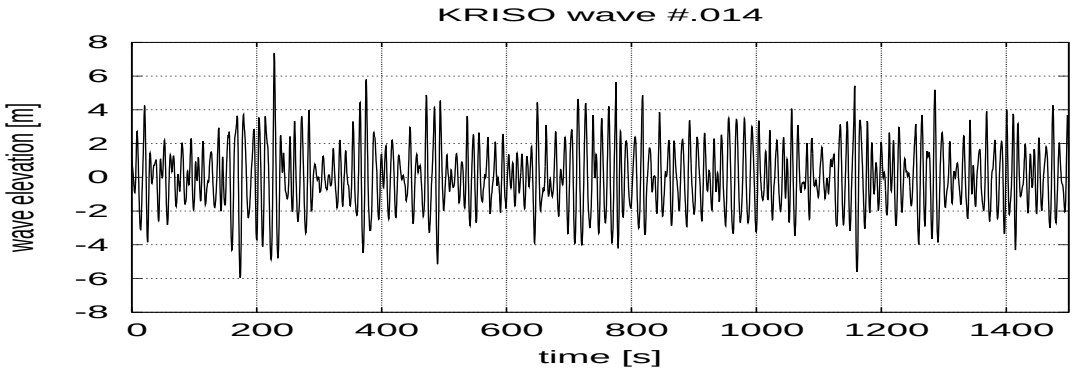

Fig. 107. Input wave $H_s = 7.0m$

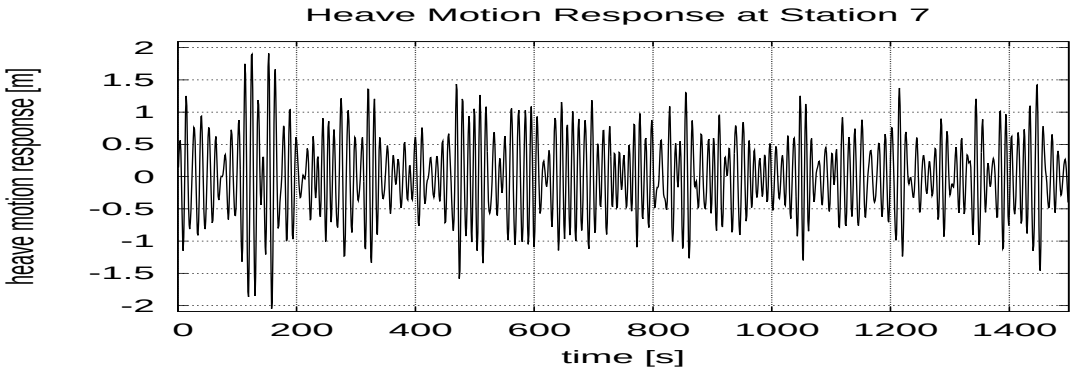

Fig. 108. Heave Motion for heading 135^o and $H_s = 7.0m$

2.4. Case 4 $H_s = 7.0m$

Figures 107 to 114 shows the input wave profile, heave, pitch, sway, roll, yaw,weatherside relative motion response and the leeward side relative motion response for KRISO wave data ID #014.The probability of exceedence of these wave are given in figures 115(a) to 116(d)

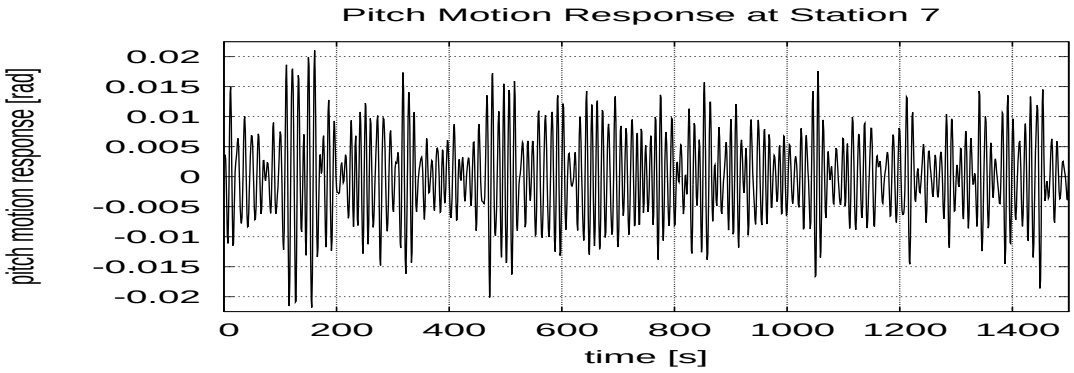

Fig. 109. Pitch Motion for heading 135^o and $H_s = 7.0m$

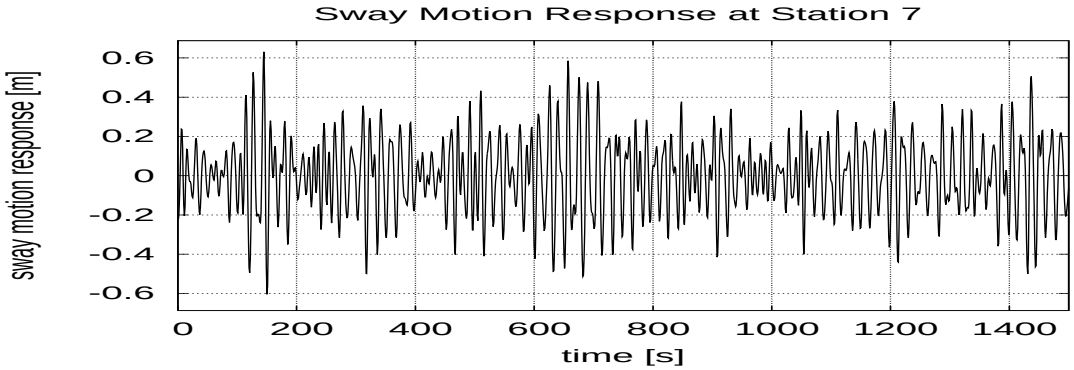

Fig. 110. Sway Motion for heading 135^o and $H_s = 7.0m$

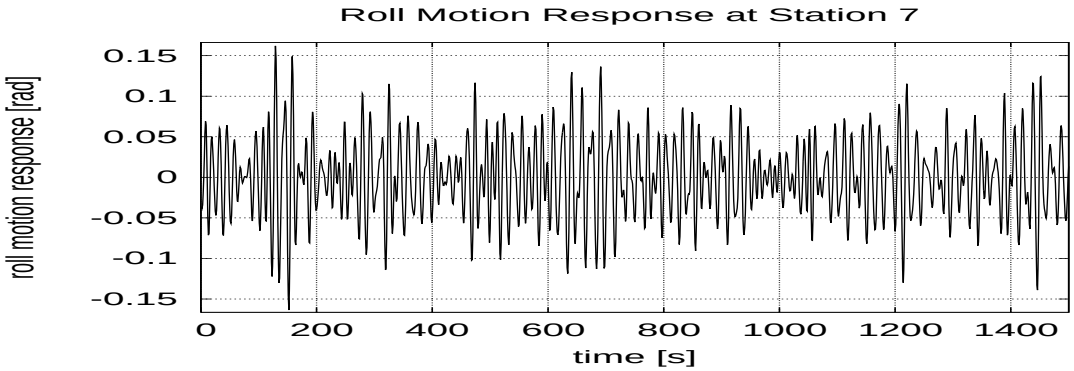

Fig. 111. Roll Motion for heading 135^o and $H_s = 7.0m$

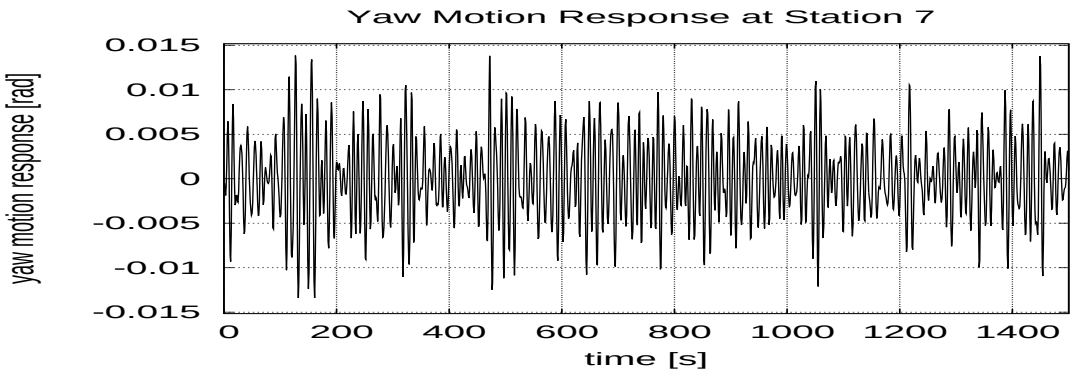

Fig. 112. Yaw Motion for heading 135^o and $H_s = 7.0m$

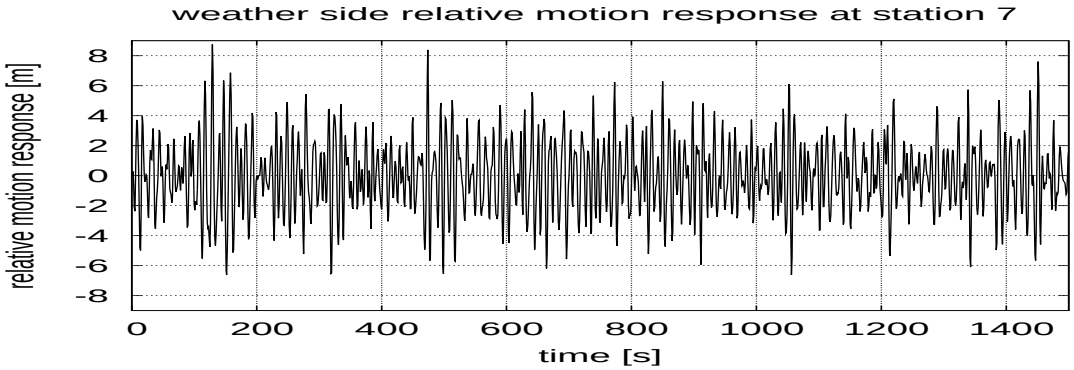

Fig. 113. Relative Motion at weather side for heading 135^o and $H_s = 7.0m$

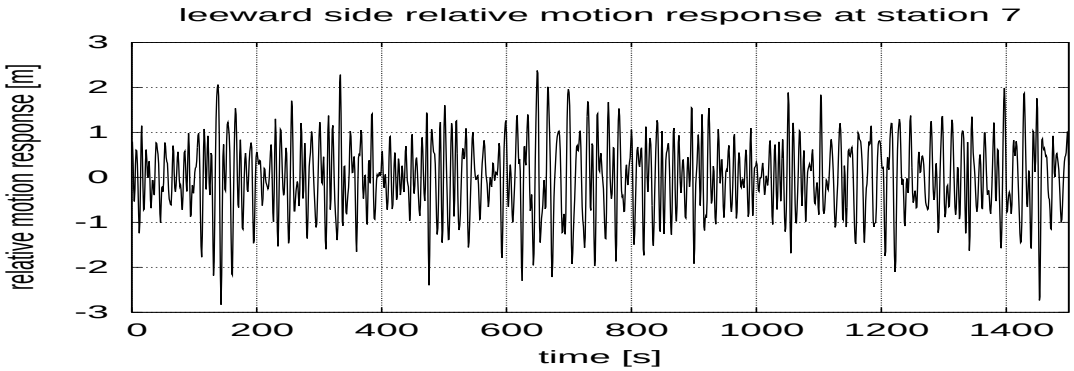

Fig. 114. Relative Motion at leeward side for heading 135^o and $H_s = 7.0m$

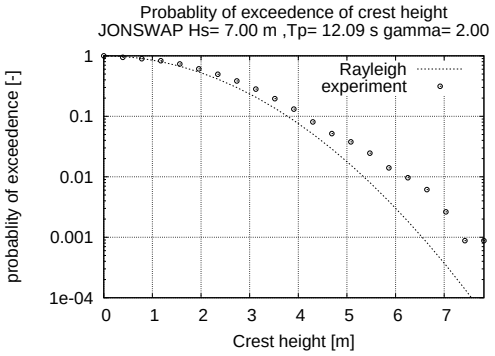

(a) input wave

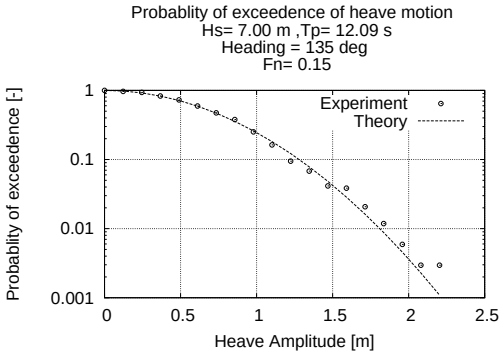

(b) heave motion

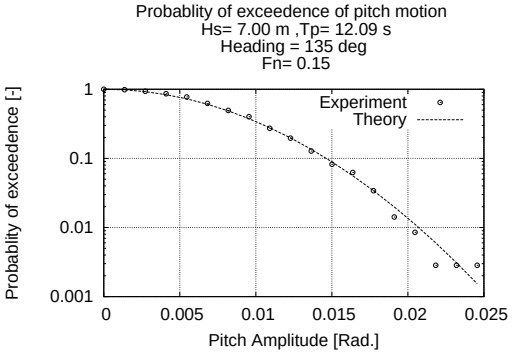

(c) pitch motion

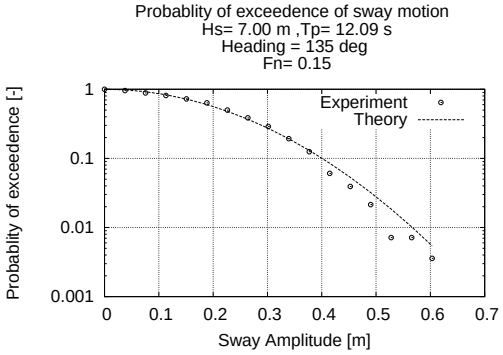

(d) sway motion

Fig. 115. Probability of exceedence for the input wave and resultant motion Hs=7.00m, Fn=0.15 and Heading = 135^o

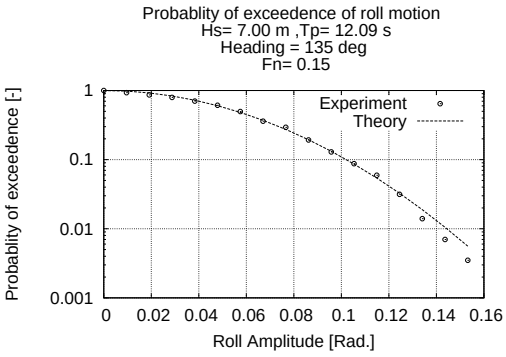

(a) roll motion

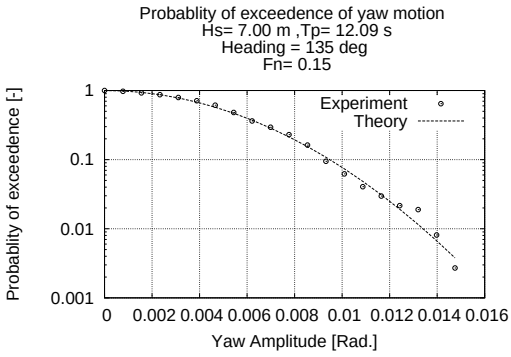

(b) yaw motion

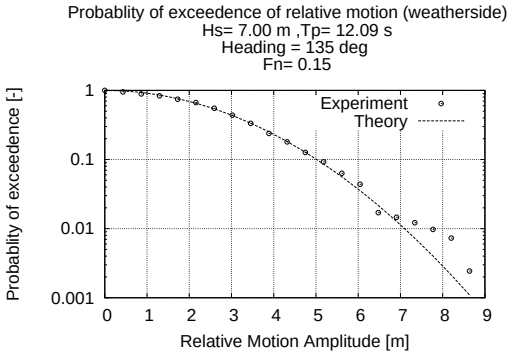

(c) vertical relative motion (weather side)

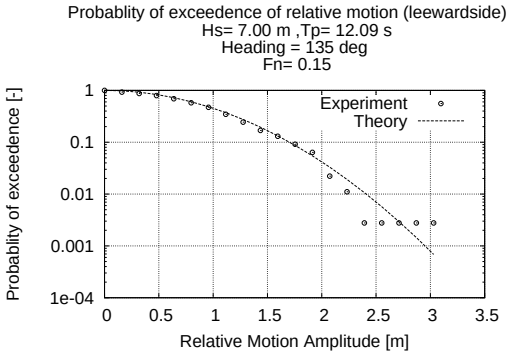

(d) vertical relative mnotion (leeward side)

Fig. 116. Probability of exceedence for the input wave and resultant motion Hs=7.00m, Fn=0.15 and Heading = 135^o

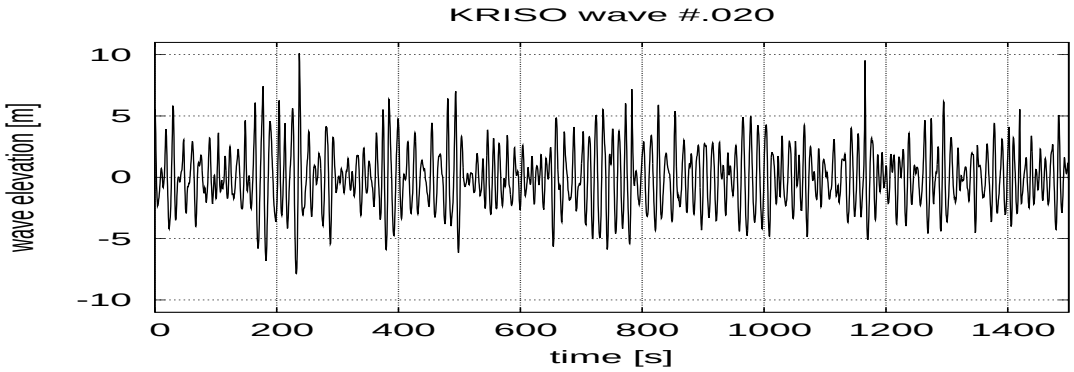

Fig. 117. Input wave $H_s = 9.0m$

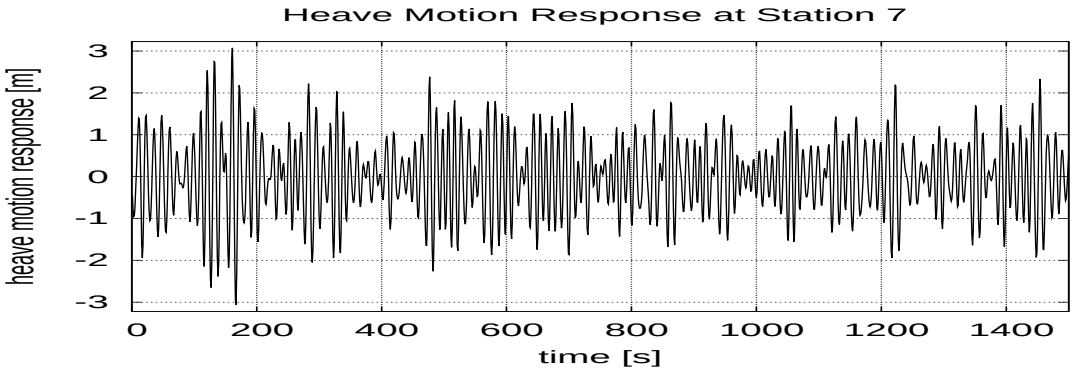

Fig. 118. Heave Motion for heading 135^o and $H_s = 9.0m$

2.5. Case 5 $H_s = 9.0m$

Figures 117 to 124 shows the input wave profile, heave, pitch, sway, roll, yaw,weatherside relative motion response and the leeward side relative motion response for KRISO wave data ID #020.The probability of exceedence of these wave are given in figures 125(a) to 126(d)

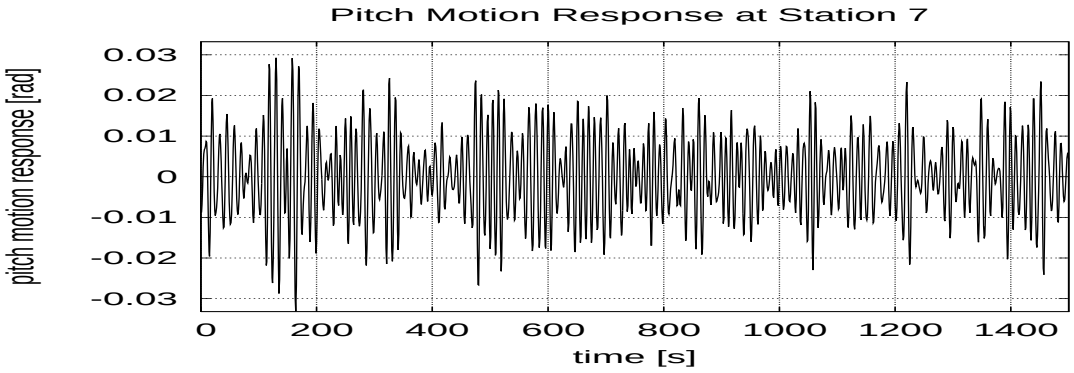

Fig. 119. Pitch Motion for heading 135^o and $H_s = 9.0m$

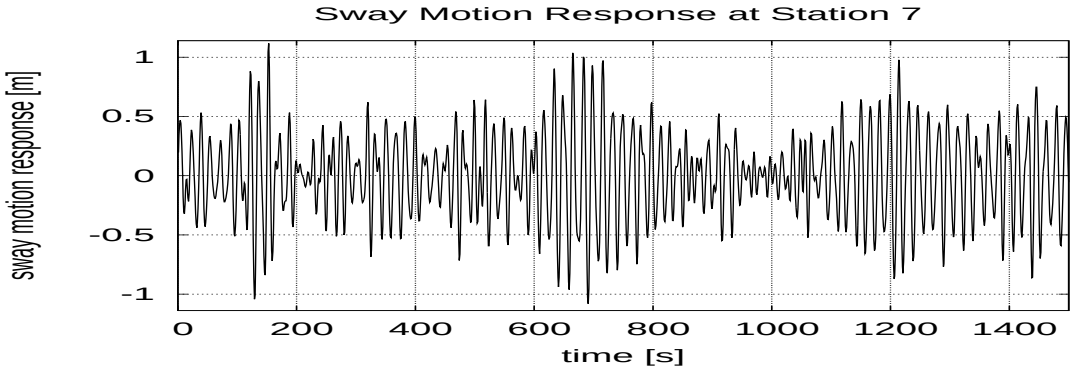

Fig. 120. Sway Motion for heading 135^o and $H_s = 9.0m$

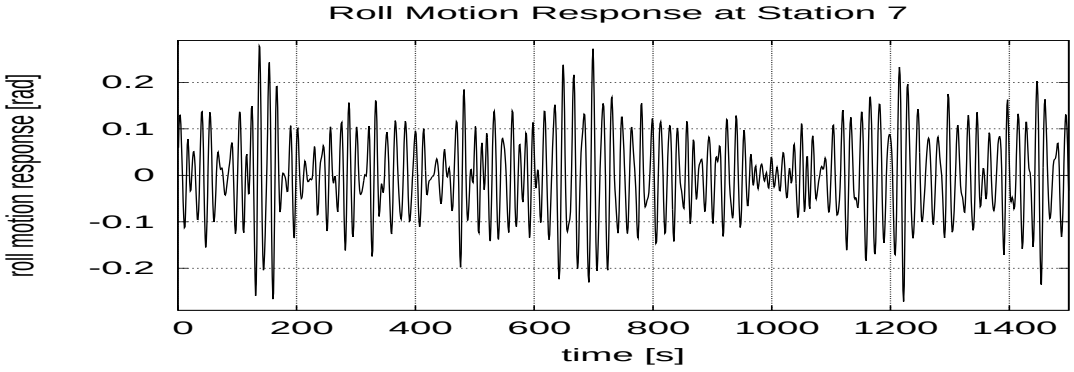

Fig. 121. Roll Motion for heading 135^o and $H_s = 9.0m$

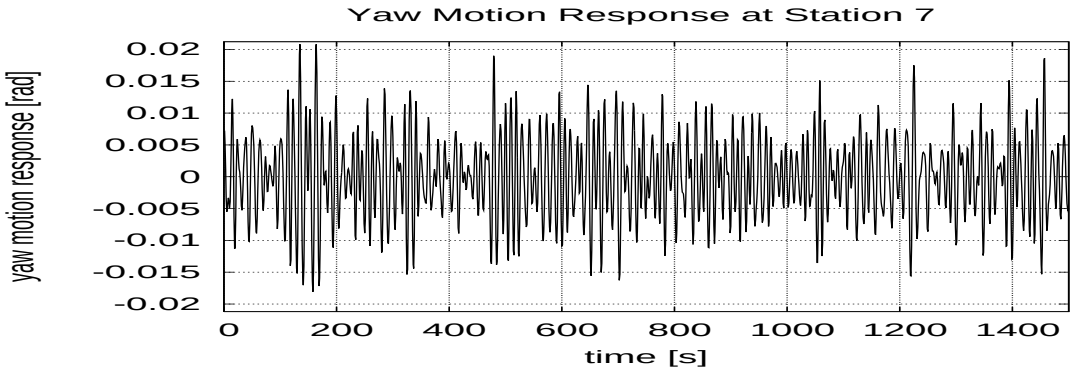

Fig. 122. Yaw Motion for heading 135^o and $H_s = 9.0m$

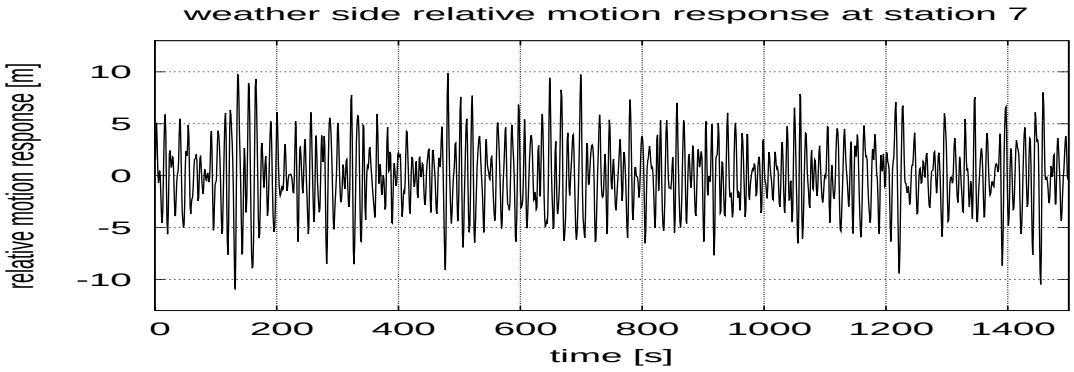

Fig. 123. Relative Motion at weather side for heading 135^o and $H_s = 9.0m$

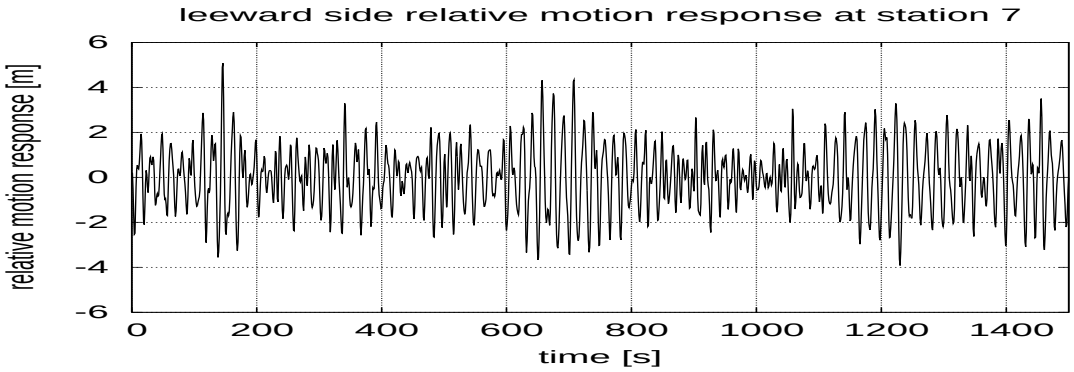

Fig. 124. Relative Motion at leeward side for heading 135^o and $H_s = 9.0m$

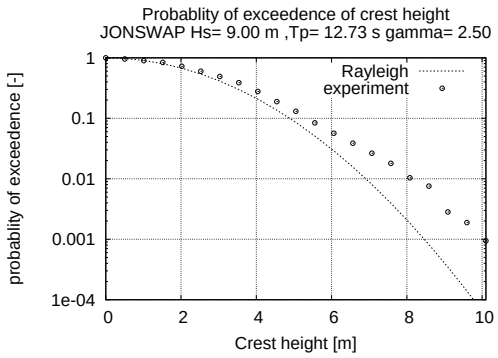

(a) input wave

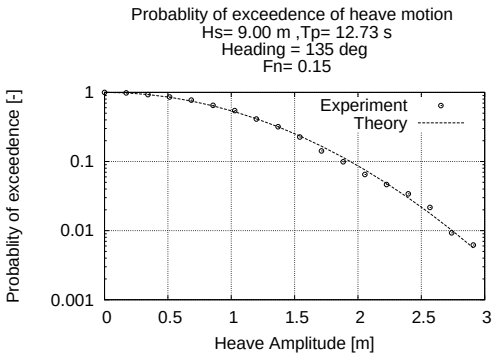

(b) heave motion

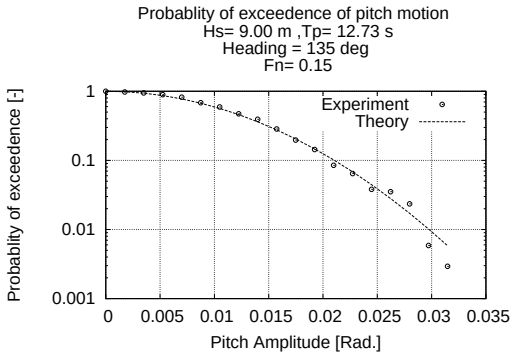

(c) pitch motion

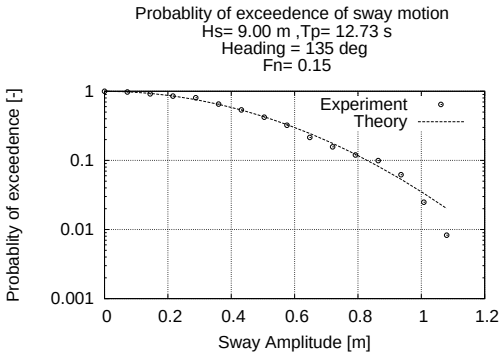

(d) sway motion

Fig. 125. Probability of exceedence for the input wave and resultant motion Hs=9.00m, Fn=0.15 and Heading = 135^o

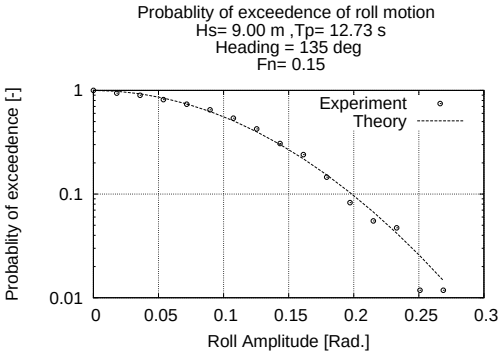

(a) roll motion

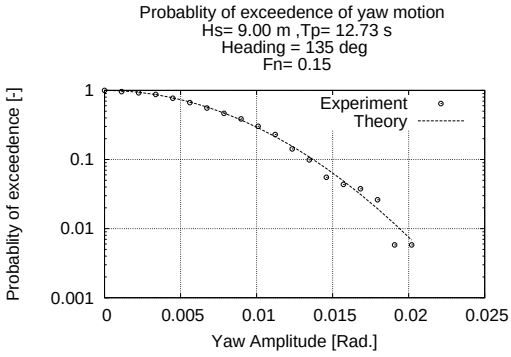

(b) yaw motion

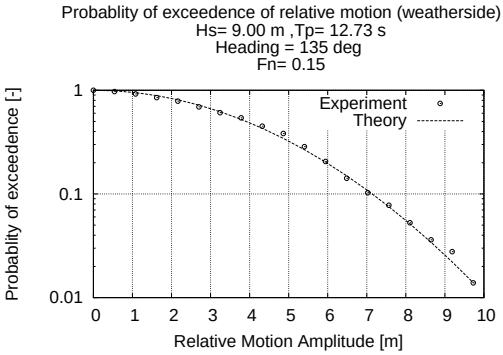

(c) vertical relative motion (weather side)

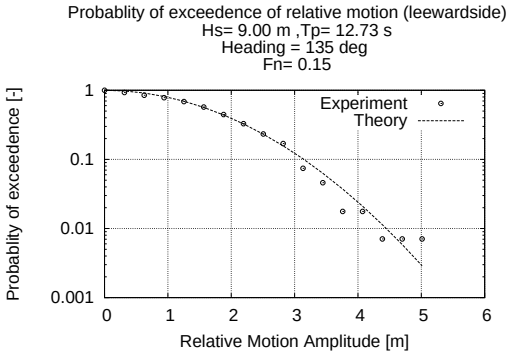

(d) vertical relative motion (leeward side)

Fig. 126. Probability of exceedence for the input wave and resultant motion Hs=9.00m, Fn=0.15 and Heading = 135^o

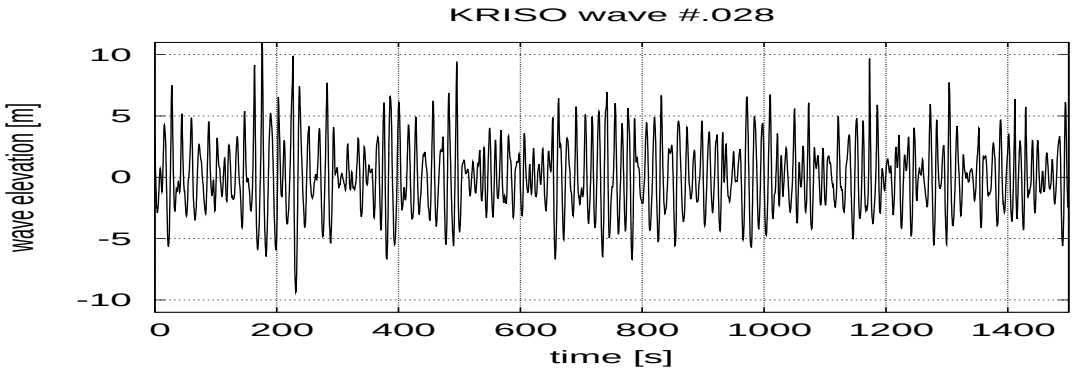

Fig. 127. Input wave $H_s = 11.0m$

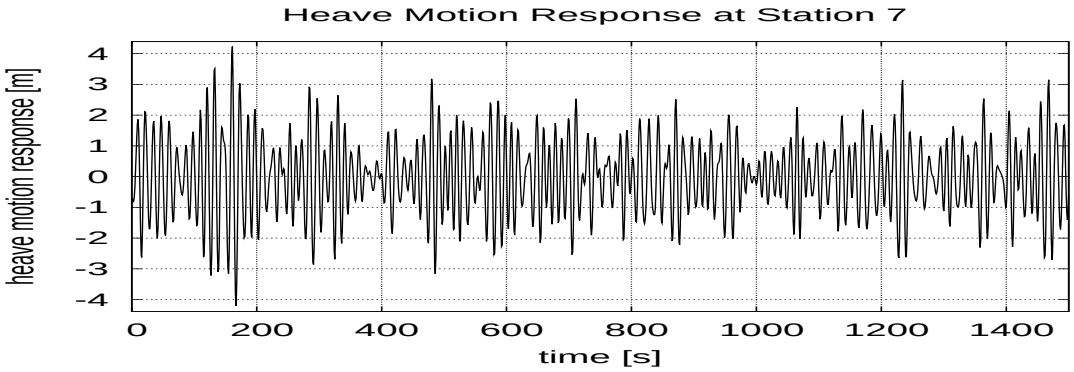

Fig. 128. Heave Motion for heading 135^o and $H_s = 11.0m$

2.6. Case 6 $H_s = 11.0m$

Figures 127 to 134 shows the input wave profile, heave, pitch, sway, roll, yaw,weatherside relative motion response and the leeward side relative motion response for KRISO wave data ID #028.The probability of exceedence of these wave are given in figures 135(a) to 136(d)

3. Most Probable Peak Value

The most probable peak values for the different sea states, for each sea condition is shown in figure 137(a) to 138.

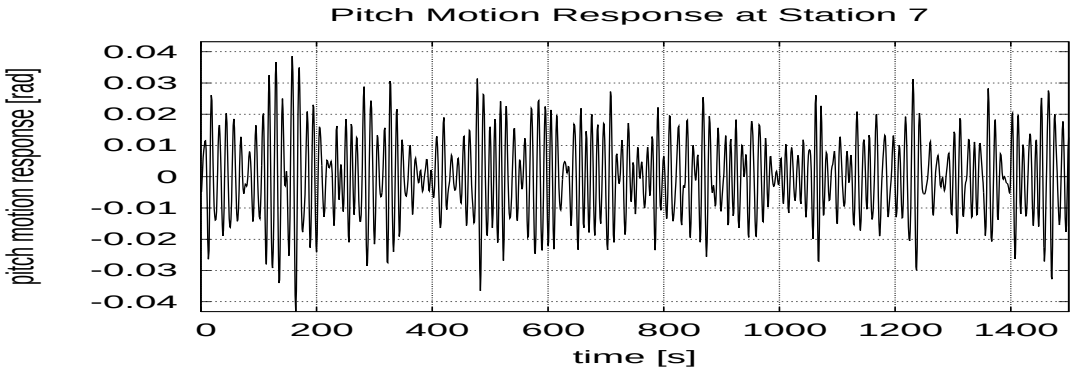

Fig. 129. Pitch Motion for heading 135^o and $H_s = 11.0m$

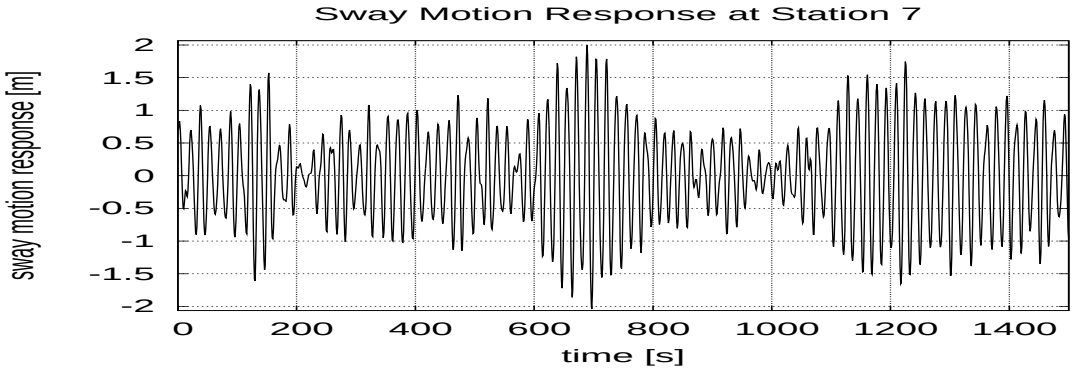

Fig. 130. Sway Motion for heading 135^o and $H_s = 11.0m$

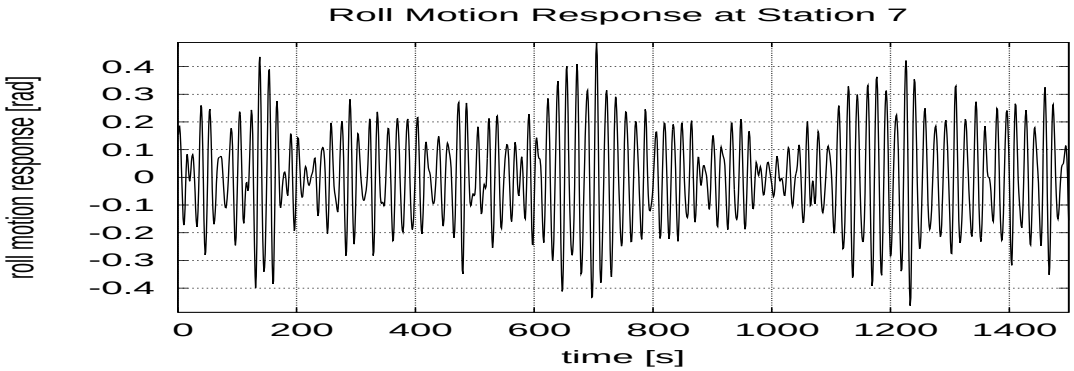

Fig. 131. Roll Motion for heading 135^o and $H_s = 11.0m$

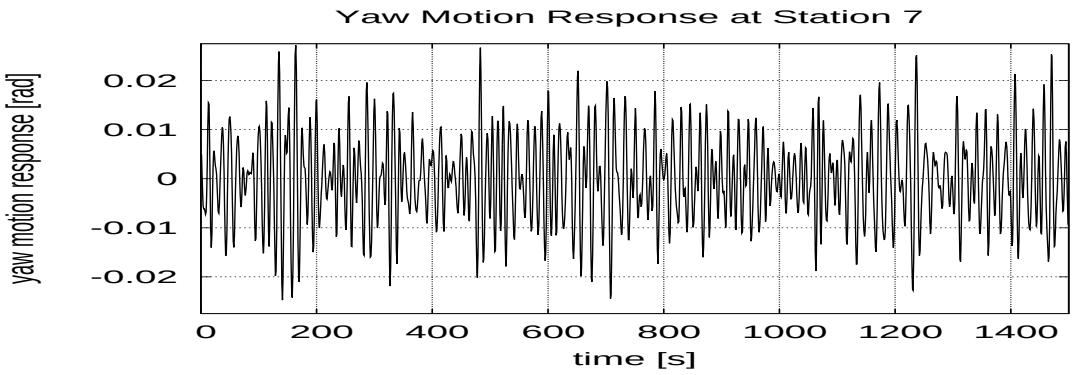

Fig. 132. Yaw Motion for heading 135^o and $H_s = 11.0m$

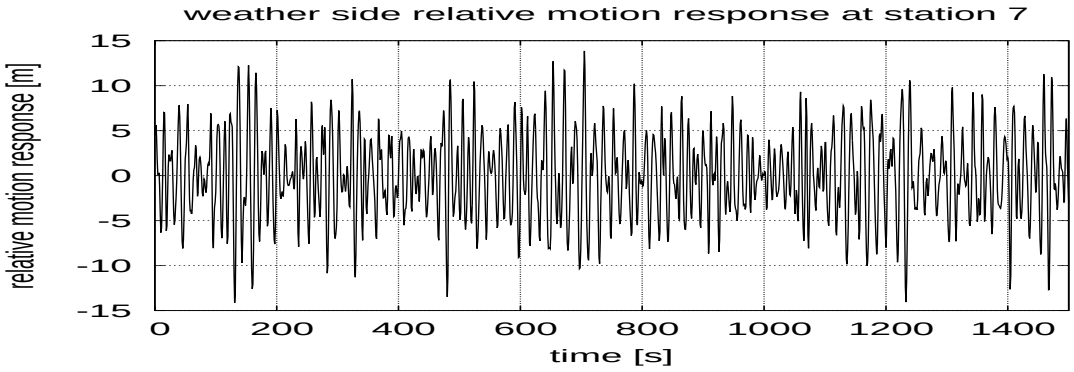

Fig. 133. Relative Motion at weather side for heading 135^o and $H_s = 9.0m$

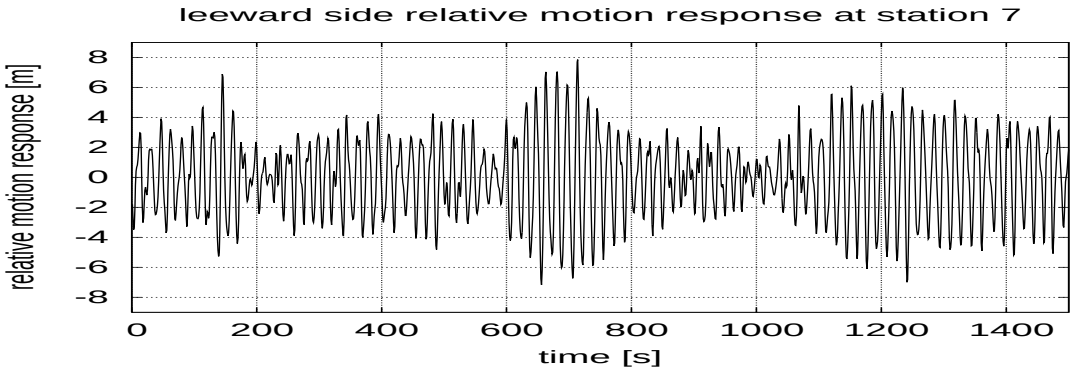

Fig. 134. Relative Motion at leeward side for heading 135^o and $H_s = 9.0m$

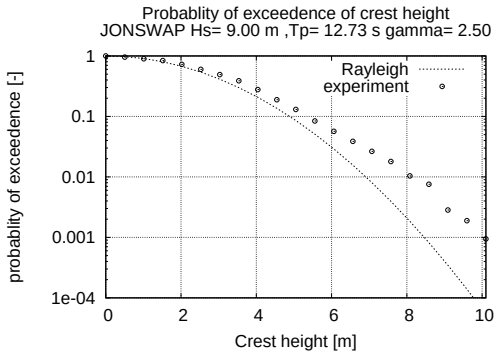

(a) input

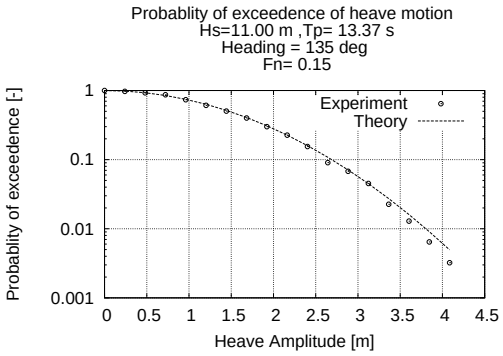

(b) heave

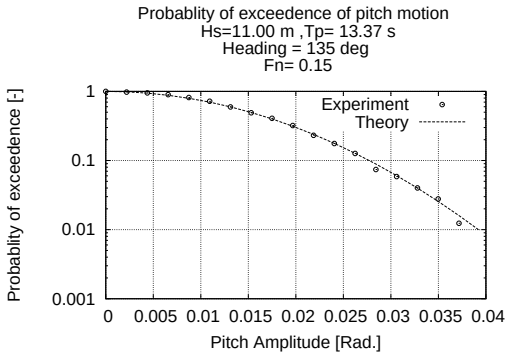

(c) pitch

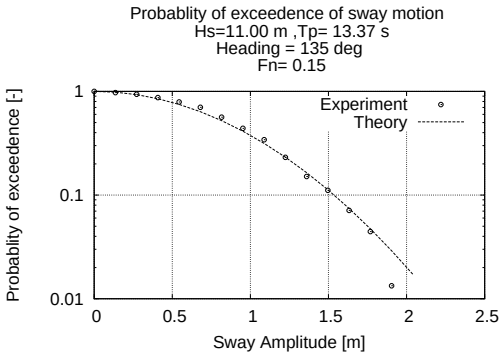

(d) sway

Fig. 135. Probability of exceedence for the input wave and resultant motion Hs=11.00m, Fn=0.15 and Heading = 135^o

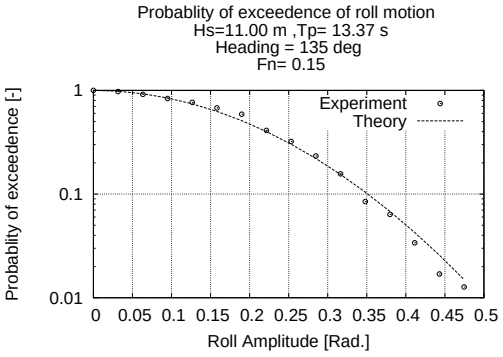

(a) roll

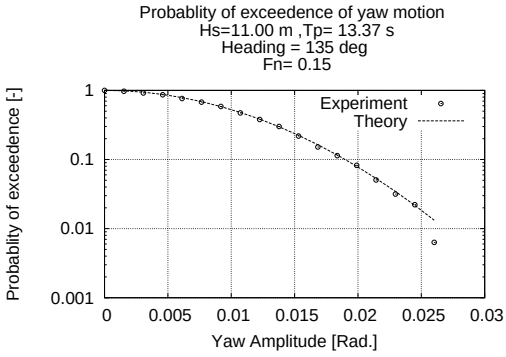

(b) yaw

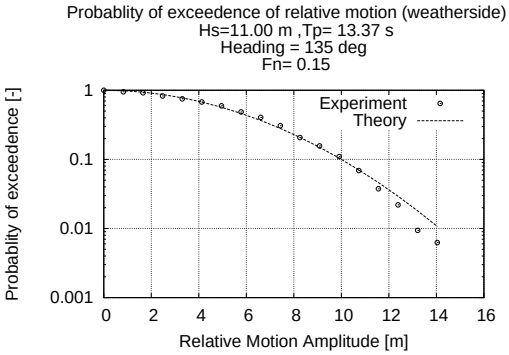

(c) vertical relative motion (weather side)

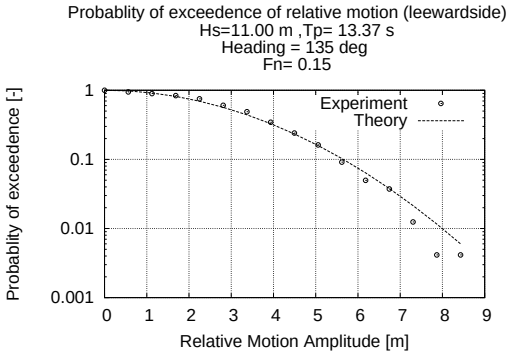

(d) vertical relative motion (leeward side)

Fig. 136. Probability of exceedence for the input wave and resultant motion Hs=11.00m, Fn=0.15 and Heading = 135^o

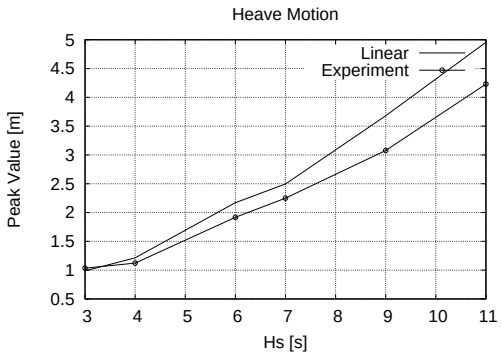

(a) heave

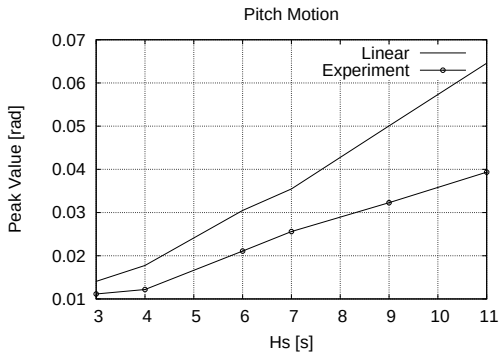

(b) pitch

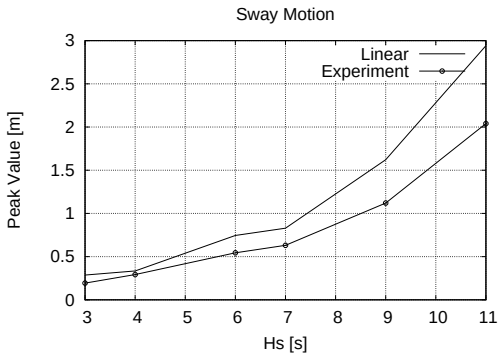

(c) sway

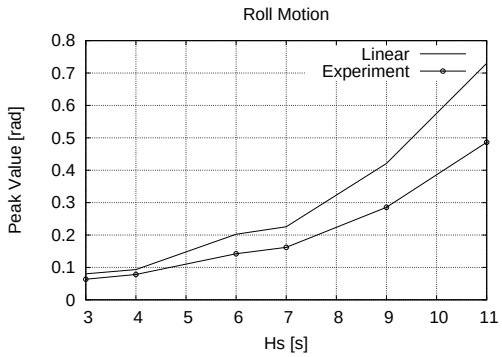

(d) roll

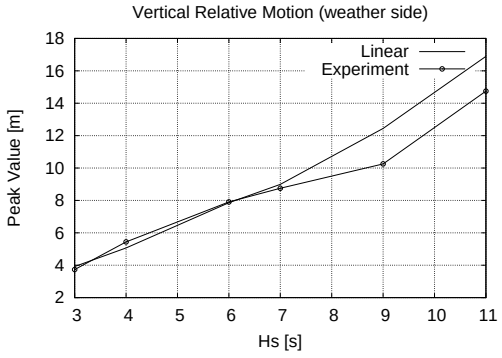

(e) weather side

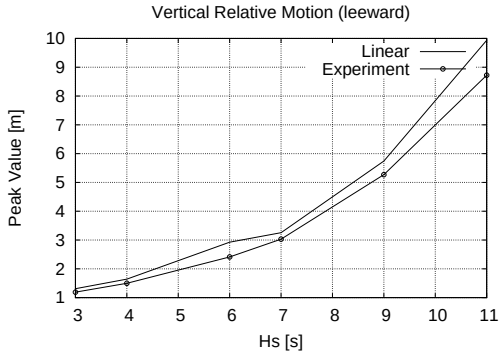

(f) leeward side

Fig. 137. Peak value comparison for heave, pitch,sway,roll and vertical relative motions (weather side and leeward side) for Fn=0.15 and Heading = 135^o

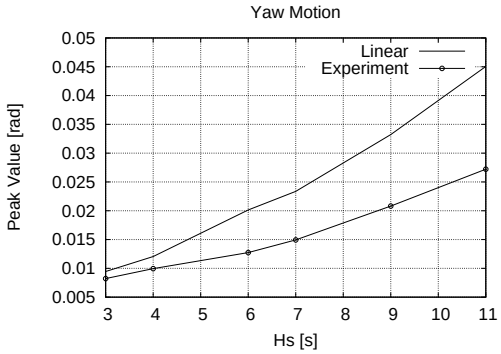

Fig. 138. Peak value comparison for yaw motion, Fn=0.15 and Heading = 135^o

CHAPTER VI

ANALYSIS RESULTS FOR HEADING = 180^O AND $F_N = 0$

The motions of the container ship SL 7 for $Fn = 0$ and headings of 180^o are calculated using the linear approach and using UNIOM.

1. Simulation Results

In this section, the results from using the linear theory and UNIOM are compared. The simulation using UNIOM is carried out for 3600 seconds, but for the plots to be readable, only 1500 seconds of data is shown. The time steps used for the simulations is 1 second. The peak values are found corresponding to a time duration of 3600 seconds.

2. Probability of Exceedence

The probability of exceedence for the wave as well as the response motions are calculated. The following pages show the input wave and the responses.

2.1. Case 1 $H_s = 3.0m$

Figures 139 to 143 shows the input wave profile, heave, pitch, sway, roll, yaw, weatherside relative motion response and the leeward side relative motion response for KRISO wave data ID #043. The probability of exceedence of these wave are given in figures 144(a) to 145

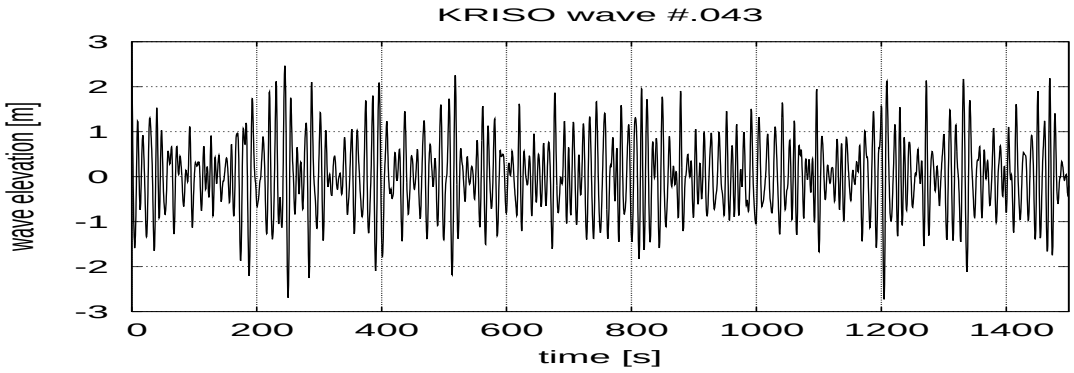

Fig. 139. Input wave $H_s = 3.0m$

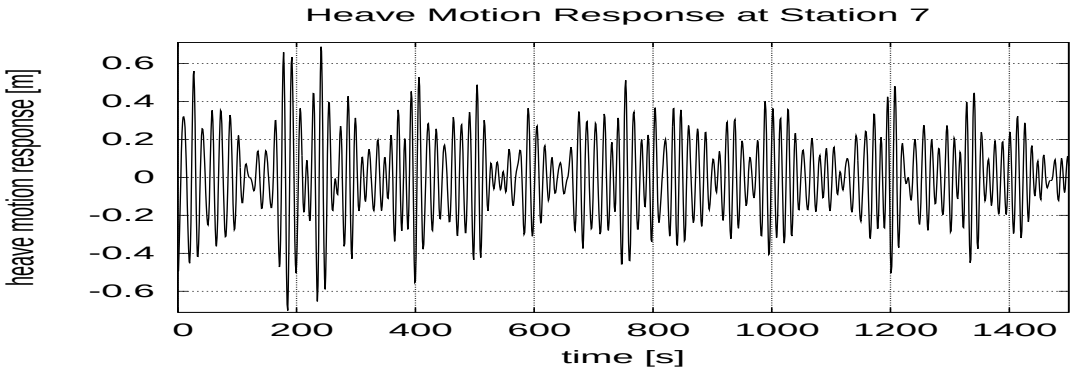

Fig. 140. Heave Motion for heading 180^o and $H_s = 3.0m$

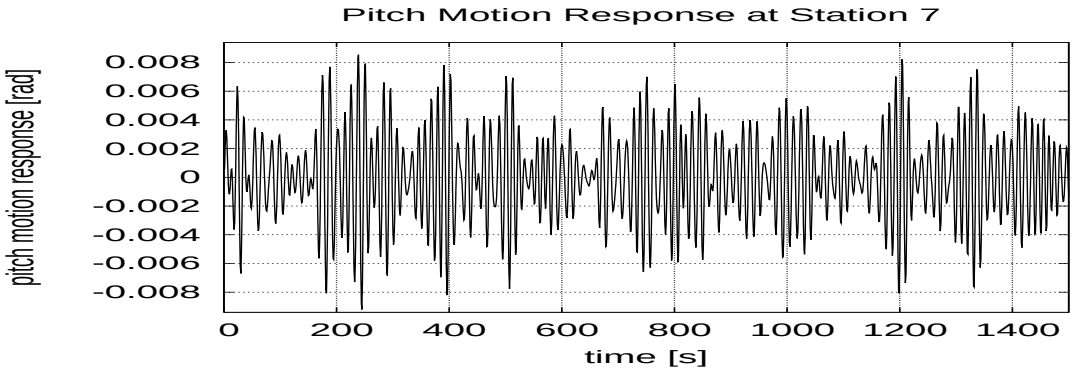

Fig. 141. Pitch Motion for heading 180^o and $H_s = 3.0m$

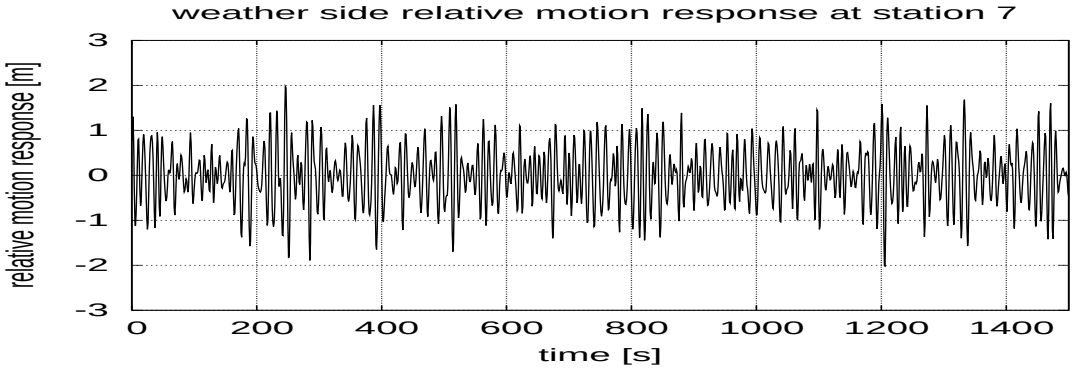

Fig. 142. Relative Motion at weather side for heading 180^o and $H_s = 3.0m$

2.2. Case 2 $H_s = 4.0m$

Figures 146 to 150 shows the input wave profile, heave, pitch, sway, roll, yaw, weatherside relative motion response and the leeward side relative motion response for KRISO wave data ID #042. The probability of exceedence of these wave are given in figures 151(a) to 152

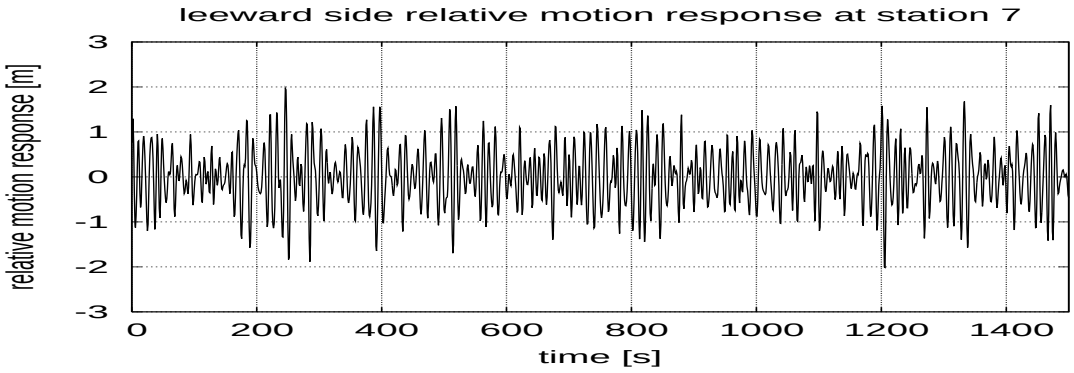

Fig. 143. Relative Motion at leeward side for heading 180^o and $H_s = 3.0m$

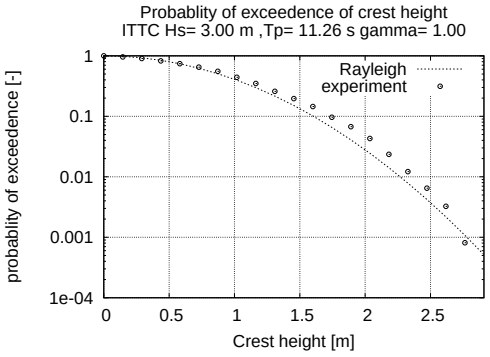

(a) Input wave

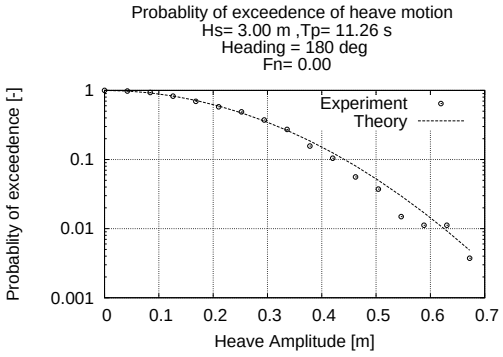

(b) Heave motion

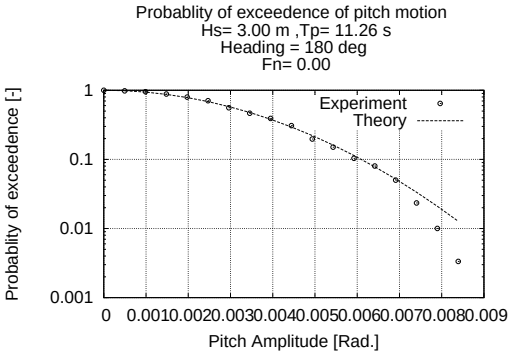

(c) Pitch motion

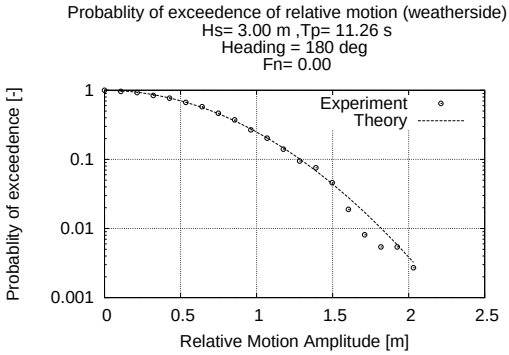

(d) vertical relative motion (weather side)

Fig. 144. Probability of exceedence for the input wave and resultant motion Hs=3.00m, Fn=0 and Heading = 180^o

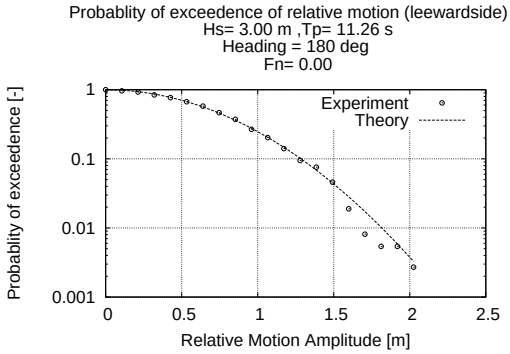

Fig. 145. Probability of exceedence for vertical relative motion (leeward side) Hs=3.00m, Fn=0 and Heading = 180^o

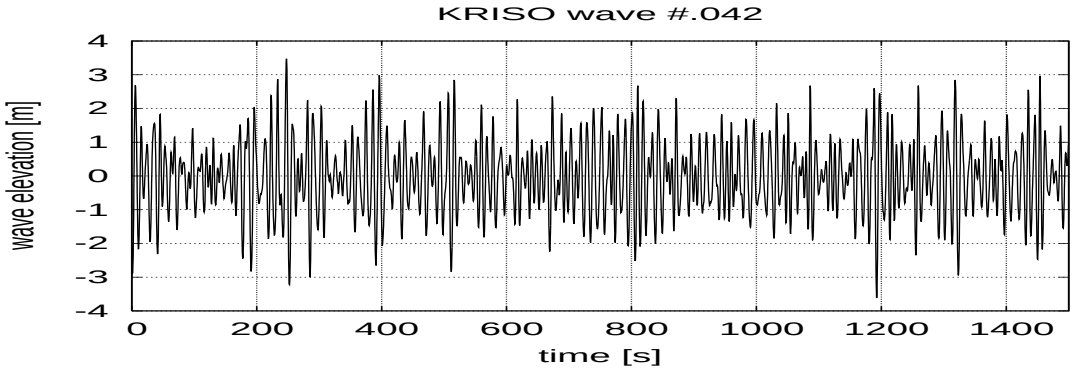

Fig. 146. Input wave $H_s = 4.0m$

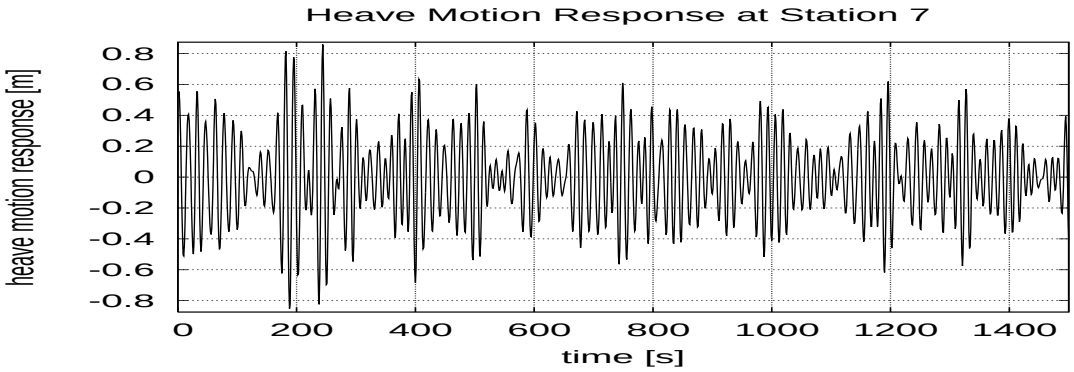

Fig. 147. Heave Motion for heading 180^o and $H_s = 4.0m$

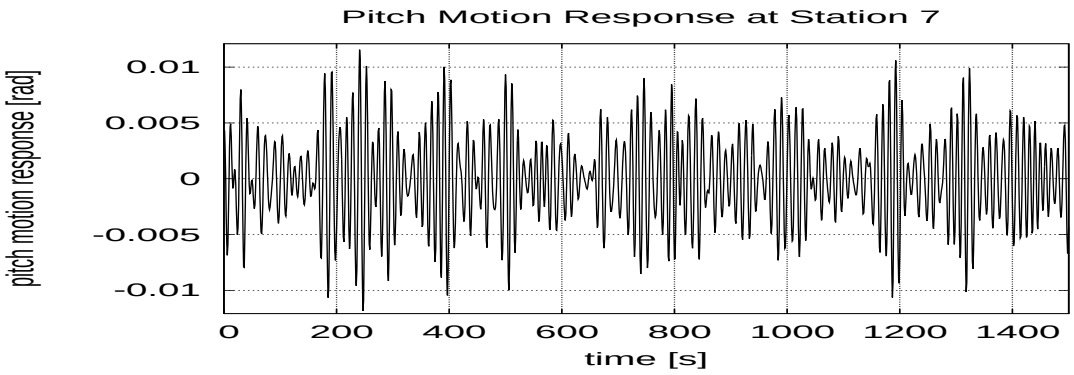

Fig. 148. Pitch Motion for heading 180^o and $H_s = 4.0m$

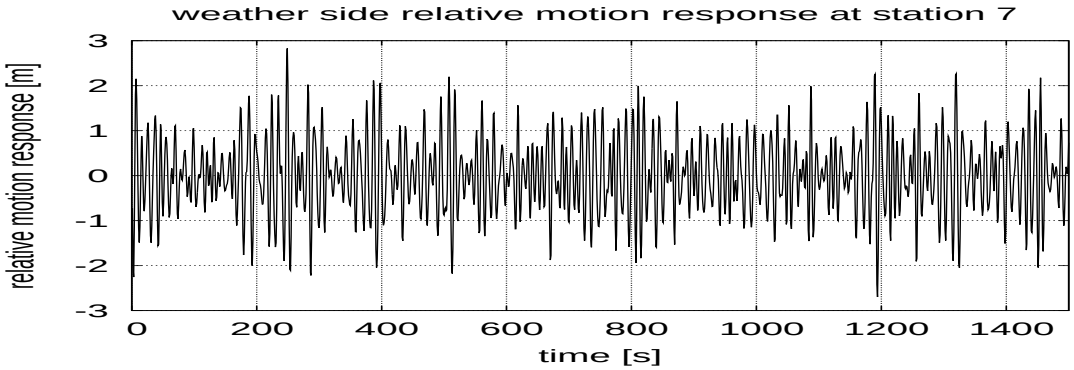

Fig. 149. Relative Motion at weather side for heading 180^o and $H_s = 4.0m$

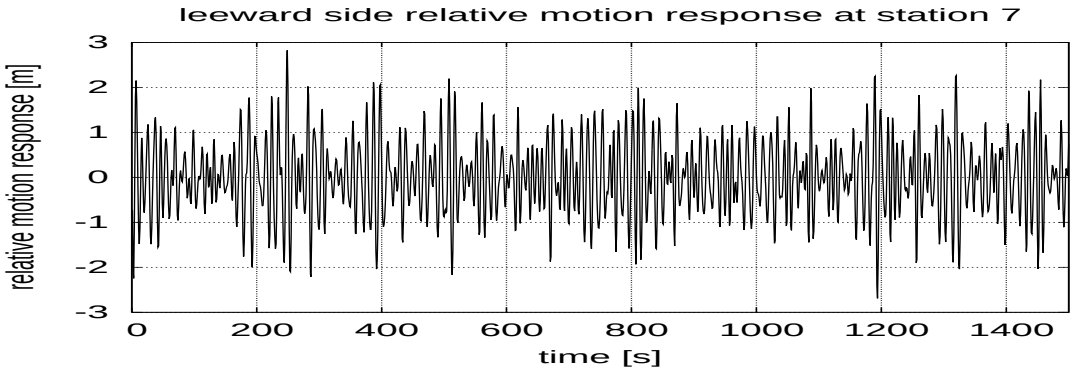

Fig. 150. Relative Motion at leeward side for heading 180^o and $H_s = 4.0m$

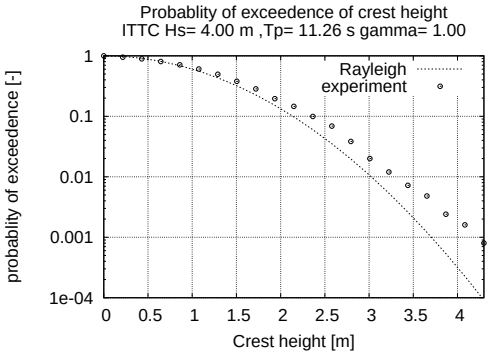

(a) input wave

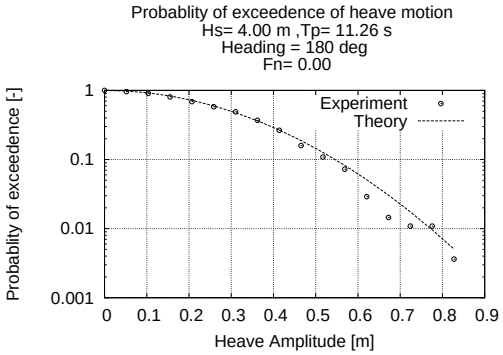

(b) heave motion

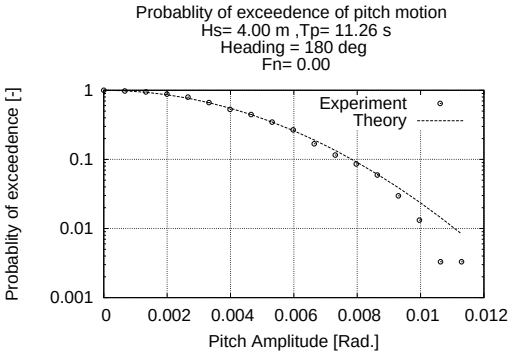

(c) pitch motion

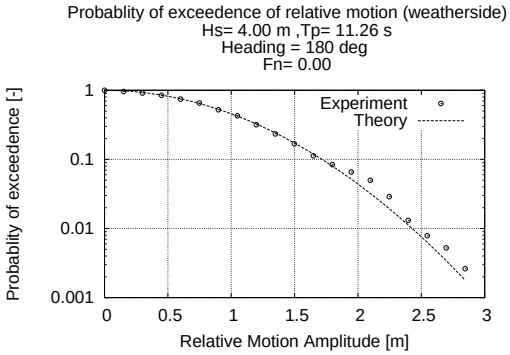

(d) vertical relative motion (weather side)

Fig. 151. Probability of exceedence for the input wave and resultant motion Hs=4.00m, Fn=0 and Heading = 180^o

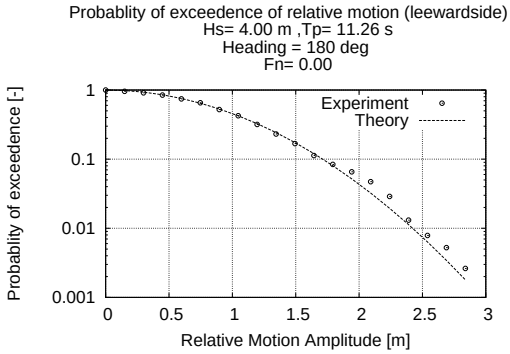

Fig. 152. Probability of exceedence for vertical relative motion (leeward side) Hs=4.00m, Fn=0 and Heading = 180^o

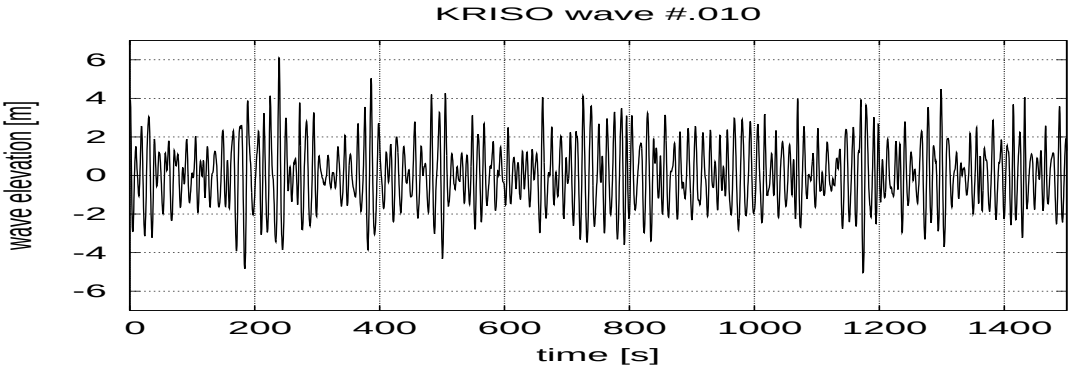

Fig. 153. Input wave $H_s = 6.0m$

2.3. Case 3 $H_s = 6.0m$

Figures 153 to 157 shows the input wave profile, heave, pitch, sway, roll, yaw, weatherside relative motion response and the leeward side relative motion response for KRISO wave data ID #010.The probability of exceedence of these wave are given in figures 158(a) to 159

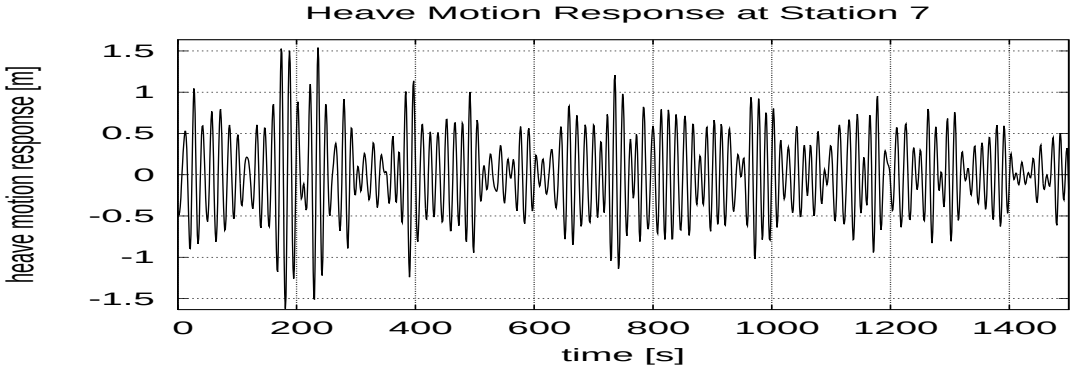

Fig. 154. Heave Motion for heading 180^o and $H_s = 6.0m$

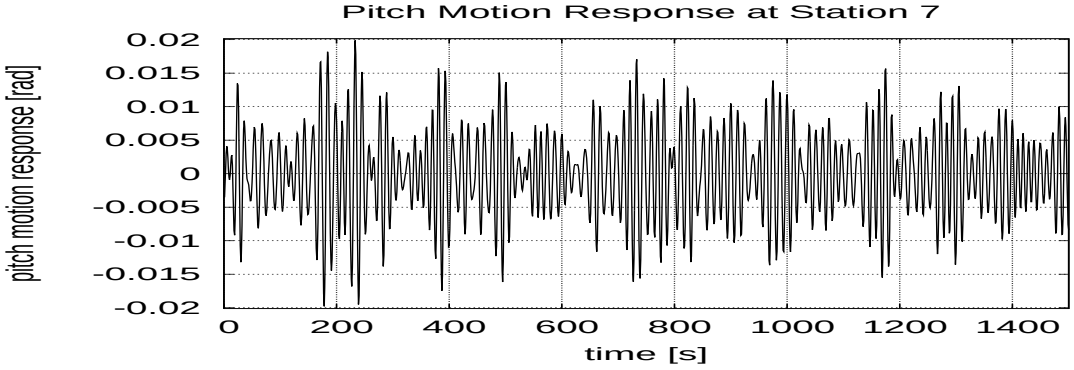

Fig. 155. Pitch Motion for heading 180^o and $H_s = 6.0m$

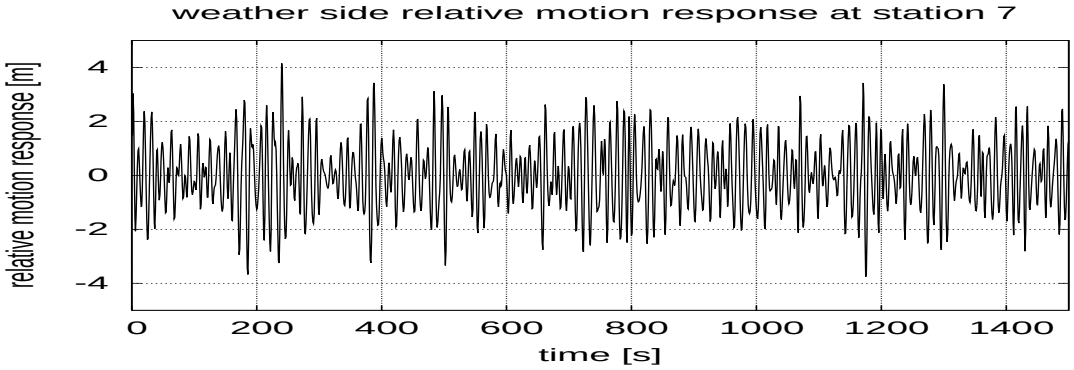

Fig. 156. Relative Motion at weather side for heading 180^o and $H_s = 6.0m$

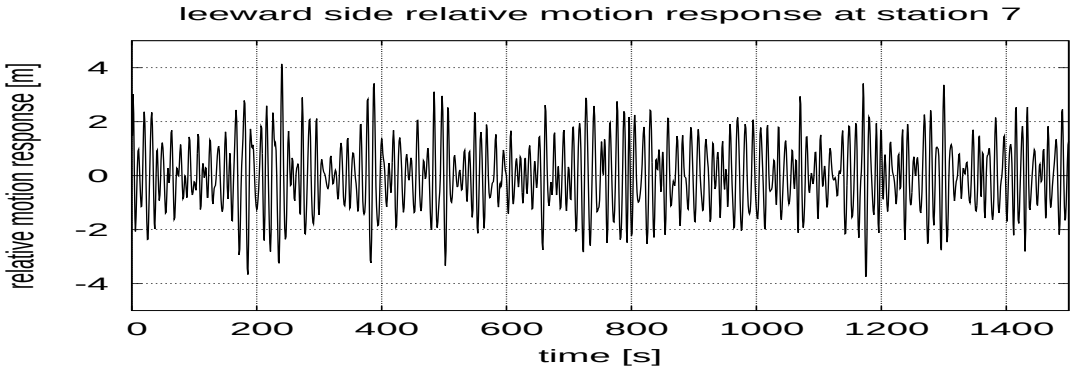

Fig. 157. Relative Motion at leeward side for heading 180^o and $H_s = 6.0m$

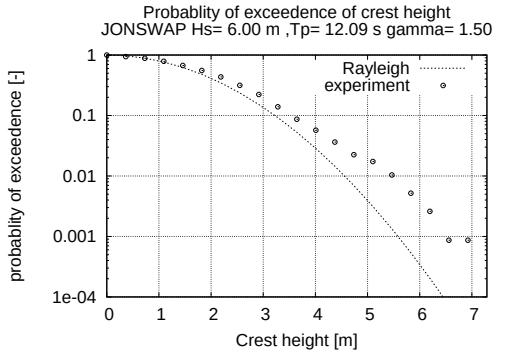

(a) vertical relative motion (leeward side)

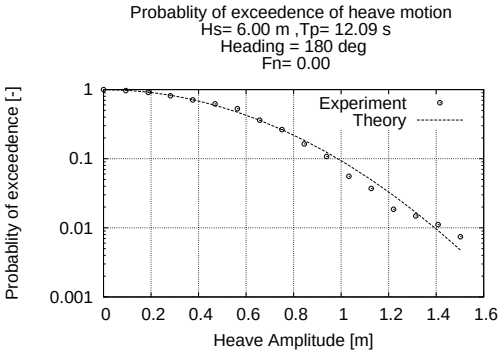

(b) heave motion

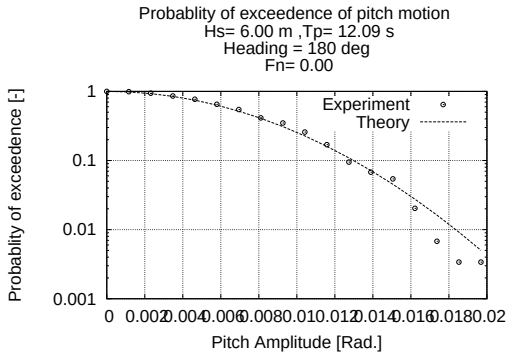

(c) pitch motion

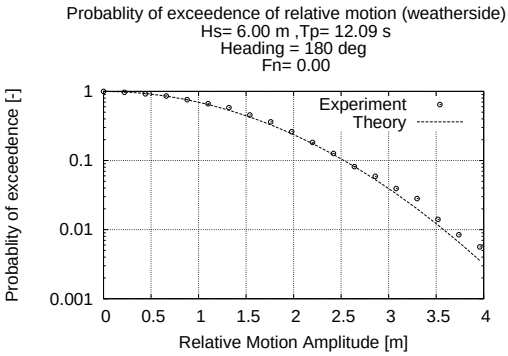

(d) vertical relative motion (weather side)

Fig. 158. Probability of exceedence for the input wave and resultant motion Hs=6.00m, Fn=0 and Heading = 180^o

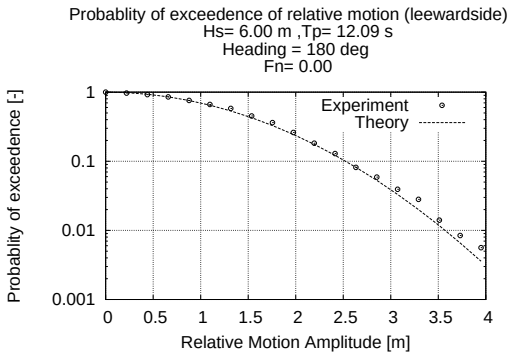

Fig. 159. Probability of exceedence for the vertical relative motion (leeward side) Hs=6.00m, Fn=0 and Heading = 180^o

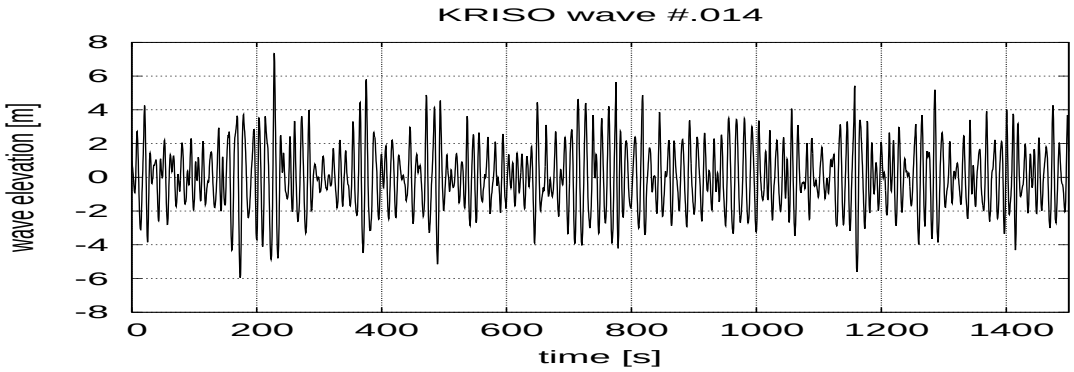

Fig. 160. Input wave $H_s = 7.0m$

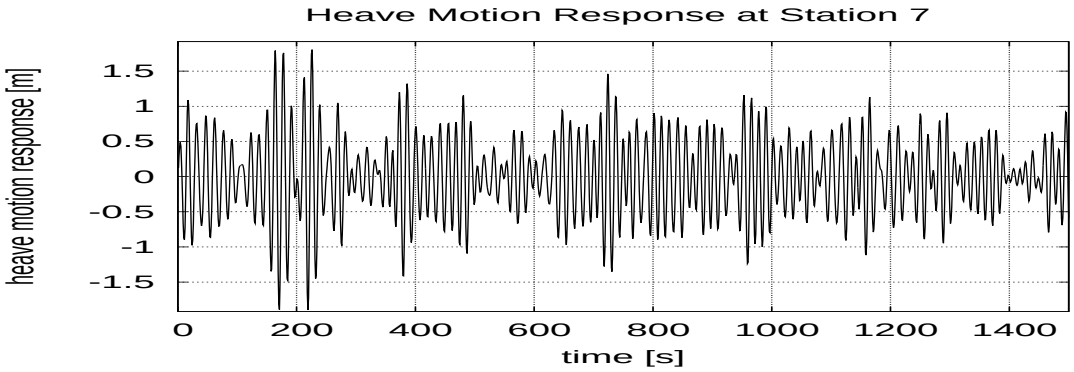

Fig. 161. Heave Motion for heading 180^o and $H_s = 7.0m$

2.4. Case 4 $H_s = 7.0m$

Figures 160 to 164 shows the input wave profile, heave, pitch, sway, roll, yaw, weatherside relative motion response and the leeward side relative motion response for KRISO wave data ID #014.The probability of exceedence of these wave are given in figures 165(a) to 166

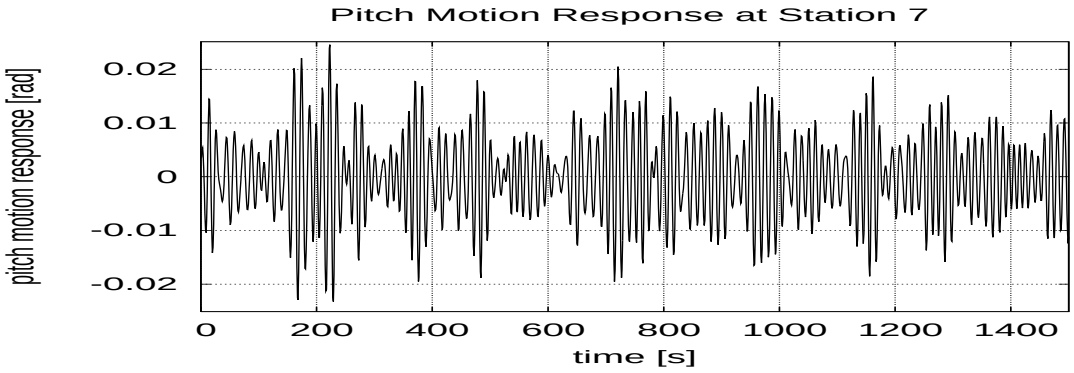

Fig. 162. Pitch Motion for heading 180^o and $H_s = 7.0m$

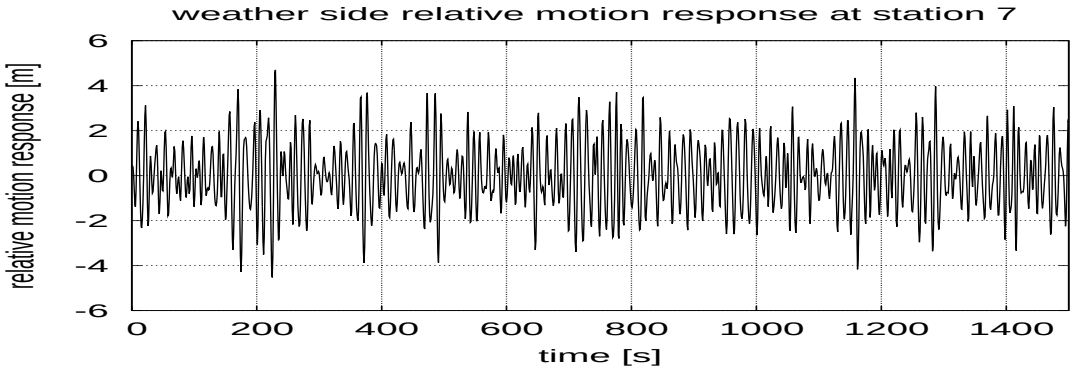

Fig. 163. Relative Motion at weather side for heading 180^o and $H_s = 7.0m$

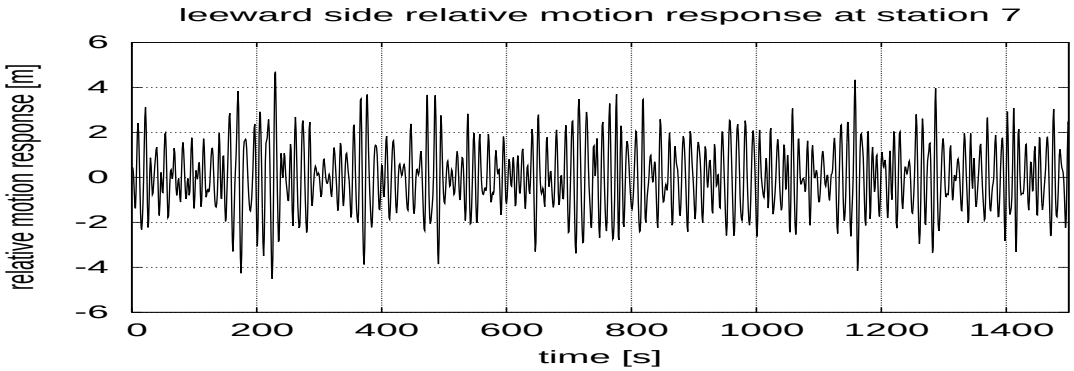

Fig. 164. Relative Motion at leeward side for heading 180^o and $H_s = 7.0m$

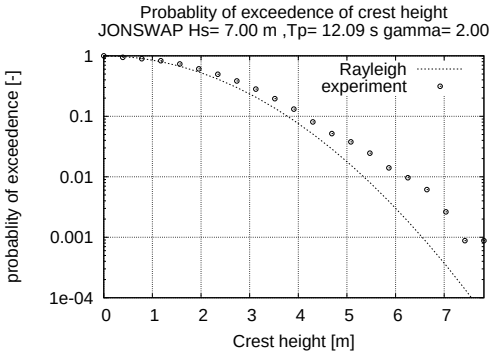

(a) input wave

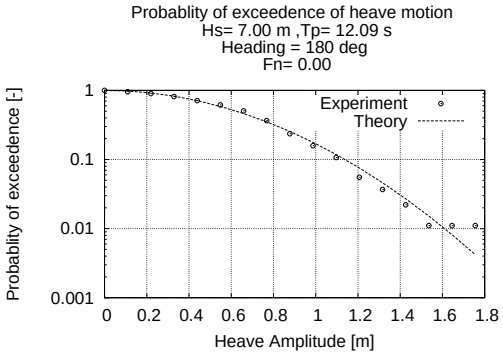

(b) heave motion

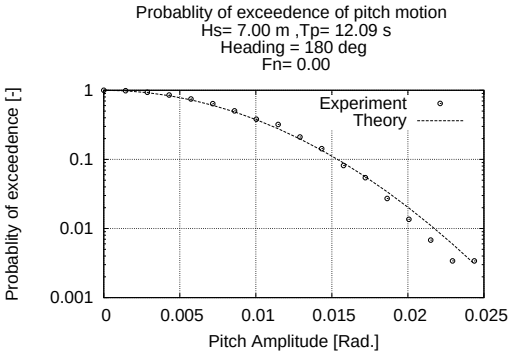

(c) pitch motion

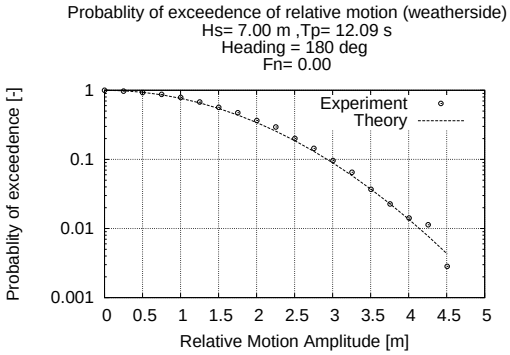

(d) vertical relative motion (weather side)

Fig. 165. Probability of exceedence for the input wave and resultant motion Hs=7.00m, Fn=0 and Heading = 180^o

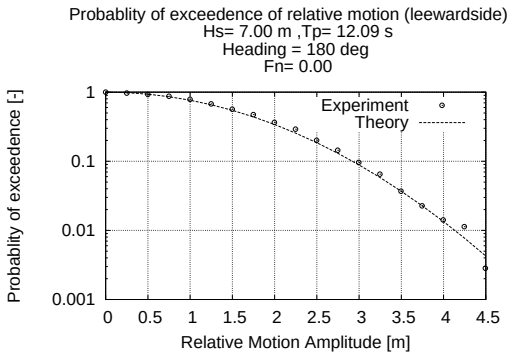

Fig. 166. Probability of exceedence for vertical relative motion (leeward side) Hs=7.00m, Fn=0 and Heading = 180^o

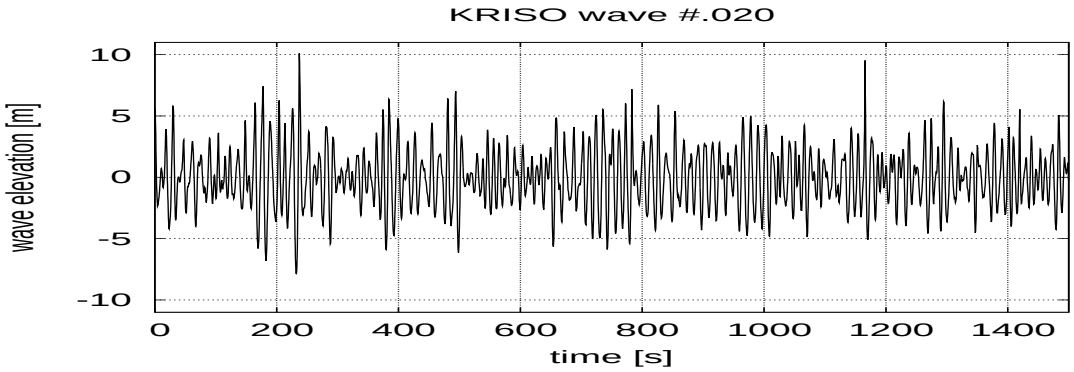

Fig. 167. Input wave $H_s = 9.0m$

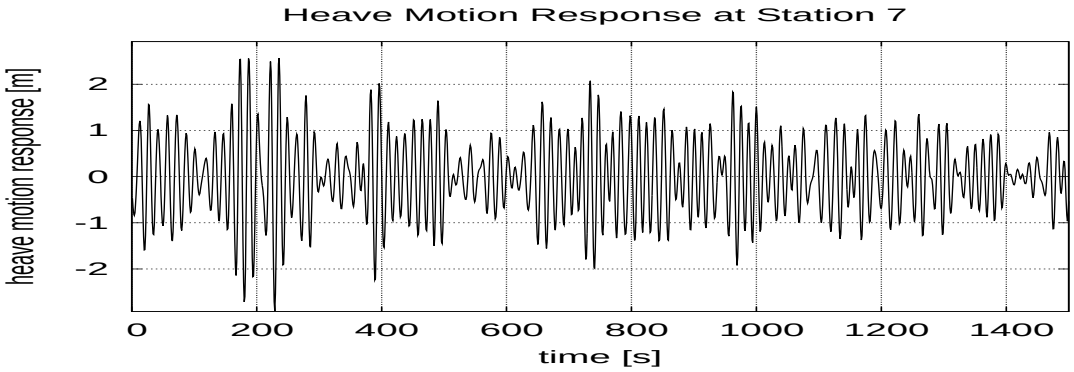

Fig. 168. Heave Motion for heading 180^o and $H_s = 9.0m$

2.5. Case 5 $H_s = 9.0m$

Figures 167 to 171 shows the input wave profile, heave, pitch, sway, roll, yaw, weatherside relative motion response and the leeward side relative motion response for KRISO wave data ID #020.The probability of exceedence of these wave are given in figures 172(a) to 173

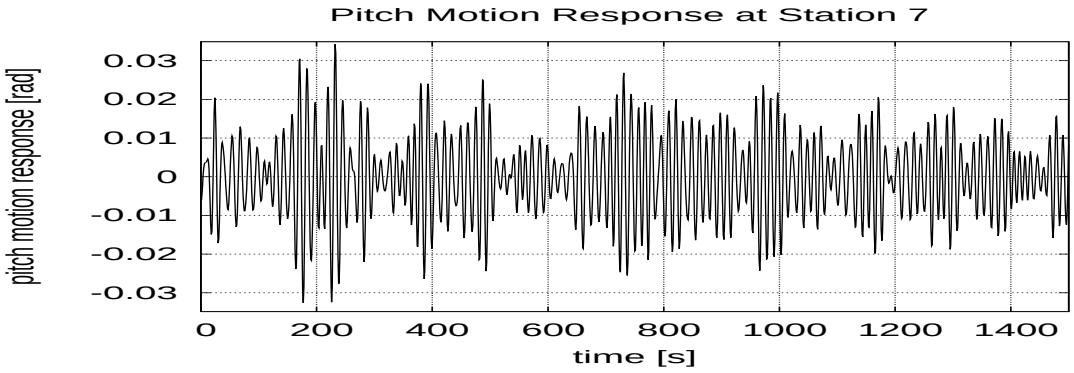

Fig. 169. Pitch Motion for heading 180^o and $H_s = 9.0m$

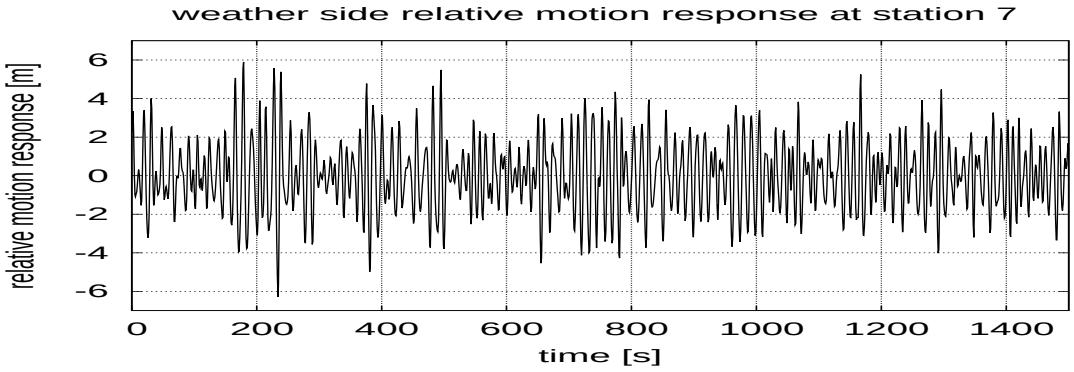

Fig. 170. Relative Motion at weather side for heading 180^o and $H_s = 9.0m$

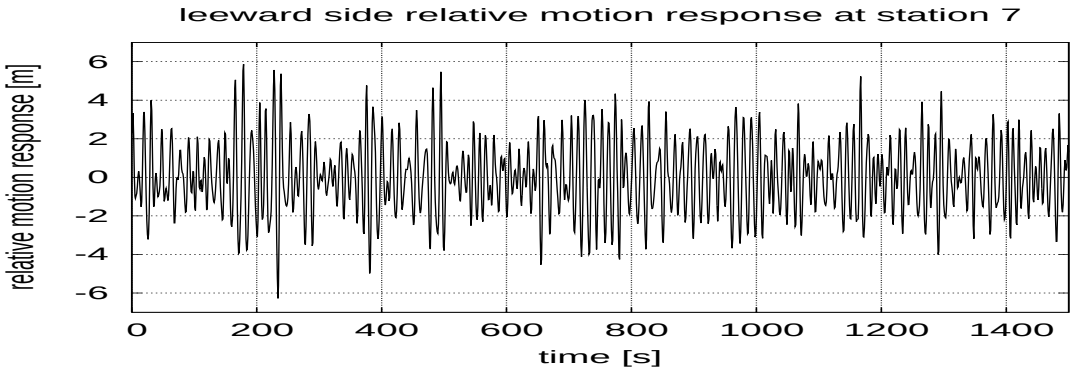

Fig. 171. Relative Motion at leeward side for heading 180^o and $H_s = 9.0m$

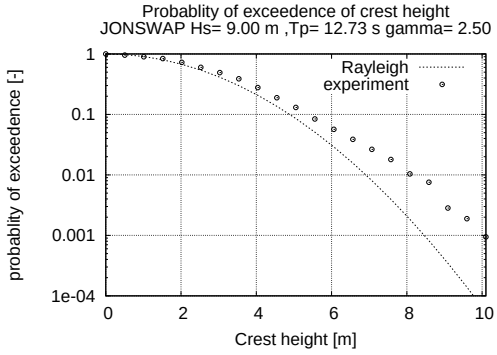

(a) input wave

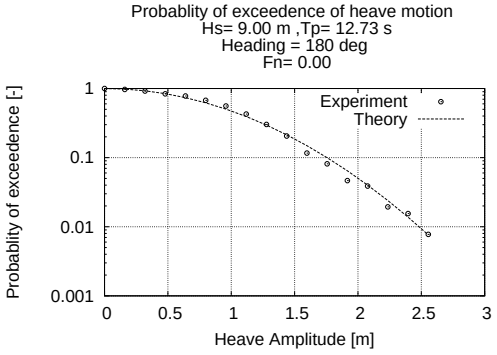

(b) heave motion

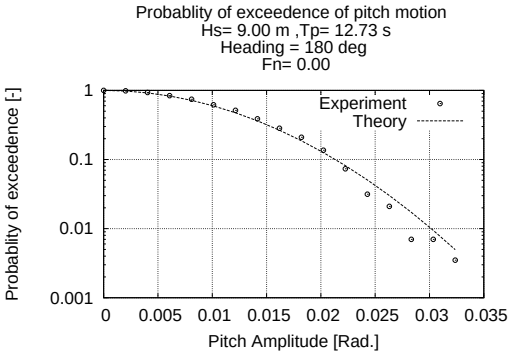

(c) pitch motion

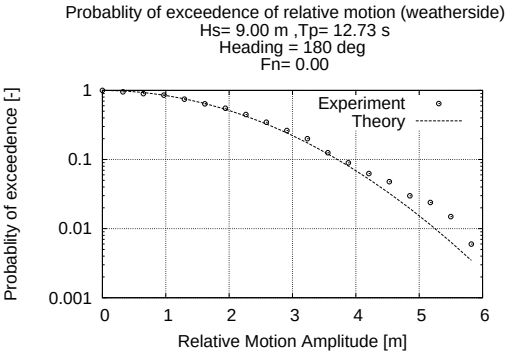

(d) vertical relative motion (weather side)

Fig. 172. Probability of exceedence for the input wave and resultant motion Hs=9.00m, Fn=0 and Heading = 180^o

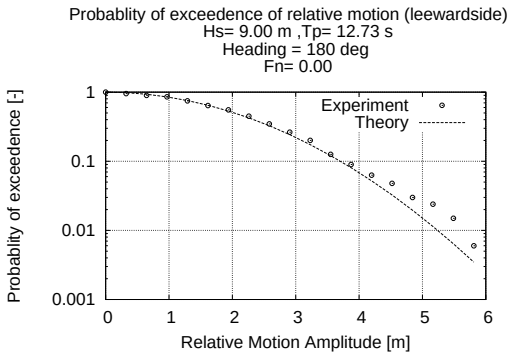

Fig. 173. Probability of exceedence for vertical relative motion (leeward side) Hs=9.00m, Fn=0 and Heading = 180^o

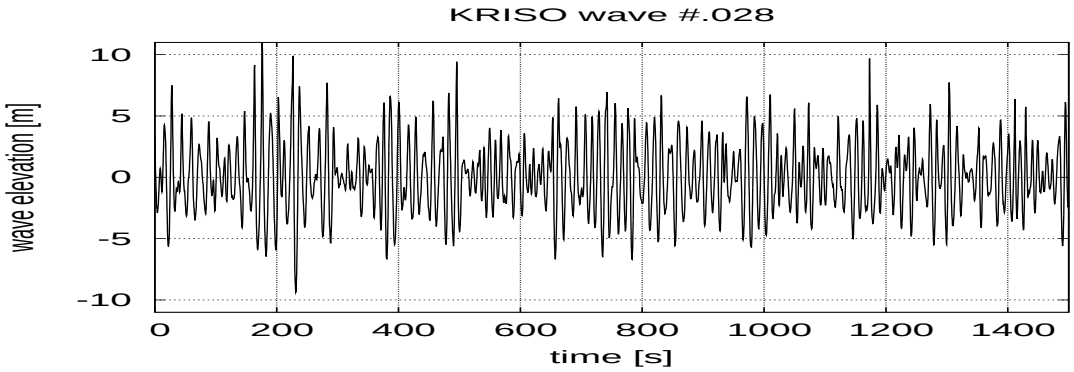

Fig. 174. Input wave $H_s = 9.0m$

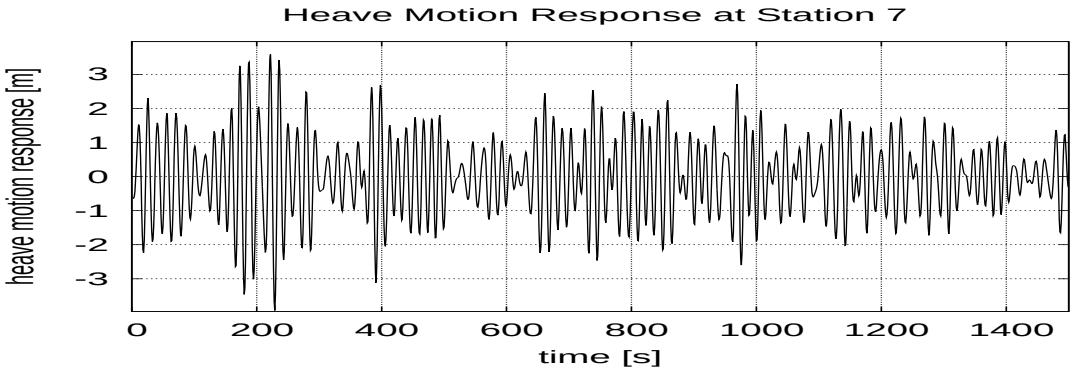

Fig. 175. Heave Motion for heading 180^o and $H_s = 11.0m$

2.6. Case 6 $H_s = 11.0m$

Figures 174 to 178 shows the input wave profile, heave, pitch, sway, roll, yaw, weatherside relative motion response and the leeward side relative motion response for KRISO wave data ID #028.The probability of exceedence of these wave are given in figures 179(a) to 180

3. Most Probable Peak Value

The most probable peak values for the different sea states, for each sea condition is shown in figure 181(a) to 181(d).

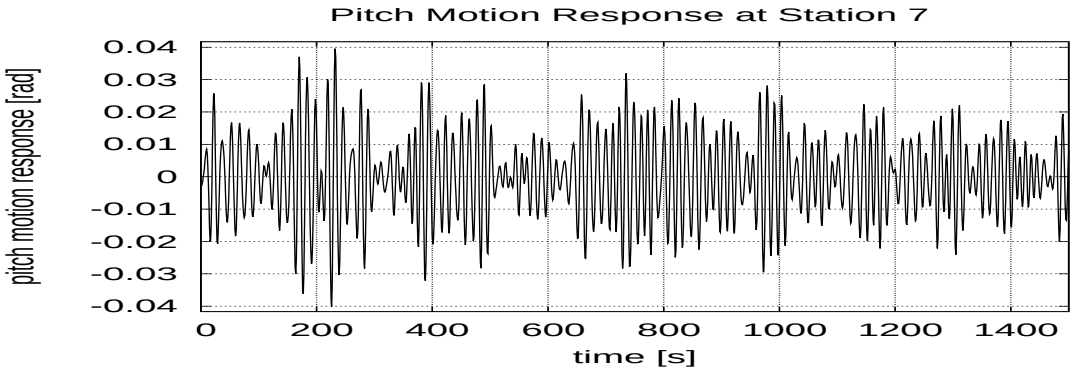

Fig. 176. Pitch Motion for heading 180^o and $H_s = 11.0m$

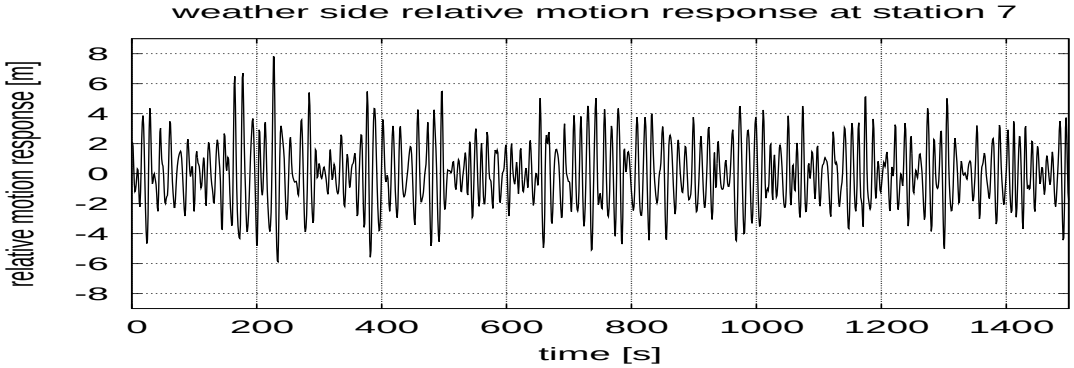

Fig. 177. Relative Motion at weather side for heading 180^o and $H_s = 9.0m$

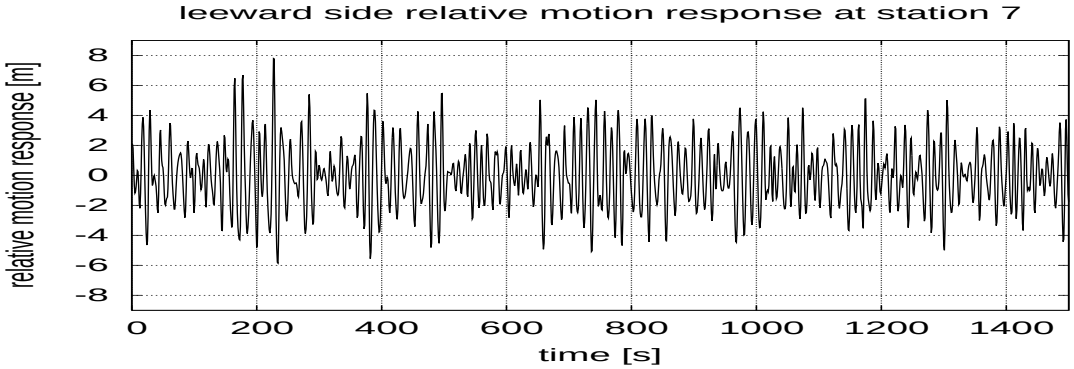

Fig. 178. Relative Motion at leeward side for heading 180^o and $H_s = 9.0m$

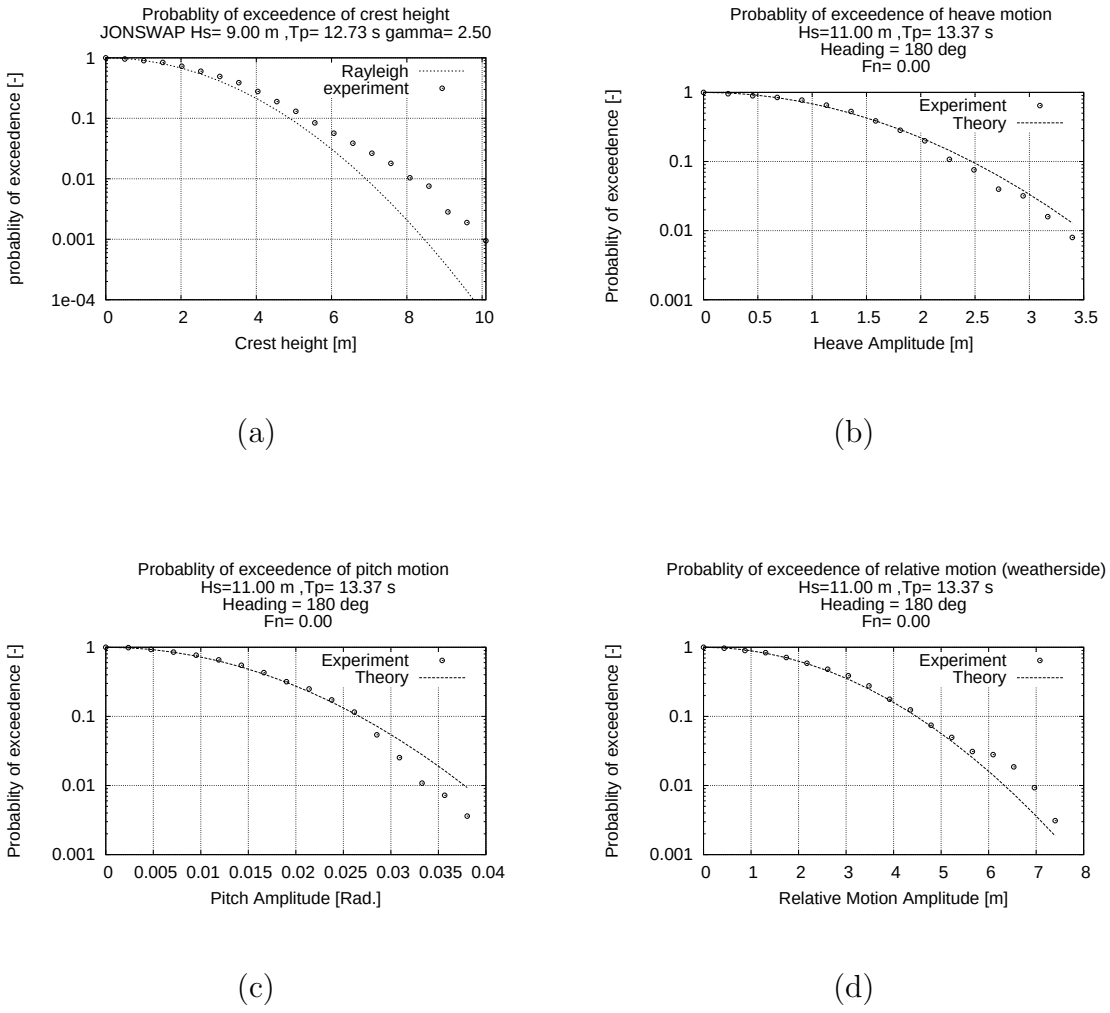

Fig. 179. Probability of exceedence for the input wave and resultant motion Hs=11.00m, Fn=0 and Heading = 180^o

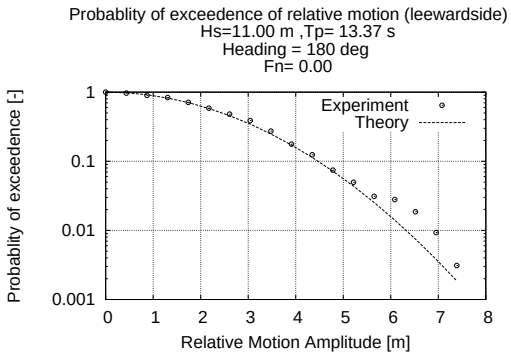

Fig. 180. Probability of exceedence for the vertical relative motion (leeward side) Hs=11.00m, Fn=0 and Heading = 180^o

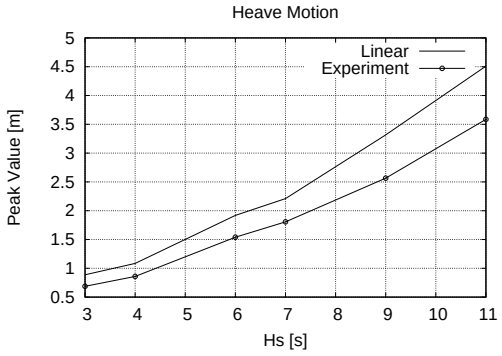

(a) heave

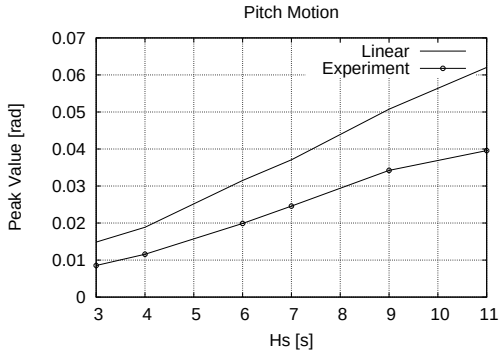

(b) pitch

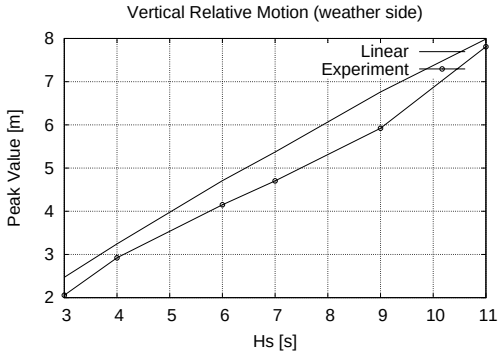

(c) weather side

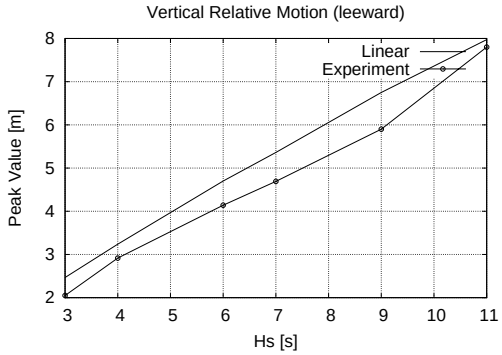

(d) leeward side

Fig. 181. Peak value comparison for heave, pitch,sway,roll and vertical relative motions (weather side and leeward side) for Fn=0 and Heading = 180^o

CHAPTER VII

SUMMARY OF ANALYSIS RESULTS

In chapters IV, V and VI we have shown exhaustive analysis results for Heading = 90^o and $F_n = 0$, Heading = 135^o , and $F_n = 0.15$, Heading = 180^o and $Fn = 0$. In this chapter the most probable peak value will be analyzed for: Case 4 - Heading = 135^o and $F_n = 0.00$ Case 5 - Heading = 180^o and $F_n = 0.15$

1. Analysis Results for Heading = 135^o AND $F_n = 0.00$

The most probable peak values for the different sea states, for each sea condition is shown in figure 182(a) to 1.

2. Analysis Results for Heading = 180^o AND $F_n = 0.15$

The most probable peak values for the different sea states, for each sea condition is shown in figure 184(a) to 184(d).

3. Observation

In all the above cases we see that the most probable peak obtained from UNIOM is lower than that obtained by the linear method.

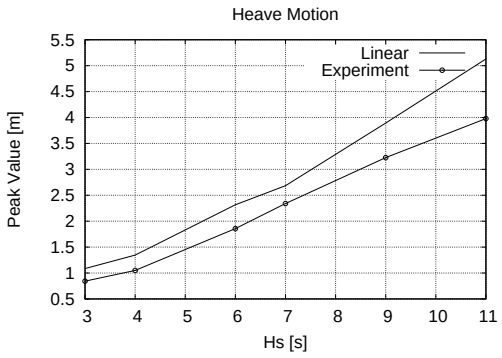

(a) heave

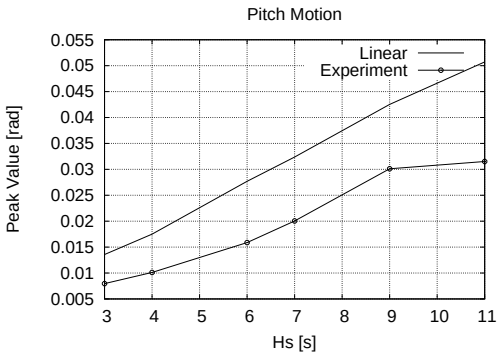

(b) pitch

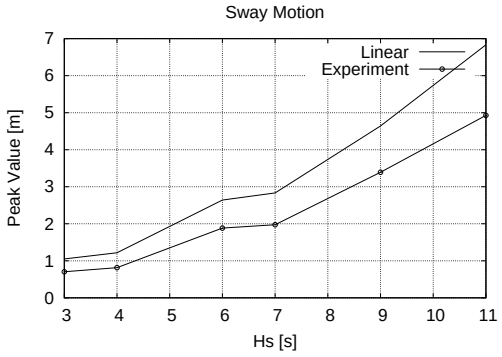

(c) sway

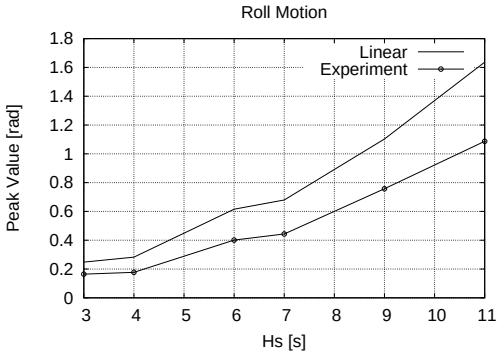

(d) roll

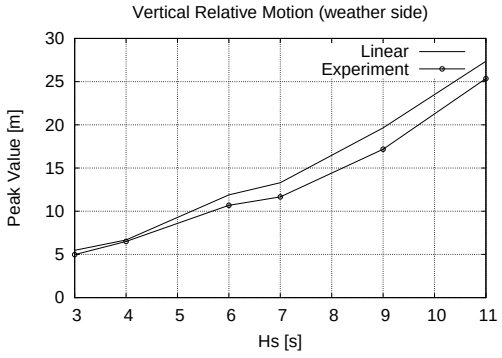

(e) weather side

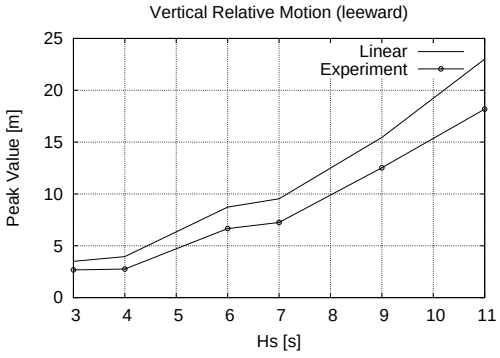

(f) leeward side

Fig. 182. Peak value comparison for heave, pitch,sway,roll and vertical relative motions (weather side and leeward side) for Fn=0.00 and Heading = 135^o

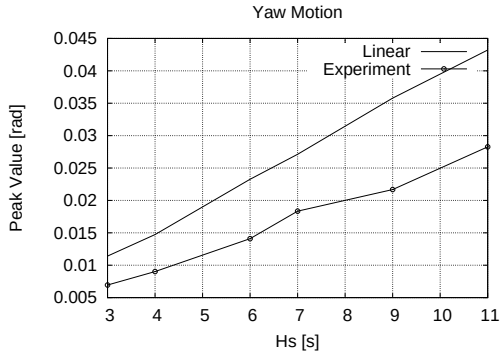

Fig. 183. Peak value comparison for yaw motion, Fn=0.00 and Heading = 135^o

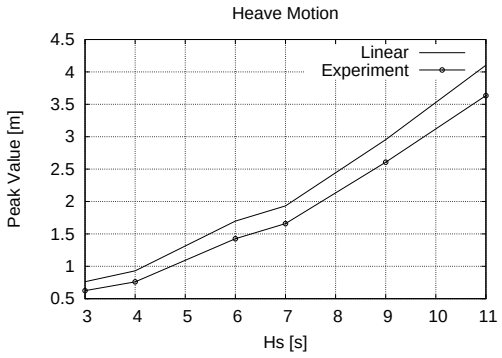

(a) heave

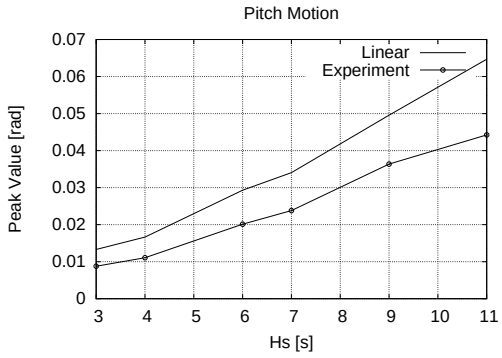

(b) pitch

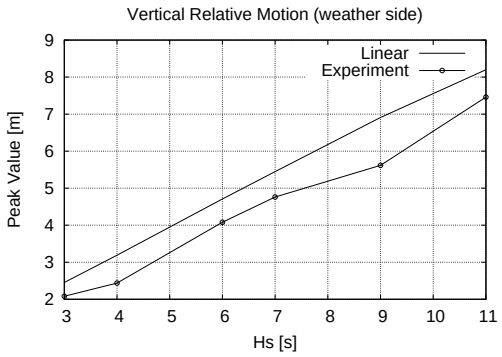

(c) weather side

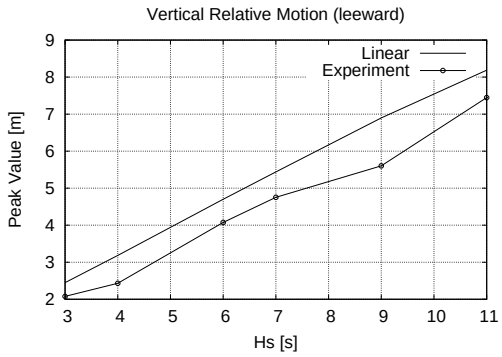

(d) leeward side

Fig. 184. Peak value comparison for heave, pitch, sway, roll, and vertical relative motions (weather side and leeward side) for Fn=0 and Heading = 180^o

CHAPTER VIII

CONCLUSION

Conventionally the responses of the ship to different sea states are calculated in the frequency domain using the linear theory. This method is prone to over-predictions for nonlinear waves. The linear approach is based on the assumption that the process is a narrow band Gaussian process. This explains why the predictions are different from the simulated values.

The study shows the validity of the UNIOM approach over the linear theory. The probability of exceedence study has shown that the responses are actually lower than those calculated using the spectral approach, thus being in line with the experiments done by Dalzell (Cummins 1973). This confirms the validity of the UNIOM approach in calculating the responses of a floating body in an irregular seaway.

The predictions using the linear method and UNIOM match closely for the lower sea states, this is apparent in figure 137(e). In this figure at low sea states, the values predicted by UNIOM overshoots the value predicted by the linear theory. However, at higher sea states there is marked difference in this and the linear theory is seen to over predict.

This trend is attributed to the fact that the lower sea states are more close to being linear whereas the higher sea states show marked nonlinear behavior. Therefore, the higher sea states show greater divsersions from the linear predictions.

Thus UNIOM seems to be applicable to predict non linear effects on vertical relative motion and other modes as well. It is hoped that this method may be developed further to be more generic. However to quantitatively conclude that this method explains the non linearity of ship motions, we require experimental data.

In the future, UNIOM can be applied to a ship sea-way system, using the

Quadratic Transfer Function (QTF) in place of the RAO. This will represent the nonlinearities in ship responses more accurately.

REFERENCES

Adil, A. 2004 Simulation of ship motion and deck-wetting due to steep random sea. Masters thesis, Texas A&M University, College Station, Texas.

Bhattacharyya, R. 1978 *Dynamics of Marine Vehicles.* John Wiley and Sons, New York.

Chakrabarti, S. K. 1994 *Offshore Structure Modeling.* World Scientific, River Edge, NJ.

Cummins, W. 1973 Pathologies of the transfer function. Report. Naval Ship Research and Development Center, Bethesda, Maryland.

Dalzell, J. 1982 An investigation of the applicability of the third degree functional polynomial model to non-linear ship motion problem. Report SIT-DL-82-9-2275. Stevens Institute of Technology, Hoboken, NJ.

Dean, R. G. and Dalrymple, R. A. 1984 *Water Wave Mechanics for Engineers and Scientists.* World Scientific, River Edge, NJ.

Journee, J. and Massie, W. 2001 *Offshore Hydrodynamics.* located at www.shipmotions.nl and accessed on March 2006.

Kim, C. H. 2006 *Non Linear Waves and Offshore Structures.* World Scientific, River Edge, NJ.

Kim, C. H., Chou, F. S. and Tein, D. 1980 Motions and hydrodynamic loads of a ship advancing in oblique waves. *Trans.* SNAME, **88**, 1, Mar, 29.

Richer, J. 2005 The effects of wave groups on the nonlinear simulation of ship motion in random sea. Masters thesis, Texas A&M University, College Station, Texas.

VITA

ADDRESS

Room # 202, Ocean Engg Division,

Dept. of Civil Engg,

Texas A&M University,

College Station,

TX-77843-3136.

EDUCATION

Master of Science in Ocean Engineering. Graduation Date: May 2006

Major : Ocean Engineering

(August 2004 - May 2006)

Texas A&M University

Bachelor of Technology in Naval Architecture and Ship Building

Major : Naval Architecture and Ship Building

(September 1997 - May 2002)

Cochin University of Science and Technology,

Cochin, Kerala, India.

EXPERIENCE Graduate Teaching assistant with the Ocean Engineering program (2005 - 2006) Naval Architect - A B Marine Consultants (2002 November - 2004 August)

The typist for this thesis was Rajith Padmanabhan.